CHAPTER 1

INTRODUCTION

The human lens contains a number of low molecular mass kynurenine-based compounds, known as UV filters. Previous studies have shown that some of these UV filters can bind to human lens proteins *in vivo*, causing modifications that are observed upon lens aging and age-related nuclear cataract. The overall aims of this study were to i) develop an efficient synthetic pathway for the major UV filter, 3-hydroxykynurenine-*O*-β-D-glucoside, for subsequent protein binding studies, and to allow facile entry to other UV filters, ii) identify and quantify novel human lens metabolites using total synthesis and spectral analysis, iii) investigate the binding of 3-hydroxykynurenine-*O*-β-D-glucoside and other lens metabolites to lens proteins, and iv) determine the effect of UV light on the UV filter-modified lens proteins and the possible role of UV light in lens aging and age-related nuclear cataract.

1.1 General Introduction

Cataract is an opacity of the lens that causes loss of vision.[1] It is the leading cause of blindness and visual impairment, accounting for approximately 41% of the estimated 38 million cases of visual impairment worldwide.[2-4] According to the Australian Institute of Health and Welfare, in 2005 almost 1.5 million Australians aged 55 or over suffered from untreated cataract in 2004, *i.e.* 31% of this age group.[5] Currently, the only treatment for cataract is surgery.

The most common form of cataract is age-related nuclear (ARN) cataract.[6] It is characterised by a progressive increase in fluorescence, yellowing/tanning and precipitation of proteins (crystallins), primarily in the inner core of the lens.[7-12] ARN cataract is a disease that occurs mainly in the elderly.[13] With the increasing average age of populations in many countries, the incidence of ARN cataract is going to rise. It is therefore imperative that non-surgical treatments be found.

The World Health Organisation has estimated that the number of blind people aged 60 years and over will increase from 22 million to 54 million by 2020 and that more than 50 million of

these will live in developing countries.[14] As a result, cataract surgery will consume an increasing proportion of the health care budget in developed countries (~$3.4 billion annually in USA), while in developing countries an even smaller portion than the current 10% of cataract patients will have their vision surgically restored.[15-17] Hence, an understanding of the mechanism of ARN cataract formation is important.

Human lens ultraviolet (UV) light absorbers, known as UV filters, have been implicated in ARN cataract formation.[18-20] An understanding of their involvement in ARN cataract, at a molecular level, is an essential first step in the development of a preventative and/or therapeutic treatment for this disease.

A detailed discussion of the human lens, its components, including lens crystallins, antioxidants and UV filters, and changes that occur in the lens upon aging and development of ARN cataract, is given in this chapter. In addition, the possible role of UV light in the formation of ARN cataract is discussed.

1.2 The human eye

The human eye (Figure 1.1) is the organ of sight. The outermost layer of the eye contains the sclera and the cornea.[21] The sclera is a white strong fibrous protective coat covering 85% of the posterior surface of the eye. The anterior portion of the eye is covered by a transparent viscoelastic tissue called the cornea. Its function is to focus incoming light onto the lens. Beneath this is the choroid, containing the iris and the ciliary body, which together are known as the uvea.[21] The iris is a ring of muscle fibres located behind the cornea and in front of the lens. It contains melanocytes, which include the pigment melanin, whose function is to prevent light scattering. The opening in the iris is the pupil, which contracts and expands in response to the brightness of the surrounding light.

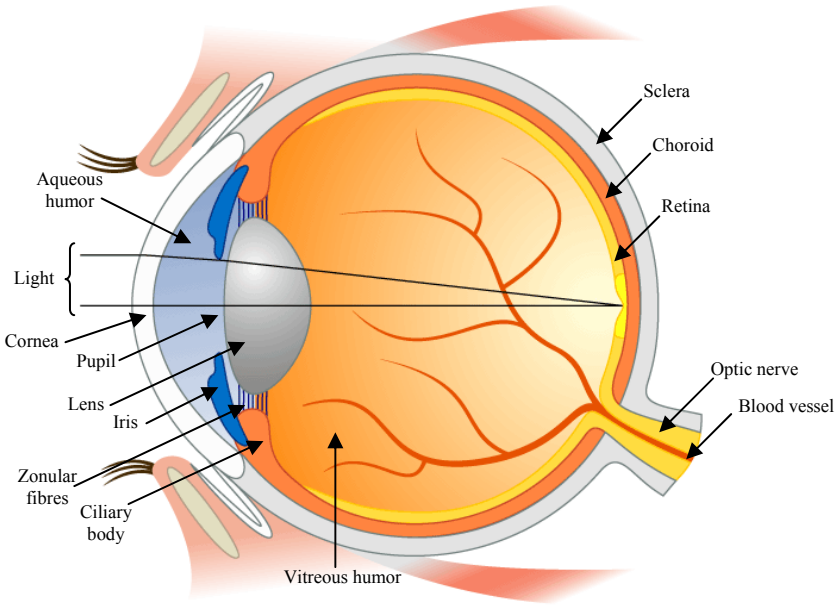

Figure 1.1: The cross-section of the human eye.[22]

The lens is a transparent tissue positioned behind the iris and the pupil. It is held in position between the aqueous and vitreous humor by the zonular fibres that attach to the ciliary body.[23] The contraction and expansion of these fibres alter the curvature of the lens, enabling adjustable focus, a process known as lens accommodation.[24] The iris and the lens are bathed in the aqueous humor, a transparent watery fluid that contains various antioxidants and maintains intraocular pressure.[23] Behind the lens is the vitreous humor, which provides support and growth factors, and also serves as a shock absorber against mechanical damage. The light focused by the lens passes through the vitreous humor and reaches the retina, the centre of the visual process. The retina is composed of photoreceptor cells (rods and cones) that receive light and the neural portion that transduces light signals through the retina to the optic nerve.[23]

1.3 The human lens

The lens is essential for human vision. It typically contributes one third of the eye's total dioptric power (the degree to which a lens converges or diverges light), and by changing its shape, it is able to fulfill the requirements of the accommodative processes. The normal human lens is a transparent, pale yellow, biconvex body contained within an elastic collagenous capsule (Figure 1.2). The capsule allows the diffusion of small molecules both into the lens tissue (*e.g.* oxygen, glucose, amino acids, fatty acids and other nutrients) and out

of the lens tissue (*e.g.* lactose and carbon dioxide).[21] The lens capsule is also elastic, which is important for controlling the lens shape during focussing. It is an avascular organ that obtains all nutrients from the aqueous and vitreous humors that bathe it.[21,24,25]

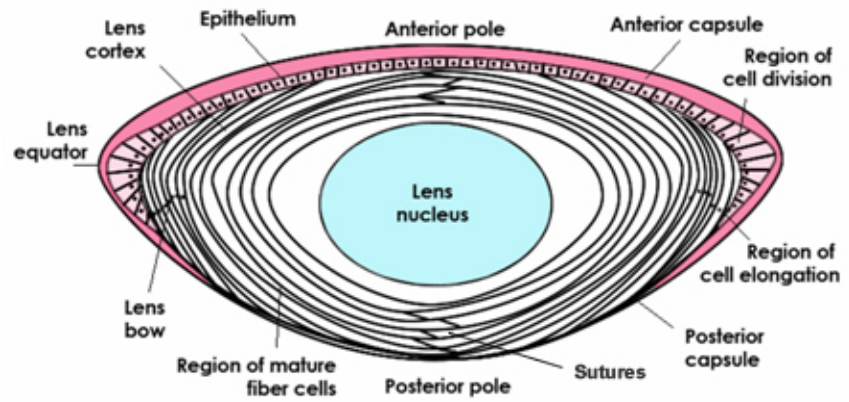

Figure 1.2: The cross-section of the human lens (adapted with modifications from Wormstone *et al.*[25] and Harding[24]).

All cells within the lens are derived from epithelial cells, which are contained in the localised region of cell division and fibre differentiation. In the normal lens, growth begins at the equatorial germinative zone, where epithelial cells differentiate into fibre cells. Fibre cells elongate from the anterior of the lens, curving around towards the posterior of the lens, where they meet in the regions called sutures. New fibre cells are laid down as concentric layers on the previously formed embryonic fibres. Fibre cells experience loss of the nuclei and other intracellular organelles, thus becoming metabolically quiescent.[26] Due to the lack of DNA and RNA, there is little or no protein turnover of lens proteins as the cell ages.[27] Therefore, cells contained within the nucleus are amongst the oldest cells in the body and have some of the oldest proteins. The lens is thus an exceptional system for the study of age-related processes.

The human lens grows continuously throughout the lifespan of an individual, with the maximum rate being observed in the foetus. Humans are born with ~1.6 million fibre cells. This reaches 3 million at age 20 and almost 3.5 million fibre cells at age 80.[28] The mass of the lens starts at ~65 mg at birth and increases to ~125 mg by the end of the first year through to ~260 mg by 90 years of age.[29]

Special anatomical and physiological features of the lens keep light-scattering to a minimum and are responsible for lens transparency in the visible region of the spectrum (400 to 800 nm).[28,30] These include a high concentration (up to 500 mg/mL) of proteins known as crystallins and anucleated fibre cells grouped in hexagonal arrays with minimal extracellular

spaces. Tight control of electrolyte balance in the lens is necessary to maintain a constant hydration level.[31] Disorganisation of the fibre membranes and the lens proteins is believed to be a factor in visual impairment.

1.4 Lens composition

The lens is comprised of ~60% water and 35% proteins (crystallins) by mass. The remainder includes varying quantities of amino acids[32,33] and trace minerals (*e.g.* sodium, potassium, copper, iron, zinc, selenium, chromium and cobalt)[34-38] and many low molecular mass compounds including antioxidants (*e.g.* glutathione (GSH), ascorbic acid, uric acid),[39-42] and, of direct interest to the present study, UV filter compounds.[39] The nature and role of the proteins, antioxidants and UV filter compounds are described in greater detail below.

1.4.1 Lens proteins

The crystallins of the human lens constitute more than 90% of the lens proteins. The other proteins present in the lens include those associated with membranes and the cytoskeleton, and enzymes involved in lens metabolism.[1] The majority of protein synthesis occurs in the lens cortex from amino acids that have been transported into the lens from the aqueous humor.

Crystallins are structural proteins responsible for the refractive properties and stability of the lens. Bovine and human lens proteins contain three distinct groups of crystallins, designated α, β and γ, based on decreasing molecular mass.[26,28,43] α-Crystallin is by far the largest of the crystallin proteins and is not sequence-related to the β- and γ-crystallins. There are two α-crystallin proteins, αA and αB, found in a three to one molar ratio in human lenses.[28] Each α-crystallin subunit is ~20 kDa, however, they exist as a heterogenous multimeric assembly with a molecular mass distribution ranging from 500 to 1000 kDa.[43] The amino acid sequence homology between αA- (acidic) and αB- (basic) crystallins is approximately 60%.[44] αA- and αB-crystallin are continuously synthesised and are found in the lens epithelial cells. While αA-crystallin is found mainly in the lens, with trace amounts in other tissues, αB-crystallin is considered to be a ubiquitous protein with measurable levels found in the brain, muscles and heart.[45-48] In addition to their structural role, α-crystallins function as molecular chaperones in

the lens, regulating protein folding and preventing non-specific protein aggregation in the intact lens.[28,44,49-52] Increased amounts of αB-crystallins have been associated with various neurological diseases, such as Alexander's disease,[53] Creutzfeldt-Jakob disease,[54] Alzheimer's disease[55] and Parkinson's disease.[55-57] The β- and γ-crystallins are structural and fibre cell specific proteins. β-Crystallins exist as multiple forms of aggregated proteins from dimers through to octamers, with molecular masses from 5 to 200 kDa.[26] β-Crystallins comprise seven proteins, βA1-A4 (acidic) and βB1-B3 (basic). The γ-crystallins exist as monomers (~20 kDa) and are sequence and structurally related to the β-crystallins.[26] Hence, they are often categorised together as the β, γ-crystallin superfamily. In human lenses, the γ-crystallins are comprised of seven proteins, γA-γF and γS, with γC, γD and γS being the dominant polypeptides.[44,58]

1.4.2 Lens antioxidants

There are several different mechanisms that protect the lens from the effects of oxidation. These include both enzymatic (superoxide dismutase, catalase and gluthathione redox cycle enzymes) and non-enzymatic factors (GSH, ascorbic acid, α-tocopherol, β-carotene, uric acid). The activities of the various protective systems are generally higher in the cortex than in the nucleus, with the epithelial layers being particularly active. This protection, however, is not absolute and low levels of damage may accumulate throughout life. The two major non-enzymatic antioxidants present in the lens are GSH and ascorbic acid.

1.4.2.1 Glutathione (GSH)

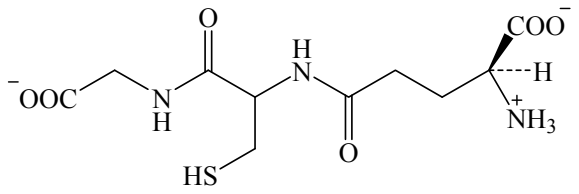

Figure 1.3: Chemical structure of GSH.

GSH (Figure 1.3) is a linear tripeptide of L-glutamic acid, L-cysteine and glycine.[59] It is present in ~1-6 mM levels in normal human lenses.[39] Its concentration is higher in the cortex than in the nucleus, with the highest concentration being in the epithelium.[39,59] GSH is considered to be the most important self-generated antioxidant in mammals.[60,61] The

sulfhydryl group on the cysteinyl portion of GSH accounts for the high electron-donating capacity (high negative redox potential) and consequently strong reducing power of GSH.[62] GSH plays a major role in the protection of cells from harmful reactive oxygen species including peroxides (*e.g.* H_2O_2), reduction of disulfides, removal of xenobiotic electrophiles and inhibition of oxidation of endogenous chemicals such as ascorbate, catechols and aminophenols.[59,63-67] In the process, GSH is oxidised to the disulfide, GSSG, which is re-reduced by the action of glutathione reductase.[59] The reactions involving glutathione and protein sulphydryl groups are summarised in Scheme 1.1.

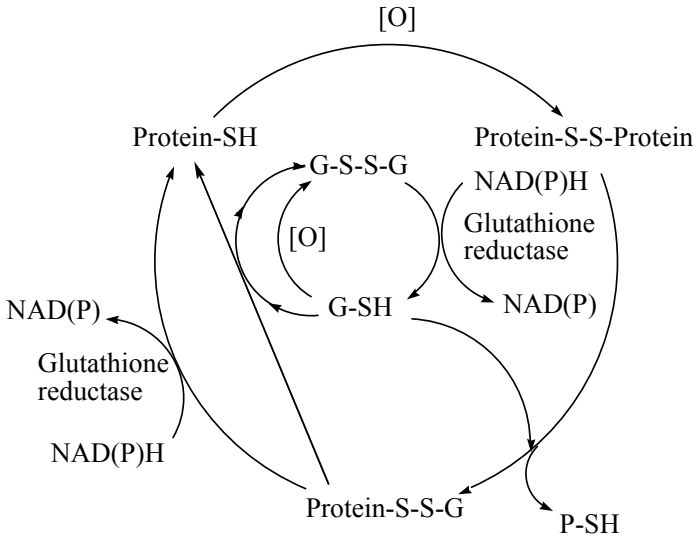

Scheme 1.1: The glutathione protective system.[64,68]

1.4.2.2 Ascorbic acid

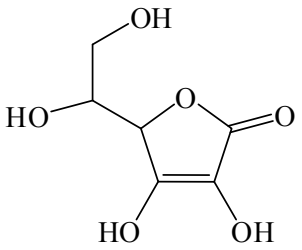

Figure 1.4: Chemical structure of ascorbic acid.

Ascorbic acid (Figure 1.4) is present in ~1-2 mM levels in normal human lenses.[69] It is capable of reacting with some activated oxygen species (*e.g.* singlet oxygen [$^1O_2$]) and free radicals (*e.g.* superoxide radical [$O_2^{\cdot-}$], hydroxyl radical [$HO^{\cdot}$], alkoxyl radical [$RO^{\cdot}$], peroxyl radical [$ROO^{\cdot}$]).[70] In the presence of trace amounts of transition metals, ascorbic acid can reduce oxygen to water.[71] Dehydroascorbic acid (DHA), an intermediate in the ascorbate oxidation pathway, can be subsequently reduced by GSH, resulting in the regeneration of ascorbic acid.[72,73] Recent experiments by Shang *et al.*[74] have suggested that ascorbic acid is an

effective scavenger of H_2O_2 in lens epithelial cells. In addition, ascorbic acid displays pro-oxidant properties. In the presence of trace amounts of iron and copper, ascorbic acid can generate peroxides, which may result in generation of hydroxyl radicals *via* reaction with reduced metals.[75-77] Major reactions found in the human lens that involve ascorbic acid are summarised in Scheme 1.2.

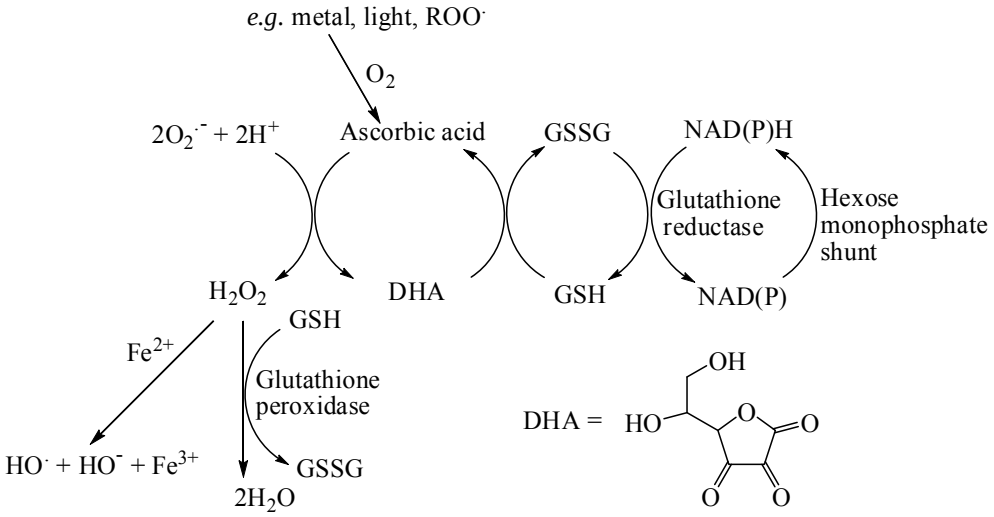

Scheme 1.2: The role of ascorbic acid as antioxidant and pro-oxidant in the antioxidative pathways in the human lens.[64,72,77,78]

1.4.3 Lens UV filters

The damaging wavelengths of UV radiation that reach the lens are in the range of 300-400 nm. The majority of this UV radiation (~90-95%) is effectively absorbed by low molecular mass lenticular UV absorbers, known as UV filters,[79,80] which are biosynthesised in the lens in the anterior cortical epithelial cells.[81] They have a maximum absorption at 360-370 nm.[80]

The major UV filters are 3-hydroxykynurenine-*O*-β-D-glucoside (3OHKG), kynurenine (Kyn) and 3-hydroxykynurenine (3OHKyn) (Figure 1.5).[80-84] In addition, 4-(2-amino-3-hydroxyphenyl)-4-oxobutanoic acid-*O*-β-D-glucoside (AHBG), 4-(2-amino-3-hydroxyphenyl)-4-oxobutanoic acid-*O*-diglucoside (AHBDG) and the glutathione adduct of 3OHKG (GSH-3OHKG) have also been identified (Figure 1.5).[85-87]

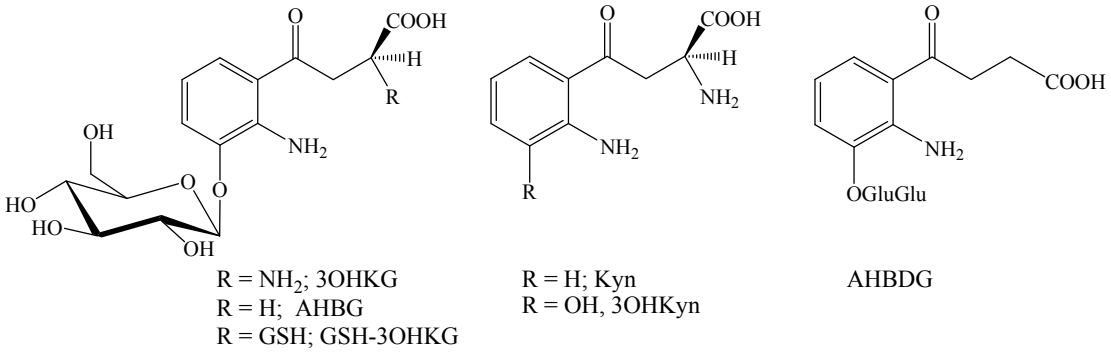

Figure 1.5: The major UV filters in the human lens.

Bova *et al.*[39] have found in normal lenses that 3OHKG is the most prevalent (~50-400 nmol/g), followed by GSH-3OHKG (~0-600 nmol/g), AHBG (~5-80 nmol/g), Kyn (~5-30 nmol/g), 3OHKyn (~2-15 nmol/g) and AHBDG (~0.2-9.8 nmol/g). These levels are comparable to levels observed in other studies,[40,81,86,88] although lower for 3OHKG (~1-7 μmol/g) and AHBG (~0.3-2.6 μmol/g) compared to the levels determined by Truscott *et al*.[85]

UV filters are believed to be involved in non-destructive photo-physical pathways upon exposure to UV light.[79,89] Following light absorption, UV filters get promoted to an electronic excited state, which undergoes a rapid and efficient physical quenching process within picoseconds.[90] This results in the regeneration of the original ground-state without formation of reactive oxygen species. The electron from the excited state returns to the ground state by either dissipating the excess energy of the excited state through heat (photothermal mode), internal vibrations, or the release of energy as a photon *via* fluorescence or phosphorescence (emission mode).[31,89]

UV filters are continuously biosynthesised in the lens from L-tryptophan (Trp) *via* the kynurenine pathway (Scheme 1.3).[80] The kynurenine pathway is the major pathway for Trp catabolism in humans and approximately 95% of the total body Trp is metabolised by this route.[91-95] The first and rate limiting step of the kynurenine pathway is the oxidative cleavage of the 2,3-double bond of the indole ring of Trp by indoleamine 2,3-dioxygenase (IDO) [EC 1.13.11.17] and incorporation of O_2 or $O_2^{\cdot-}$ to produce *N*-formyl-L-kynurenine.[93,95-97] *N*-Formyl-L-kynurenine is then hydrolysed by a formamidase [EC 3.5.1.9] to form Kyn. Kyn is subsequently metabolised by kynurenine 3-hydroxylase [EC 1.14.13.9] to form 3OHKyn.[93,95] 3OHKyn is then glucosylated to yield 3OHKG, which has a half-life of 2-48 h.[81,91] This glucosylation is lens specific in humans and primates. The specific glucosyl transferase involved has still not been determined, however investigations carried out by Wong *et al.*[98] on

bilirubin glucoside have suggested that the enzyme is a microsomal uridine diphosphate (UDP) glucosyl transferase.

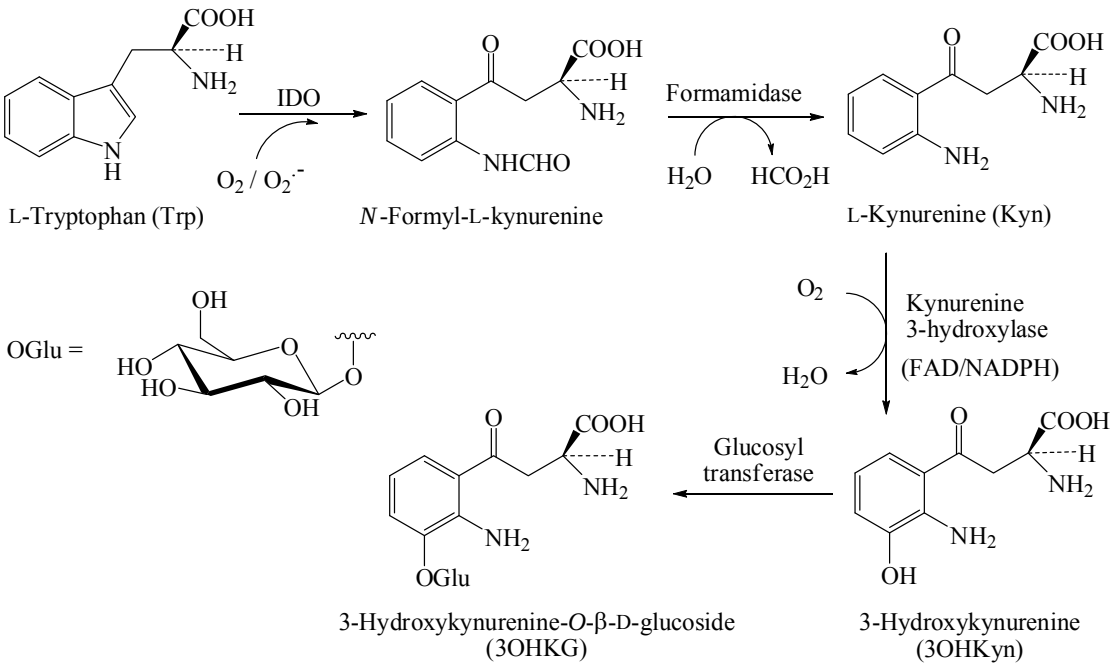

Scheme 1.3: The kynurenine pathway of tryptophan metabolism.[94-96,99]

The UV filters 3OHKG, Kyn and 3OHKyn are unstable under physiological conditions in the human lens and deaminate non-enzymatically to yield α,β-unsaturated carbonyl compounds.[100,101] It has been recently shown that the deaminated product of 3OHKG can undergo further reactions in the human lens, including reduction by reduced nicotinamide dinucleotide (phosphate) (NAD(P)H) or Michael addition with GSH, to yield AHBG and GSH-3OHKG, respectively (Scheme 1.4).[86,100]

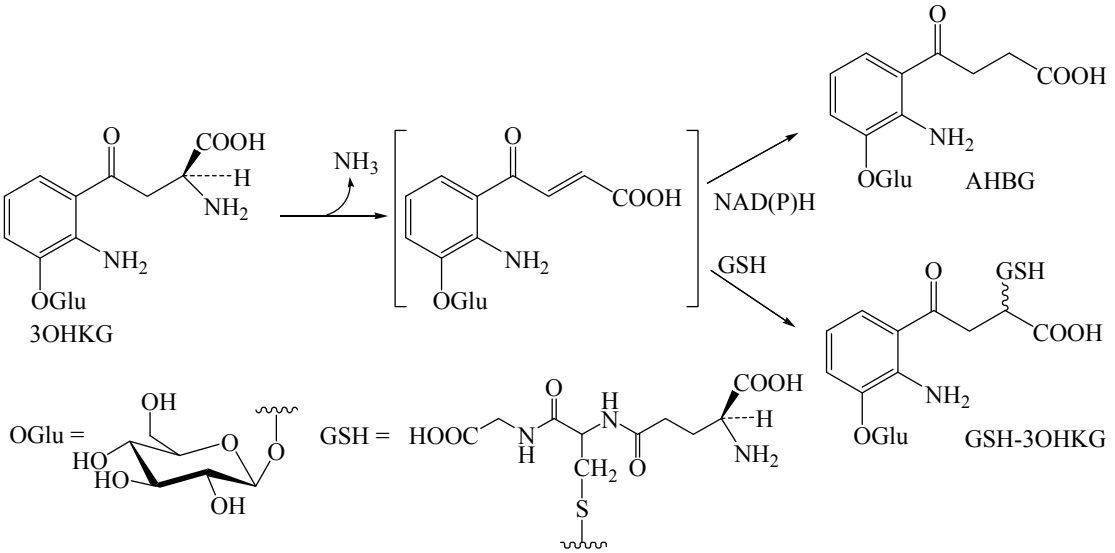

Scheme 1.4: The biosynthetic pathway for formation of AHBG and GSH-3OHKG.[85,86,100]

Taylor *et al.*[87] have proposed that further glucosylation of AHBG, *via* glucosyl transferase, yields the diglucoside AHBDG (Figure 1.5). Enzymatic studies have determined that AHBDG is a β-linked diglucoside, however the nature of the diglucosidic link (1 → 6 or 1 → 4) remains to be determined. Analyses of human lens extracts have also shown that a range of low molecular mass compounds are present with 'UV filter' properties. These had not been identified at the time of commencement of this study.

1.5 Normal human lens aging

As the lens ages a broad spectrum of molecular, biochemical and structural changes occur. The specifics of these changes as a result of normal aging are discussed below.

1.5.1 Colouration and fluorescence in human lenses

Young human lenses are a colourless to pale yellow colour. With age, an increase in lens colouration is observed.[102,103] The absorption of light by the human lens increases exponentially with age, extending to approximately 500 nm.[102,104] Accumulation of pigments seems to be at least partly responsible for age-dependent colouration of the human lens.[105] It has been suggested that lens colouration arises through the attachment of UV filters[106,107] and glycation of crystallins.[108,109]

The colouration of the lens is accompanied by a corresponding increase in lens fluorescence.[103] Fluorophores of blue and green fluorescence, with excitation and emission maxima at ~360/420-440 nm and 435/500-520 nm, respectively, have been found.[110,111] In addition, a general increase in optical density has been observed, leading to increased scattering of light rather than a true absorption.[112] These changes affect colour perception.[113]

1.5.2 Lens barrier formation

The fibre cells of the nucleus rely on the transport of water-soluble nutrients, such as GSH, from the metabolically-active outer cortex and epithelium into the lens nucleus.[114] Without any vascular system and little extracellular water (5% of total lenticular water), the major mode of transportation is thought to be *via* diffusion, through gap junctions.[115] After middle-age, a barrier to diffusion of small molecules into the lens nucleus appears.[116] The barrier

dimensions coincide approximately with the junction of the nuclear and cortical region, however the molecular basis for this barrier is still under investigation.[115,116] As a consequence of the barrier, unstable molecules (*e.g.* UV filters, ascorbic acid, NAD(P)H and GSH) that cross the barrier into the nucleus will have a greater residence time within the nuclear region, and this is likely to result in a greater extent of reaction/decomposition of the compounds and a diminished chance of damage repair. In addition, the nuclear concentration of GSH falls and its response to oxidative stress may also be reduced.[116] Since interception of deaminated UV filters and ascorbic acid by GSH or NAD(P)H is compromised, it is an inevitable consequence of the barrier that the long-lived proteins in the nucleus become modified.[63,117,118] As protein turnover in the human lens is negligible, *i.e.* nuclear proteins are as old as the individual, these modifications can accumulate over the lifetime of an individual. As a result protein tertiary structure and function may be altered and possibly predispose the aged lens to ARN cataract.[119,120]

1.5.3 Decrease in antioxidants

As a result of aging and barrier formation, the level of GSH in the human lens decreases.[59,121-123] The nuclear GSH concentration decreases from ~4.5 mM in a young lens to ~1 mM by the ninth decade, while the cortical concentration decreases from ~6 mM in a young lens to ~3 mM by the ninth decade.[39,121] The activity of γ-glutamylcysteinyl synthetase in the human lens has been shown to decline with age to very low levels, suggesting that this is partly responsible for the several-fold decline of human lenticular GSH content with age.[67,123-125] In contrast, the ability of the lens to reduce oxidised GSH (GSSG) by glutathione reductase is not significantly different in old compared to young human lenses.[124] A small decline in GSH levels may be due to the formation of GSH-3OHKG, as a result of GSH Michael addition to deaminated 3OHKG.[86] A significant increase in GSH-3OHKG levels has been found in human lenses after ~50 years of age, with the most pronounced increase in the nuclear region.[39] As the decrease in the activities and/or levels of lenticular antioxidants has been found to be the highest in the nuclear region, the proteins in this region are more susceptible to oxidative damage and post-translational modifications.

1.5.4 Post-translational modifications of proteins

Most of the proteins in the lens nucleus were formed *in utero*. It is therefore not surprising that they become modified over the lifetime of an individual, due to interaction with both endogenous and exogenous factors. There are two classes of post-translational modifications (PTMs); those that cause either a decrease or no change in the molecular mass (neutral or subtractive modifications) and those that result from the addition of molecules to the polypeptide (additive modifications). The neutral or subtractive modifications include truncation and racemisation. Deamidation is also included in this group as it results in only 1 Da molecular mass increase. Glycosylation, phosphorylation, methylation, acetylation, carbamylation and UV filter modifications are additive modifications. In general, PTMs are likely to influence crystallin conformation, aggregation state or solubility. However, as the additive PTMs can lead to greater alteration in chemical properties of amino acids, it is possible that they are responsible for the colouration of lens proteins, aggregation, increased light scattering and eventual loss of lens transparency; these changes may predispose the lens to the formation of cataract.

1.5.4.1 Neutral or subtractive modifications

1.5.4.1.1 Truncation, racemisation and deamidation

An increase in truncations at the *N*- and *C*-termini of α-, β- and γ-crystallins has been shown to occur with age.[126-131] *N*- and *C*-truncated βB1- and αA-crystallins show different aggregation behaviour and chaperone activity compared to the native macromolecules.[132,133] In addition, racemisation of L-amino acids to D-amino acids in proteins is one marker of the aging process.[134-136] Racemisation proceeds *via* the removal of the α-carbon proton to form a planar carbanion.[137] Factors such as the position of an amino acid in a peptide chain, the R substituent of the amino acid and the alteration of the protein microstructure affect this process.[137] In particular, racemisation of L-aspartic acid (Asp) has been observed at a rate of 0.14% per year in normal and cataractous lenses.[134] Accumulation of D-Asp in high molecular mass aggregates and water insoluble proteins has been identified.[135] Racemisation of tyrosine (Tyr) residues is of particular significance, since Tyr residues are generally important in hydrophobic interactions within proteins.[138] Furthermore, deamidation of glutamine (Gln) and asparagine (Asn) to glutamic (Glu) and Asp, respectively, results in formation of more polar carboxylate anions, which may encourage ionic interactions in the proteins, leading to

conformational changes.[139] Wilmarth *et al.*[140] have found deamidation to be one of the major age-related PTMs, being significantly more abundant in the water-insoluble proteins of aged lenses.

1.5.4.2 Additive modifications

1.5.4.2.1 Carbamylation, acetylation, phosphorylation and methylation

Carbamylation of ~45-60% of accessible *N*-termini of γB-, γC- and γD-crystallins and acetylation of ~10-12% of these carbamylated crystallins has been detected in adult lenses.[141] Whether *N*-carbamylation and *N*-acetylation are co- or post-translational processes is still not known. The carbamylated and acetylated *N*-termini of 11-day old lenticular γC- and γD-crystallins have been found in yields of 2-3%.[141] The presence of *N*-carbamylation and *N*-acetylation in young lenses suggests that this modification may not be detrimental to protein solubility and function.[141] In addition, acetylated *C*-terminal Lys-70 has been identified on αA-crystallin.[142] This modification is of potential significance as it is located in a region that may impact in a negative manner on the chaperone activity of αA-crystallin.[142] Phosphorylation of α- and β-crystallins has also been observed at serine (Ser), threonine (Thr) and Tyr residues and it has been estimated to be present at levels ≤ 5%.[129,143] In contrast, methylation of exposed cysteine (Cys) residues in adult lenses has been recently reported to be at levels of ~50% in γD-crystallins and 12% in γC- and γB-crystallins.[141] Methylation of γS-crystallins has also been found to be higher in the nucleus than in the cortex, while methylation of γC-crystallins is similar throughout the lens.[141,144] It has been proposed that methylation and glutathionylation (though this may be of lower significance due to the known GSH decrease in older lenses) may be beneficial by inhibiting the formation of intra- and intermolecular disulfide bonds.[123,145]

1.5.4.2.2 Glycation

Non-enzymatic glycation of proteins *via* the Maillard reaction occurs by condensation of reducing carbohydrates (*e.g.* glucose) or dicarbonyl compounds (*e.g.* glyoxal and methylglyoxal) with protein free amino groups (*e.g.* lysine [Lys] and arginine [Arg]) to form covalent adducts called Amadori products.[146-148] The first step in this reaction is the formation of a Schiff base between a reducing sugar and an amino group on the protein, followed by an Amadori rearrangement to yield a relatively stable ketoamine adduct.[149] These primary

products may undergo subsequent oxidation to form compounds known as advanced glycation end (AGE) products. These products may accumulate in long-lived proteins such as crystallins and lead to colouration, fluorescence and protein cross-linking.[150-156] Diabetes mellitus is a risk factor for lens protein glycation, resulting in, for example, twice as much glucitol-lysine compared to control samples.[154]

As described in Section 1.4.2.2, ascorbic acid is essential for lens defense mechanisms. However, it can inflict damage when the cell's defenses are weakened, such as during aging.[157] *In vitro* experiments have revealed that the oxidation products of ascorbic acid (*e.g.* L-dehydroascorbic acid, L-diketogulonic acid, oxalic acid, L-erythrulose and L-threonic acid) can rapidly react with lens proteins through glycation, yielding brown and fluorescent products that absorb light > 300 nm and fluoresce at λ_{ex} 350 and λ_{em} 400-450 nm. These products resemble those found in aged or cataractous lenses.[108,109,118,158-160] In addition, cross-links and aggregation, copper chelation and production of reactive oxygen species (*e.g.* $^1O_2$, $O_2^{-\cdot}$), especially under UVA irradiation, have also been observed following ascorbylation.[161-166] Due to the higher concentration of ascorbic acid (~1-2 mM) compared to glucose levels (~1 mM) and the higher reactivity of ascorbic acid, ascorbic acid-derived PTMs are regarded as more significant than those from glucose.[146,160] In addition, ascorbic acid on air can glycate lens proteins 9-fold and cross-link proteins 90-fold more rapidly than either glucose or fructose.[146] Several AGE products have been identified in human lens proteins following enzymatic digestion.[109,159,160,166] These AGE products include pentosidine,[167,168] N^{ε}-carboxymethyllysine and N^{ε}-carboxyethyllysine,[169] vesperlysine A,[148,155] glucosepane,[156] K2P,[159] 3-lysine-lactic acid,[149] imidazolium salts (GOLD and MOLD),[170,171] glyoxal-lysine amide (GOLA) and glycolic acid-lysine amide (GALA),[172] oxalate monoalkylamide[173] and methylglyoxal-derived hydroxyimidazolones (MG-H1 and MG-H2).[159,174] The concentration of most known AGE products analysed in human lenses to date range from 10-500 pmol/mg lens protein. Selected AGE products are shown in Figure 1.6.

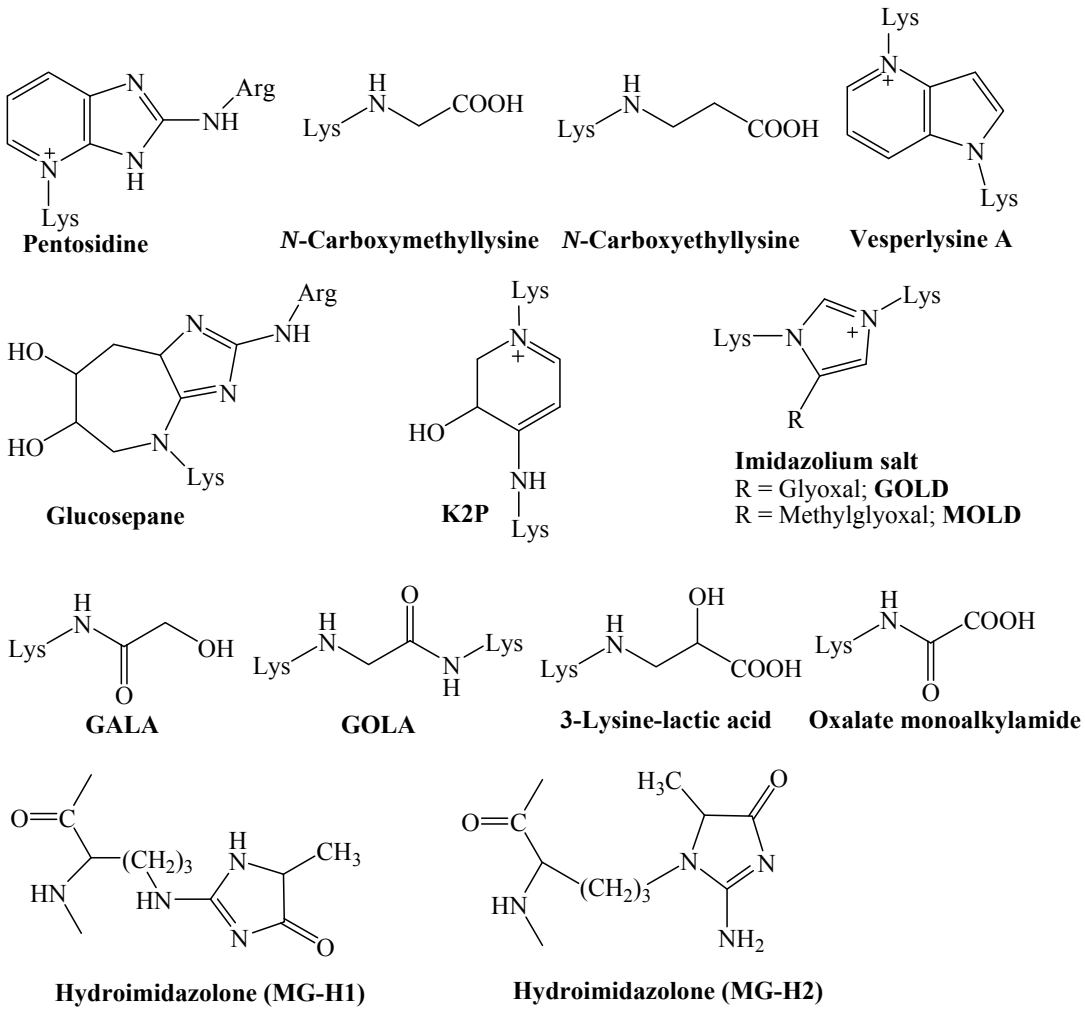

Figure 1.6: Selected AGE products found in human lenses.

1.5.4.3 UV filter modifications

With age, UV filter levels (*e.g.* 3OHKG, Kyn and 3OHKyn) decline at a rate of ~12% per decade in both the nucleus and cortex of human lenses.[39] This decrease in free UV filters is accompanied by an increase in the concentration of UV filters covalently-bound to lens proteins.[18,19,175,176] The level of Kyn and 3OHKG bound to lens proteins correlates directly to the level of lens colouration and fluorescence.[18,19] For example, the resultant fluorescence of protein bound-Kyn (λ_{ex} 410 nm and λ_{em} 490 and 525) is comparable to the fluorescence observed from aged lenses (λ_{ex} 420-435 nm and λ_{em} 500-520 nm).[18] Therefore, UV filter binding to lens proteins appears to be one of the mechanisms involved in the increase of lens fluorescence during aging and cataract.

As previously described, UV filters have been found to be unstable at physiological pH, resulting in deamination (Scheme 1.5).[85,86] Deaminated Kyn and 3OHKyn are able to bind to

nucleophilic amino acid residues, such as Cys, histidine (His) and Lys, on lens proteins *in vitro*, while *in vivo* studies suggest that preferential binding occurs at Cys residues.[18,20,176,177] The specific binding sites for Kyn and 3OHKyn on human lens crystallins remain to be determined. In addition, recent *in vivo* studies have revealed four 3OHKG binding sites at Cys residues of lens crystallins in older normal human lenses.[120] No *in vitro* studies with 3OHKG and lens proteins have been previously carried out.

In a study on aged human lens nuclei, the mean values of UV filter protein modifications were found to be 1307 pmol/mg protein of 3OHKG, 37 pmol/mg protein of Kyn and 9 pmol/mg protein of 3OHKyn, compared to the mean values of free UV filters of 534 pmol/mg protein for 3OHKG, 16 pmol/mg protein for Kyn and 3 pmol/mg protein for 3OHKyn.[176] The amount bound to cortical proteins was markedly less (~20-fold) for 3OHKG and Kyn compared to the nuclear proteins. No binding of 3OHKyn to cortical lens proteins was detected. Due to the very high protein concentration in the lens, it is not surprising that nucleophilic amino acid residues of lens proteins react *in vivo* to form protein adducts with the reactive deaminated UV filters. This binding seems to be particularly exacerbated after middle-age, following the formation of the lens barrier.[176] As the lens proteins are not replaced, these modifications can accumulate and predispose the lens proteins to the cross-linking, insolubilisation, precipitation and photo-oxidation seen in ARN cataract. Photo-oxidation occurs through the generation of reactive oxygen species upon exposure to the wavelengths of light that penetrate the cornea. This is discussed further in section 1.6.2.

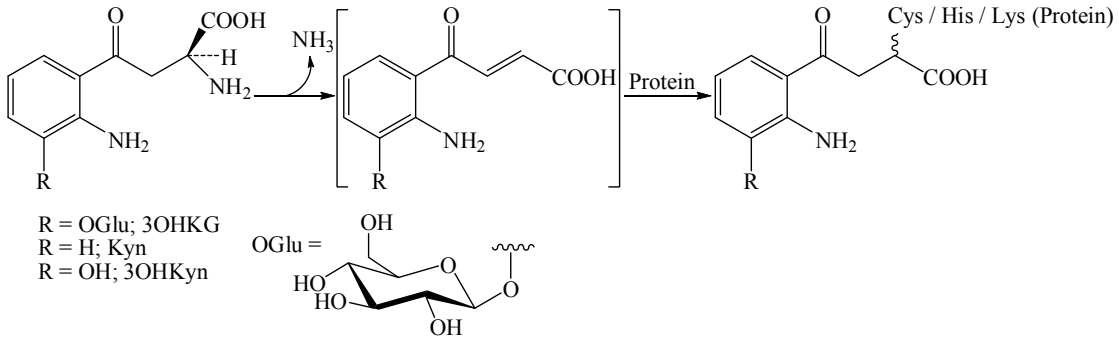

Scheme 1.5: Binding of 3OHKG, Kyn and 3OHKyn to nucleophilic amino acid residues.

1.6 Cataract – Age-Related Nuclear cataract

With age many lenses become cataractous. A cataract is a clouding of the eye's naturally transparent lens.[25] The most common type of cataract is age-related nuclear (ARN) cataract,

which accounts for approximately 60% of all cataract cases.[178] Symptoms of a developing cataract include double or blurred vision, sensitivity to light and glare, loss of night vision, seeing halos and frequent changes in eyeglass prescriptions. In addition to these problems, cataracts affect colour vision. This is best illustrated by the change in Claude Monet's (1840-1926) impressionistic style of painting after development of bilateral ARN cataract.[179] In 1918 Monet described his progressive vision loss: "I no longer perceived colours with the same intensity, I no longer painted light with the same accuracy. Reds appear muddy to me, pink insipid and lower tones escaped me." His earlier (1899) and later (1923-25) paintings of the Japanese Bridge demonstrate the remarkable change in colour perception and the loss of detail that cataract patients experience (Figure 1.7).[179]

Figure 1.7: The Japanese Bridge painted by Claude Monet in 1899 (top) and 1922 (bottom).[180]

1.6.1 Lens changes upon ARN cataract development

When compared to normal aged lenses, ARN cataract is characterised by pronounced lens colouration, fluorescence, oxidation, cross-linking and insolubility of proteins.[9-11,181] Nuclear opacification and non-tryptophan fluorescence appear to increase with the severity of the cataract. Thus ARN cataract lenses have been classified (I-V) according to the severity of the colour change (Figure 1.8).[7]

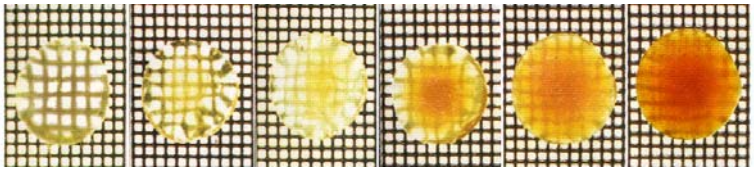

Figure 1.8: Pirie's classification of nuclear cataract using slit lamp photographs (adapted from Duncan[64]).

In addition to the more pronounced alterations noted above, changes that occur to lens proteins with the development of ARN cataract seem to take place through a mechanism different from that observed in normal aging. Oxidation is a hallmark of ARN cataract.[182] This may be due to an increase in specific oxidants such as H_2O_2 or $^1O_2$ or because of a decrease in the ability of the lens to protect itself against oxidative damage.[64] It has been suggested that oxidation starts in the lens nucleus and gradually spreads outwards through the addition of further molecules to a growing insoluble network of modified proteins.[64] With the development of age related cataract, a large decrease in lenticular GSH (up to 80%)[183-185] and ascorbic acid[186] is observed. GSH loss is mainly due to oxidation since the levels of GSSG rise significantly.[60] This is more pronounced in the lens nucleus, which may be a result of the lens barrier.[116] As the major roles of GSH are to protect protein thiol groups from oxidation/aggregation, scavenge damaging reactive oxygen species (*e.g.* H_2O_2) and produce reducing equivalents for enzymes involved in maintenance of redox equilibria, it can be expected that a decrease in the reduced GSH concentrations may have deleterious effects.[187]

More than half of protein sulfhydryl (PSH) groups and almost half of the methionine (Met) residues on lens proteins are oxidised in advanced cataract lenses.[11,188,189] The free sulfhydryls of Cys residues are among the most reactive functional groups in proteins. Oxidation of Cys residues in lens crystallins results in the formation of mixed disulfides with low molecular mass thiols such as GSH (PSSG), Cys (PSSC) and γ-glutamylcysteine (Protein-S-S-γ-glutamylcysteine) and with high molecular mass thiols such as proteins, forming protein-

protein disulfide bonds (PSSP).[68,187,190,144,191-193] Mixed sulfoxides have also been found to increase with nuclear colouration, however quantitatively they seem to be minor protein S-thiolation products.[190] Although the physiological role(s) of PSSP are not well understood, there is a correlation between these modifications and the colour/opalescence and aggregation of the nuclear crystallins.[144,190,194,195]

The *N*-terminal domain of α-crystallins may play a role in the process of cross-linking and colouration seen in cataract, suggesting that α-crystallins may be binding to denaturated crystallins *via* their chaperone activity.[196] Some of these aggregates are greater than 5 x 10^7 Da, large enough to scatter light and contribute to the loss of lens transparency.[197] Some aggregations involve non-disulfide yellow/tanned protein aggregates that are insoluble in either 8 M urea, 6 M guanidine hydrochloride or 1% sodium dodecyl sulphate in the presence of reducing agents (*e.g.* β-mercaptoethanol). These aggregates represent over 50% of the yellow protein fraction in advanced cataractous lenses.[10,11] They are detected to a greater extent in the nuclear region of the lens and correlate with the increased colouration of the lens proteins seen with the progression of cataract. Some chromophores potentially involved in cross-linking have been isolated and identified as either Trp oxidation products[198,199] or AGE products.[155,167,169]

In contrast to Kyn and 3OHKG, 3OHKyn is an *o*-aminophenol that can readily auto-oxidise at neutral pH under oxidative conditions, such as in ARN cataract. Previous studies have shown that *o*-aminophenols can undergo complex oxidative processes due to the formation of highly reactive quinone imine intermediates. These can react with amine side chains of amino acids, converting the protein into a redox-reactive substrate.[200-202] 3OHKyn has been observed to form at least five oxidation products, including xanthommatin (1) (λ_{max} 436 nm), hydroxanthommatin (2) (λ_{max} 450 and 490 nm) and 4,6-dihydroxyquinolinequinone carboxylic acid (3) (λ_{max} 350 and 460 nm) as predominant species (Figure 1.9).[203-212] These products are known to be highly coloured (red-brown) and spectroscopic studies of cataractous lenses have proven that the majority of brown pigments are composed of xanthommatin (1).[213] Model studies have shown that incubation of 3OHKyn with lens proteins, under oxidative conditions, results in yellow/tanned products that resemble ARN cataractous material.[20,106,119] The cross-linking capacity of 3OHKyn is enhanced by (but not dependent on) the reduction of metal ions.[214] Aquilina *et al.*[203,215] have shown that *in vitro* 3OHKyn oxidative products can cross-link the peptides (GlyLys, GlyGly and ThrLysProArg) through the formation of benzoxazole (4) or benzimidazole (5) adducts (Figure 1.9). It has

been suggested that this cross-linking may lead to crystallin aggregation and precipitation.[203,215]

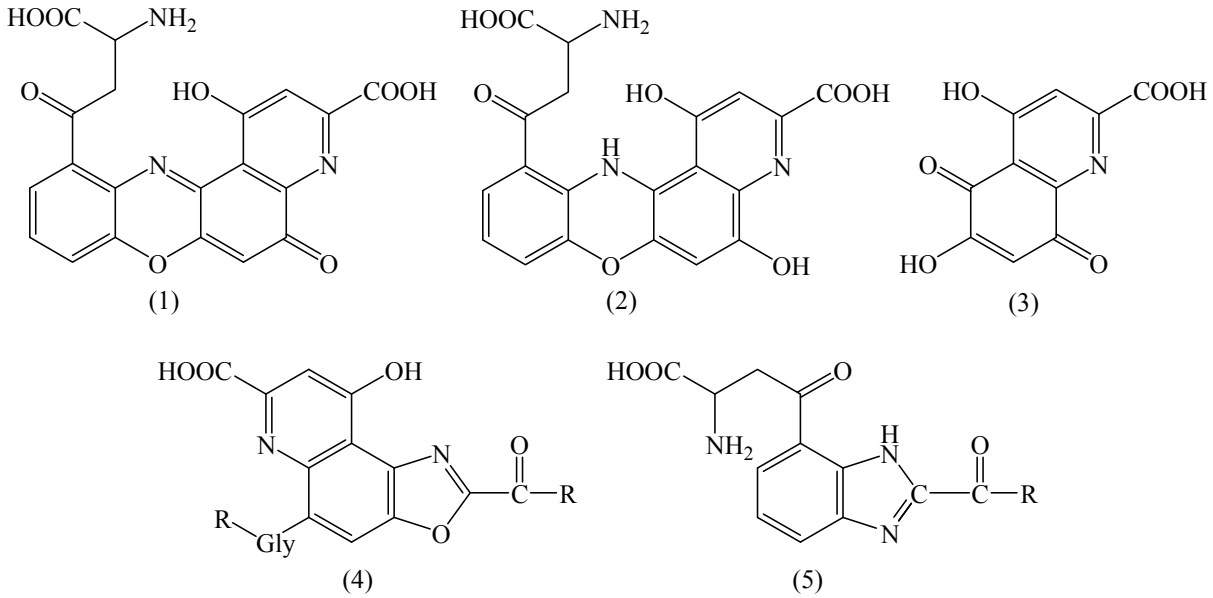

Figure 1.9: Possible oxidation products of 3OHKyn: xanthommatin (1), dihydroxanthommatin (2), 4,6-dihydroxyquinolinequinone carboxylic acid (3), and benzoxazole (4) and benzimidazole (5) adducts. R = amino acid or peptide.

The other non-disulfide cross-links so far identified are known to be AGE products, the majority of which are formed *via* Lys and Arg residues. These include pentosidine, vesperlysine, MOLD/GOLD, K2P, oxalate monoalkylamide and glucosepane (Figure 1.6, Section 1.5.4.2.2).[156,159,167,168,170,171,173] Significantly higher levels of these AGE products have been detected in cataractous lenses and water-insoluble proteins, as compared to water-soluble proteins.[148,159,172,173,216]

1.6.2 Possible factors in cataract formation

From the above discussion, it is clear that oxidation of lens proteins takes place during cataract formation. Oxidising agents capable of modifying proteins can originate from many sources, both endogenous (*e.g.* inflammation, enzymatic processes, electron transport chains [*e.g.* mitochondria and cytochrome P_{450} system]) and exogenous (*e.g.* nutritional deficiency, air pollutants, UV light, ionising radiation and tobacco smoke).[3,217-220] In this study, the significance of UV light and reactive oxygen species in lens protein modifications, and their relevance to ARN cataract, was investigated.

1.6.2.1 UV light and ARN cataract

UV light has been suspected for many years to be a factor involved in the development of cataract.[221-224] Since the biological effects of UV light vary significantly with wavelength, UV light has been divided into UVC (< 280 nm), UVB (280-320 nm) and UVA (320-400 nm).[225] UVC light does not reach the earth as it is absorbed by O_3 and O_2 (for wavelengths < 280 nm and < 240 nm, respectively), while UVA and UVB wavebands can reach the Earth's surface.[31] The human cornea absorbs wavelengths below 300 nm and hence these wavelengths are not transmitted to the lens and retina. The lens absorbs strongly in the 300-400 nm region, protecting the retina from photochemical damage and possibly enhancing contrast sensitivity and reducing chromatic aberration (Figure 1.10).[79,89,225]

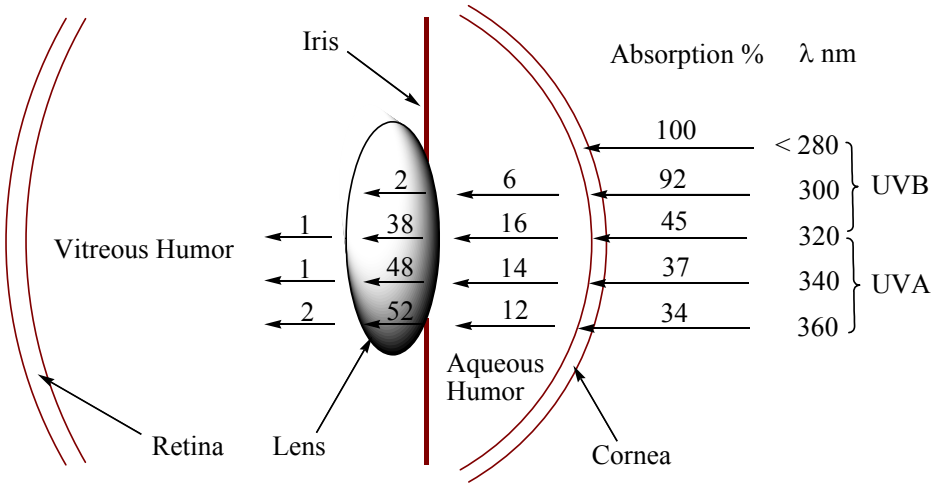

Figure 1.10: Diagram of the eye illustrating the wavelengths of light that are transmitted and absorbed by the human eye (adapted with modifications from Sliney[226]).

UVA light is known to play a role in photochemically-induced damage of cells, not by directly damaging DNA, peptides, lipids, sugars and vitamins as do the shorter wavelengths (UVB), but by generation of photoproducts.[227-229] Several detailed analyses of UV-related cataract epidemiology, link UV exposure with cortical and possibly with posterior-subcapsular cataract.[2,230-232] Recently, a correlation between occupational sun exposure and nuclear cataract has also been shown.[233]

1.6.2.2 Lens photosensitisers

UV light above 300 nm is nearly totally absorbed by the chromophores of the human lens, such as aromatic groups of freely diffusible small molecules (*e.g.* UV filters) and proteins.

UV light induced photo-oxidative damage of lens constituents (*e.g.* proteins) can take place either through the direct absorption of radiation by that molecule (Type I photochemistry) or though an indirect process involving a photosensitiser (Type II photochemistry).[165]

In the direct route, light (< 300 nm) is absorbed predominantly by the aromatic amino acids Trp and Tyr.[234] This photochemically initiated process activates, for example, Trp to produce *N*-formyl-L-kynurenine, kynurenic acid, β-carbolines, anthranilic acid, xanthurenic acid and other photoproducts and their derivatives, which are known to accumulate in the nucleus of cataractous lenses.[3,198,235-241] Furthermore, *N*-formyl-L-kynurenine, kynurenic acid and xanthurenic acid are believed to be involved in $^1O_2$ generation.[3,242-244] Since the cornea would normally filter out most of the light below 300 nm, very little light of this wavelength would reach the lens. This makes it unlikely that the accumulation of modified proteins in the nucleus of the lens is due to direct photo-oxidation of nuclear proteins.

A more likely route of protein modification would be through a photosensitiser involving UV light in the region of 300-450 nm. A photosensitiser is a chromophore that absorbs light in the selected region, forming an excited state species, which can then transfer energy to another species such as ground state molecular oxygen to give $^1O_2$. $^1O_2$ may then induce biological damage.[31,245]

When free in solution, Kyn, 3OHKyn and 3OHKG are inefficient sensitisers of oxidative damage,[79,89,237,246,247] however this may not be the case in the protein bound state. In an early study by van Heyningen,[248] it was demonstrated that exposure of lens proteins to UV light in the presence of lens fluorescent compounds (Kyn derivatives) resulted in coloured and oxidised proteins, primarily at Tyr residues, that were resistant to proteolytic digestion compared to proteins exposed to UV light in the absence of the additives. The author hypothesised the products of Kyn may be binding to lens proteins and causing photo-oxidative damage.[248] This was also supported by the subsequent findings that illuminated (> 295 nm) solutions of 3OHKyn did not result in formation of fluorescent products, while illumination of 3OHKyn in the presence of Gly (used to mimic the environment of the lens) generated blue and green fluorophores.[249] The formation of these fluorophores was greatly reduced in the presence of penicillamine, a free radical scavenger.[249] The authors suggested that both fluorophores resulted from the photochemically induced covalent attachment of 3OHKyn to Gly. In the human lens, these reactions can explain the age-related loss of UV

filters with the concomitant formation of fluorophores covalently attached to lens proteins.[249,250]

More recently, Parker *et al.*[247] have shown that covalent binding of Kyn to lens proteins *in vitro,* followed by exposure to UV light (> 305 nm), results in the generation of H_2O_2 and low concentrations of protein peroxides. It has been previously shown *in vitro* that H_2O_2 can oxidise amino acid residues on proteins, particular at Cys, Met, Trp and Tyr residues, resulting in lens opacification, accumulation of mixed disulfides, changes in electrolyte balance and protein insolubilisation.[251-255] The pattern of protein damage was comparable to that found in human cataract.[251] Furthermore, in the same study of Parker *et al.*,[247] protein-bound Tyr residues were oxidised to di-tyrosine (di-Tyr) and 3,4-dihydroxyphenylalanine (DOPA) upon exposure of Kyn-modified lens proteins to UV light (> 305 nm). This hydroxylation of Tyr and phenylalanine (Phe) residues in proteins has been previously shown to increase with severity of nuclear cataract.[256] A separate study has shown that 3OHKyn can generate $O_2^{\cdot-}$ and H_2O_2 in the presence of Cu^{2+} and promote cross-linking of α-crystallins.[257]

The UVA sensitiser activity is primarily located in the human lens water insoluble fraction.[162-164,166] Assays of this fraction *in vitro* have shown the generation of 1.0 μmol h^{-1} mg $protein^{-1}$ $^1O_2$ ($k \sim 1\text{-}3 \times 10^9$ dm^3 mol^{-1} s^{-2})[164] and 35 nmol h^{-1} mg $protein^{-1}$ $O_2^{\cdot-}$ ($k \leq 1 \times 10^7$ dm^3 mol^{-1} s^{-1})[162] in response to 250 J cm^{-2} of absorbed light, which is equivalent to 5-6 months of exposure to bright sunlight for 2 h each day at noon. H_2O_2 has also been detected on exposure to high doses of UVA (1.5 kJ cm^{-2}).[258,259]

The generation of photoproducts upon exposure to UV light can also be attributed to endogenous ascorbate-mediated Maillard reaction products (discussed in section 1.5.4.2.2).[157,235] The photochemistry of glycated lens proteins has been studied extensively by B. Ortwerth's group. The ascorbylation of lens proteins *in vitro* results in highly cross-linked and fluorescent proteins that upon exposure to UVA light generate of $O_2^{\cdot-}$, H_2O_2 and $^1O_2$, with the last of these being the dominant species produced. This suggests Type II photochemistry.[109,162,164]

Overall, photosensitiser-mediated reactions appear to play an important role in lens photochemistry and possibly cataract formation. The evidence in support of this is substantial, but not conclusive. Further details on this will be discussed in this thesis.

1.7 Aims

1.7.1 General aims

The human lens UV filters (*e.g.* Kyn, 3OHKyn and 3OHKG) are capable of protecting lens proteins from damage when they are free in solution. However, they are intrinsically unstable and can covalently bind to lens proteins. Their binding to the lens proteins appears to be a significant factor in the changes that occur upon lens aging and in the formation of ARN cataract. With the recent finding that protein-bound Kyn samples upon exposure to UV light generate reactive oxygen species and protein damage,[247] the investigation of the binding of 3OHKG, the major UV filter, to lens proteins, and the effect of UV light on proteins modified with 3OHKG and 3OHKyn, were major aims of this study. Given the importance of UV filters in human lens chemistry, and the likelihood lenses still contain a number of unidentified UV filters, an additional aim was to identify novel human lens metabolites and examine their reactivity.

1.7.2 Specific aims

1. To synthesise the non-commercially available 3OHKG, for subsequent protein binding studies, by a synthetic route that would also allow facile entry to other UV filters (Chapter 2 and 3)

2. To identify and quantify novel human lens metabolites using a combination of isolation from human lenses, total synthesis and spectral analysis (Chapter 4)

3. To investigate the abilities of UV filters and their metabolites to bind to lens proteins and to physically characterise UV filter-bound lens proteins (Chapter 5)

4. To investigate the effect of UV light on the UV filter-modified lens proteins (Chapter 6)

CHAPTER 2

A CONVENIENT SYNTHESIS OF 3OHKG

The overall aim of this chapter was to synthesise 3-hydroxykynurenine-*O*-β-D-glucoside (3OHKG) in sufficient quantity for protein binding studies (Chapter 5). An additional aim was to ensure that the synthetic method allowed facile entry to other human lens UV filters, such as 3-hydroxykynurenine (3OHKyn) and 4-(2-amino-3-hydroxyphenyl)-4-oxobutanoic acid-*O*-β-D-glucoside (AHBG) (Chapter 3), using inexpensive precursors and a green chemistry approach where possible.

2.1 Introduction

Three methods have been reported for the synthesis of 3OHKG,[260-262] however a cost effective, safe and high yielding method that can allow for the synthesis of a wide range of UV filters would be ideal.

Heckathorn *et al.*[260] and Real and Ferré[261] reported similar syntheses of 3OHKG by glucosylation of the commercially available, but expensive (AU$103/25 mg), 3OHKyn, with 2,3,4,6-tetra-*O*-acetyl-α-D-glucopyranosyl bromide (ABG) under basic conditions (Scheme 2.1). The acetylated 3OHKG (6), produced in 25-30% yield,[260] was subsequently deprotected by alkaline hydrolysis to yield 3OHKG in unreported yields. While these are short syntheses, they are inflexible and do not allow entry to a range of other UV filter compounds.

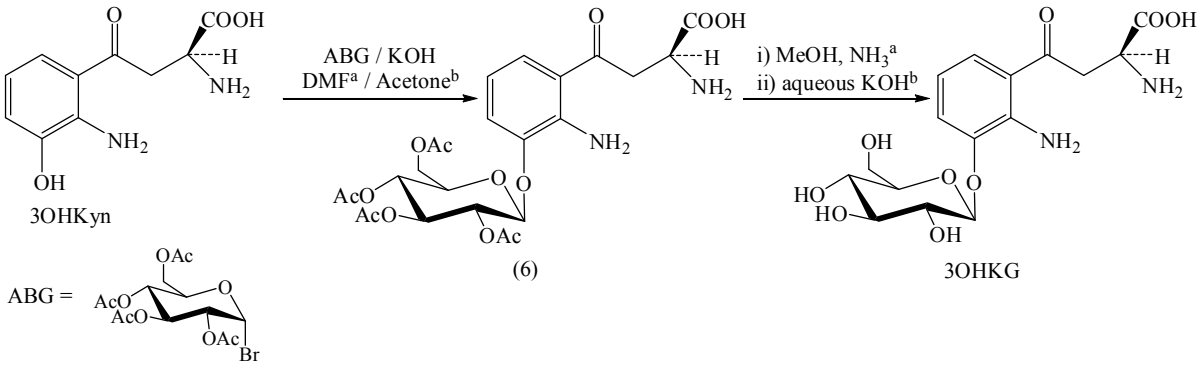

Scheme 2.1: Synthesis of 3OHKG from 3OHKyn by [a] Heckathorn *et al.*[260] and [b] Real and Ferré.[261]

Manthey *et al.*[262] reported the synthesis of 3OHKG from the acrylic acid (7) (Scheme 2.2). This was obtained from the commercially inexpensive starting material 3-hydroxyacetophenone (8), *via* nitration to 3-hydroxy-2-nitroacetophenone (9) and subsequent aldol condensation with barium glyoxylate under acidic conditions.[263] After methylation of the acrylic acid (7) to give the methyl ester (10) (45%), the phenolic group was reacted with ABG in the presence of $Hg(CN)_2$ and K_2CO_3 to yield the methyl ester glucoside (11) in 61% yield. Treatment of the methyl ester glucoside (11) in aqueous NH_3, followed by hydrogenation and alkaline hydrolysis gave 3OHKG in 13.2% yield from the acrylic acid (7).

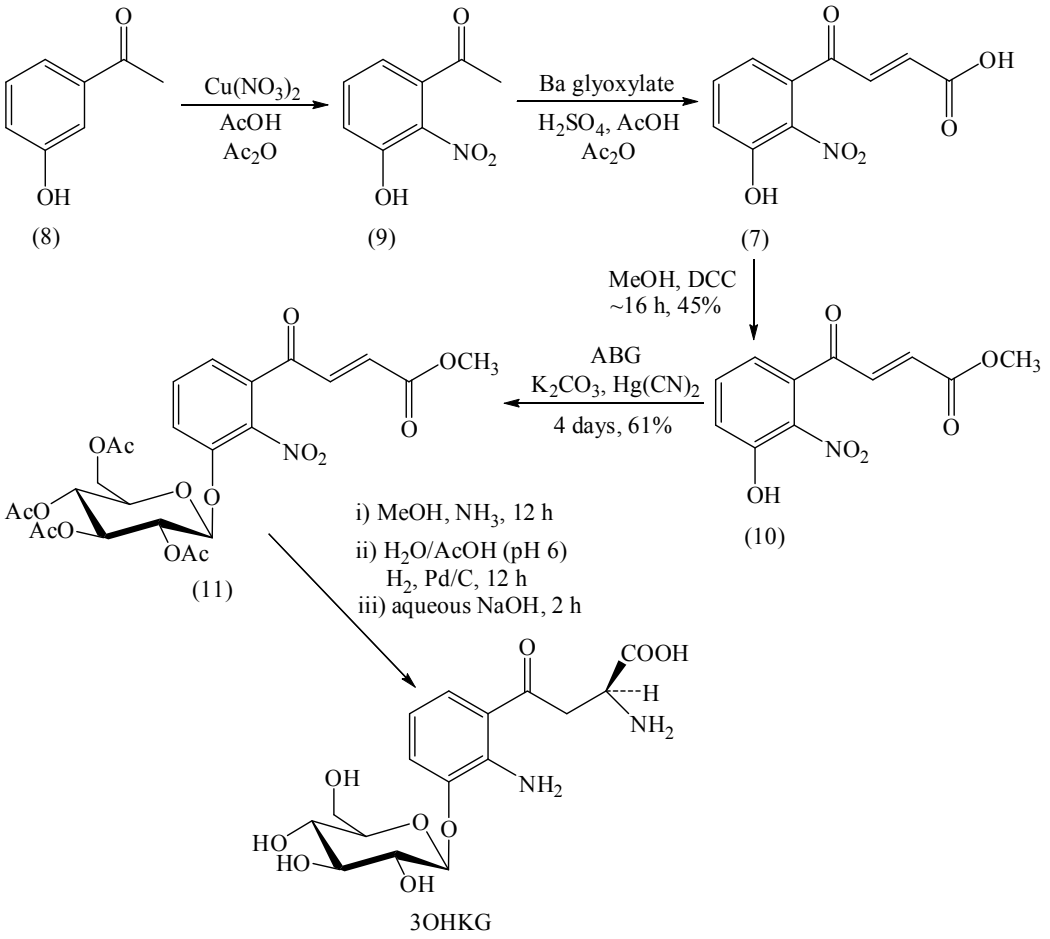

Scheme 2.2: Synthesis of 3OHKG by Manthey *et al.*[262]

In this study, the synthesis of 3OHKG from 3-hydroxyacetophenone (8), using Manthey *et al.'s* method,[262] was chosen due to the acrylic acid (7) also allowing entry to a range of other UV filter compounds (Chapters 3 and 4). However, as some of the original conditions for the synthesis of the acrylic acid (7) and subsequent steps to form 3OHKG used hazardous reagents and were time consuming, this study also investigated methods to make the synthesis less hazardous and more efficient.

2.2 Results and Discussion

2.2.1 Synthesis of 3-hydroxy-2-nitroacetophenone (9)

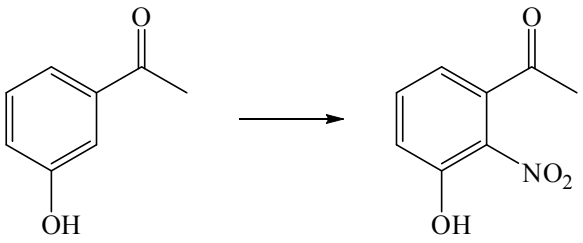

(8) (9)

The nitration of 3-hydroxyacetophenone (8) to afford 3-hydroxy-2-nitroacetophenone (9) has been reported by Butenandt *et al.*,[263] using copper nitrate in the presence of acetic anhydride and AcOH. This is an effective reagent mixture for nitration of aromatic compounds, under what is known as the "Menke conditions".[264,265] The proposed mechanism involves formation of acetyl nitrate followed by electrophilic aromatic substitution (Scheme 2.3).[266,267] Kluge *et al.*[268] and Butenandt *et al.*[263] also reported the synthesis of 3-hydroxy-2-nitroacetophenone (9) by employing a mixture of concentrated HNO_3 and H_2SO_4. The "Menke condition" was chosen for these studies as it offered milder conditions compared to the Kluge *et al.'s* method.[268]

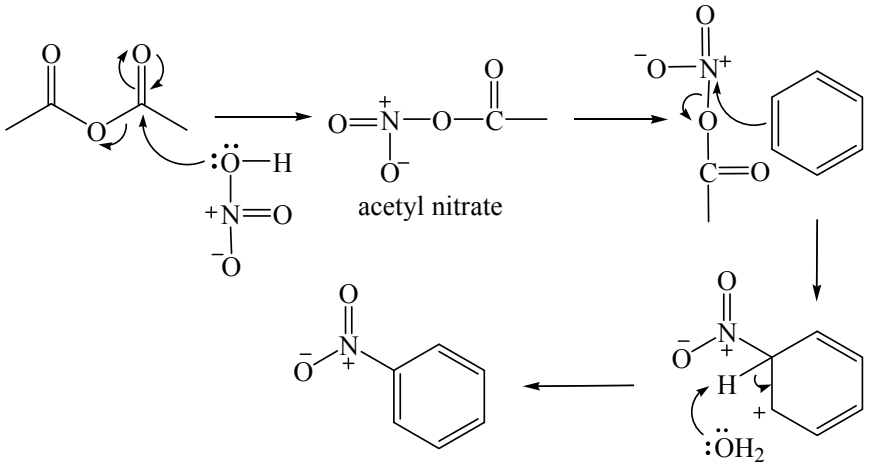

Scheme 2.3: The mechanism of electrophilic nitration of an aromatic ring by "Menke conditions".[266,267]

Following the reaction conditions of Butenandt *et al.*,[263] 3-hydroxyacetophenone (8) was dissolved in glacial AcOH and acetic anhydride. The reaction was cooled to 10-15°C and ~1.2 mol equivalents of copper nitrate hemi(pentahydrate) ($Cu(NO_3)_2 \cdot 2.5H_2O$) were added over 3 h. After an additional 5 h of stirring at 10-15°C, the green suspension, which still showed starting material by TLC, was placed in the fridge overnight. The next day, the mixture was warmed to 10-15°C and the reaction was continued following the addition of ~0.6 mol equivalents of $Cu(NO_3)_2 \cdot 2.5H_2O$. After 8 h, the green suspension was worked up by precipitation of the desired material and extraction of the filtrate. Apart from the desired 2-nitro compound (9), TLC showed the 4- (12) and 6-nitro (13) products, as expected due to the strong *o*,*p*-directing and activating phenolic group (Figure 2.1). By TLC, the 4-nitro product appeared to be produced in the highest yield, while the 2-nitro product was produced in the lowest yield, presumably due to steric hindrance. Due to the strong deactivating effect of the nitro group and low reaction temperature, dinitration was not observed in this study.

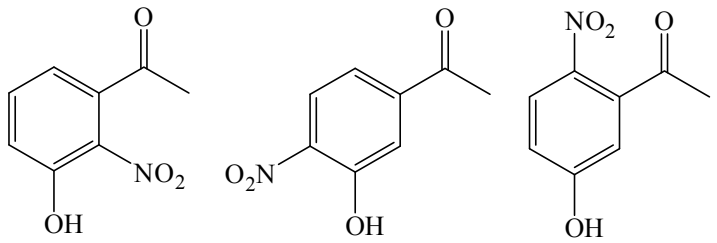

(9) (12) (13)

Figure 2.1: The products seen upon nitration of 3-hydroxyacetophenone by "Menke conditions": 3-hydroxy-2-nitroacetophenone (9); 3-hydroxy-4-nitroacetophenone (12); 3-hydroxy-6-nitroacetophenone (13).

3-Hydroxy-2-nitroacetophenone (9) was successfully purified by two successive normal phase column chromatography steps, with DCM and 5:1 toluene/EtOAc (v/v), respectively, instead of using the time consuming and hazardous benzene recrystallisation reported in the literature.[263] Column chromatography eluting with DCM allowed partial elimination of the 6-nitro (13) product (R_f 0.79) and total elimination of the 4-nitro (12) product (R_f 0.09), while elution with 5:1 toluene/EtOAc (v/v) allowed further purification of the 2-nitro (9) (R_f 0.36) from the 6-nitro (R_f 0.57) product. This gave 3-hydroxy-2-nitroacetophenone as a yellow solid in 25% yield, compared to the 18% yield described in the literature.[263] The low yields of 3-hydroxy-2-nitroacetophenone compared to the other two isomers can not be substantially altered due to the directing and steric effects present in the aromatic system. The sharp melting point at 138°C (lit. 134-136°C[268] and 138°C[263]) and ^{1}H NMR spectral analysis indicated that the product was pure. ^{1}H NMR showed three doublets of doublets at δ 7.59 (*J*

7.3, 8.5), δ 7.23 (*J* 1.2, 8.5) and δ 6.85 (*J* 1.2, 7.3), due to the aromatic protons at ArH-5, ArH-6 and ArH-4, respectively, and one singlet at δ 2.50 due to the methyl group.

2.2.2 Synthesis of 4-(3-hydroxy-2-nitrophenyl)-4-oxobut-2-enoic acid (7)

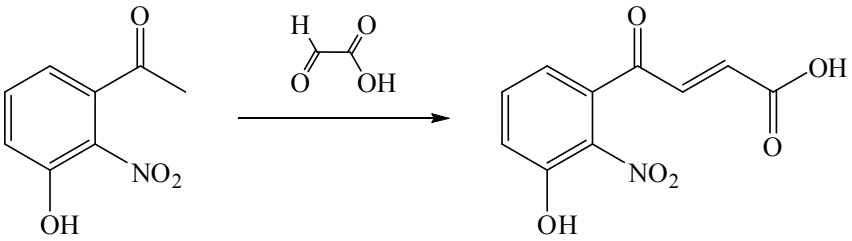

(9) (7)

Butenandt *et al.*[263] have reported the synthesis of the acrylic acid (7) using 9.5 mol equivalents of barium glyoxylate in H_2SO_4, AcOH and acetic anhydride (to remove any excess of water as a by-product of the reaction) at 68-70°C. This gave the acrylic acid in 62% yield after 3 days of reaction. The repetition of this procedure by previous members of our group gave the acid in varying and often low yields. Work up was difficult due to the thick consistency of the reaction mixture and the reaction was also found to be very unreliable. An increase in reaction temperature of around 5°C led to virtually no product and little recovery of the starting material.

A previous member of our group (D. Kalinowski[269]) investigated other procedures, including that of Szoke *et al.*,[270] which has been reported for the condensation of glyoxylic acid with related ketones (*e.g.* 4-hydroxy-3-nitroacetophenone). This procedure involved the heating of the ketone with 1 mol equivalent of glyoxylic acid monohydrate in H_3PO_4 for 2 days to give the desired enone in ~51% yield. The method was trialled for the synthesis of the acrylic acid (7), however it did not seem to be promising, as the reaction could not be pushed to completion even after the addition of 4 mol equivalents of glyoxylic acid monohydrate. The reaction mixture turned black and a dark baseline material was observed by TLC, possibly due to decomposition of the starting material or product under the acidic conditions. Another method was reported for the synthesis of the related enones (*e.g.* synthesis of 4-(3,5-dichloro-4-methylphenyl)-4-oxobutenoic acid from 1-(3,5-dichloro-4-methylphenyl)ethanone) using acetic anhydride, AcOH, H_2SO_4 and 1 mol equivalent of glyoxylic acid.[271] This method was investigated by D. Kalinowski with different mol equivalents of glyoxylic acid monohydrate (1, 2 and 4.5).[269] This method yielded a brown reaction mixture with the desired product in

only 19% yield with 4.5 mol equivalents of glyoxylic acid monohydrate. Slightly lower yields were obtained with 1 and 2 mol equivalents of glyoxylic acid monohydrate.[269]

The solvent-free aldol condensation reactions of aromatic aldehydes (*e.g.* *p*-methylbenzaldehyde) and aromatic ketones (*e.g.* acetophenone) have been investigated by grinding of reactants in the presence of NaOH as a base catalyst.[272-275] Raston *et al.*[273] reported highly chemoselective aldol condensation reactions that proved to be high yielding and produced only small quantities of acidic aqueous waste. For example, the reaction between 3,4-dimethoxybenzaldehyde and 2,3-dihydroinden-1-one in the presence of 1 mol equivalent of NaOH resulted in the desired enone in 77% yield. Repetition of this procedure by D. Kalinowski proved to be unsuccessful for the synthesis of the acrylic acid (7), however 40% yield was obtained for the aldol product with 3-hydroxyacetophenone (8) as the starting material.[269] It was suggested that the lower reactivity of 3-hydroxy-2-nitroacetophenone (9) might be due to the electron withdrawing 2-nitro group pulling electron density away from the carbonyl and hence reducing the reactivity of this moiety.

Bianchi *et al.*[276] have reported the synthesis of 4-(2,3-dimethoxyphenyl)-4-oxo-2-butenoic acid in 22% yield by melting 1 mol equivalent of glyoxylic acid monohydrate with 2,6-dimethoxyacetophenone at 120°C and ~20 mm Hg (to remove the water produced). This procedure was examined in detail by D. Kalinowski and it was found to be optimised by the use of 10 mol equivalents of glyoxylic acid monohydrate, yielding a mixture of the desired acrylic acid (7), the aldol (14) and the ester (15) in ~5 : 1 : < 1 ratio (Scheme 2.4).[269]

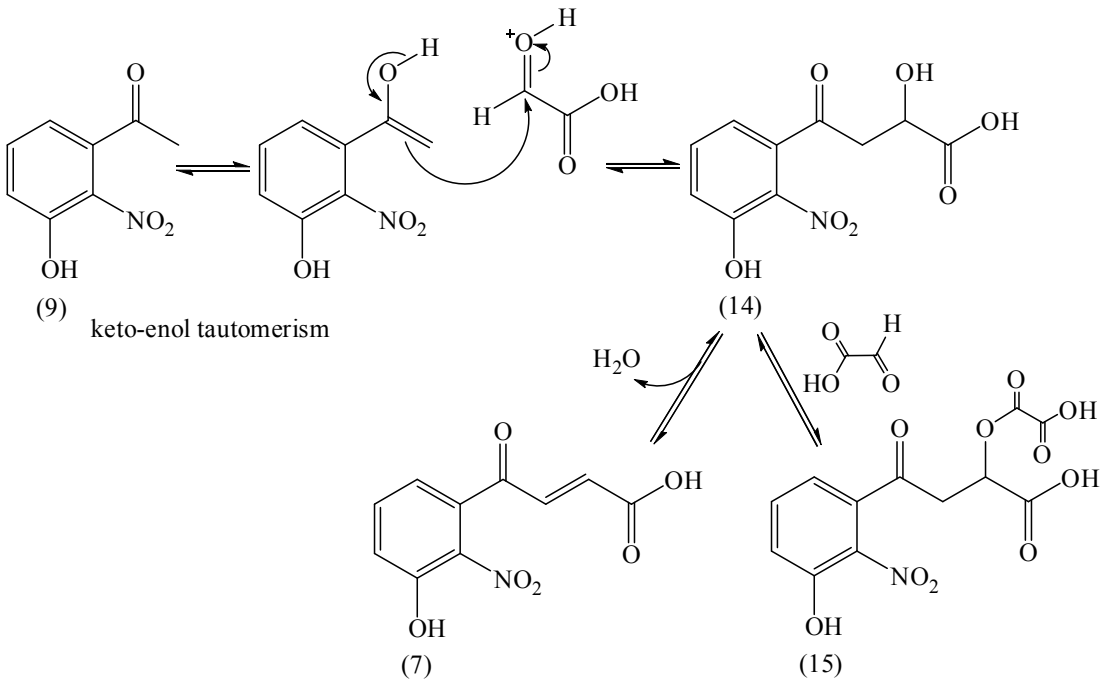

Scheme 2.4: Synthetic pathway towards the aldol (14), the acrylic acid (7) and the ester (15).

2.2.2.1 Method 1 and 2

Initially in this study, the optimised method of Bianchi *et al.*[276] from D. Kalinowski was the preferred method for the synthesis of the acrylic acid (7). 3-Hydroxy-2-nitroacetophenone (mp 138°C) was combined with melted glyoxylic acid monohydrate (~10 mol equivalents, mp 49-52°C, bp 100°C) at 60°C and the reaction temperature was increased to 120°C. In addition to a brown baseline spot, after 7 h, TLC revealed the presence of the acrylic acid (7), based on comparison with an authentic sample. Subsequent additions of glyoxylic acid monohydrate (~1 mol equivalent) over the course of the reaction (after 7 and 14 h) proved to be essential for the complete formation of the product. This was not surprising as glyoxylic acid monohydrate boils at 100°C at atmospheric pressure so some losses were expected due to evaporation. It was also found to slowly decompose at 120°C under vacuum, yielding a brown baseline spot on TLC. The desired acrylic acid (7) was the major compound observed after 24 h of reaction. In addition, the aldol (14) and the ester (15) products were found in trace quantities. This presumably occurred due to the high mol equivalents of glyoxylic acid monohydrate in the reaction.

To isolate the product, the reaction mixture was cooled to RT, dissolved in brine, extracted with DCM and purified by normal phase column chromatography. The poor solubility of the thick and sticky reaction mixture required a considerable amount of solvent to be used

(Method 1). The difficulty in handling the sticky mixture may be the reason for the moderate yields of the desired material (~42%). Thus, in subsequent experiments the hot reaction mixture was adsorbed onto normal phase silica, followed by column chromatography purification. This resulted in the elimination of time consuming extraction step and gave an improved yield of 55% (Method 2). The melting point of 157-159°C (lit.[263] 158°C) indicated that the acrylic acid (7) was obtained in high purity. The ^{1}H NMR spectrum showed a distinct *trans*-configuration of the side chain protons with a coupling constant of 16.2 Hz (2H). ES-MS displayed a molecular ion at *m/z* 238 ($M+H^{+}$), which is consistent with the expected mass of 237 Da.

2.2.2.2 Method 3

In order to optimise the reaction yield further, the application of microwave chemistry was investigated for the synthesis of the acrylic acid (7). In recent years, microwave-assisted chemical reactions have attracted great interest because of the simplicity of the process, enhanced reaction rates and greater selectivity.[277,278] Microwave chemistry not only offers substantial improvement in yields over conventional heating but can be conducted under solvent-free conditions, eliminating the use of hazardous solvents. The success of microwave synthesis is due to rapid conversion of microwave energy into thermal energy. This is dependent on physical constants (*e.g.* dielectric loss [the amount of microwave energy that is lost to the sample by being dissipated as heat]) of the reagents used. The high absorbing solvents are those that have dielectric loss greater than 14, for example small chain alcohols, dimethyl sulfoxide and formic acid.[278]

The application of microwave chemistry in aldol condensation reactions has been reported.[273,279-281] In this study, both solids, 3-hydroxy-2-nitroacetophenone (9) (mp 138°C) and glyoxylic acid monohydrate (~11 mol equivalents, mp 49-52°C, bp 100°C) were mixed and placed into the cavity of a focused microwave reactor (CEM Discover) at 110°C. It was anticipated that the acidity provided by glyoxylic acid monohydrate would be sufficient to catalyse the dehydration of the aldol intermediate (14) to yield the acrylic acid (7). Due to the obvious decomposition of glyoxylic acid monohydrate, as seen by the generation of the brown baseline material on TLC in a control reaction, two separate additions of ~1.2 mol equivalents each of this reactant were made after 6 and 12 h. The temperature was maintained at 110 ± 1°C and a power of ~50 W was employed during the reaction (Figure 2.2). The pressure was

kept to a minimum (< 5 psi). The reaction was carried out for 17 min. The brown reaction mixture was adsorbed onto normal phase silica and purified by normal phase column chromatography to give the acrylic acid (7) in 60% yield. The reaction side products, the aldol (14) and the ester (15) were not observed by TLC.

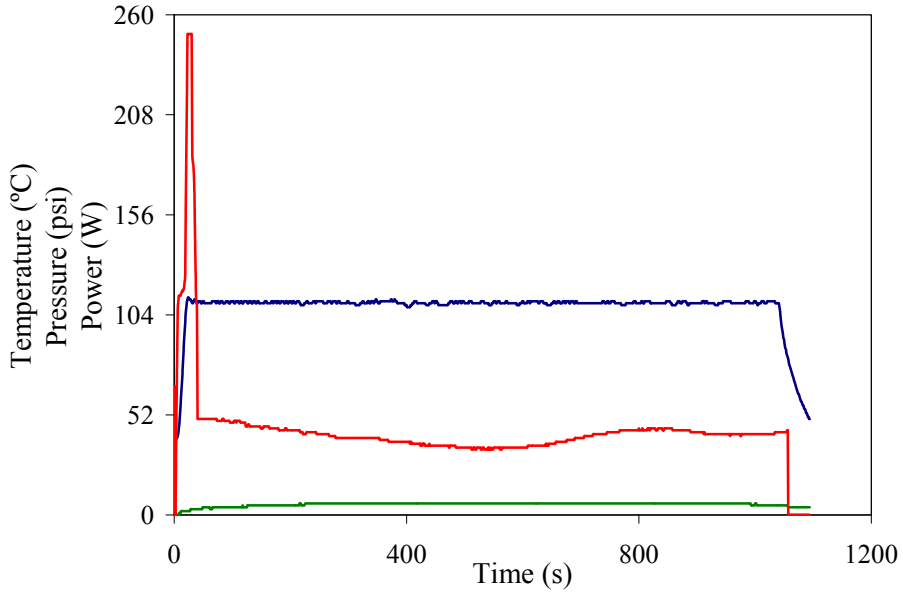

Figure 2.2: Temperature (blue), pressure (green) and power (red) measurements during the synthesis of the acrylic acid (7) in the cavity of a focused microwave reactor (CEM Discover) at 110°C.

As a result of this study, the acrylic acid (7) was synthesised with an improved reaction time, from 24 h to 17 min, and reaction yield, from 42% to 60% in comparison to the previous methods investigated by our group. This was achieved by the use of solvent-free conditions, elimination of the extraction step prior to column chromatography purification and application of the microwave technology.

2.2.3 Synthesis of methyl 4-(3-hydroxy-2-nitrophenyl)-4-oxobut-2-enoate (10)

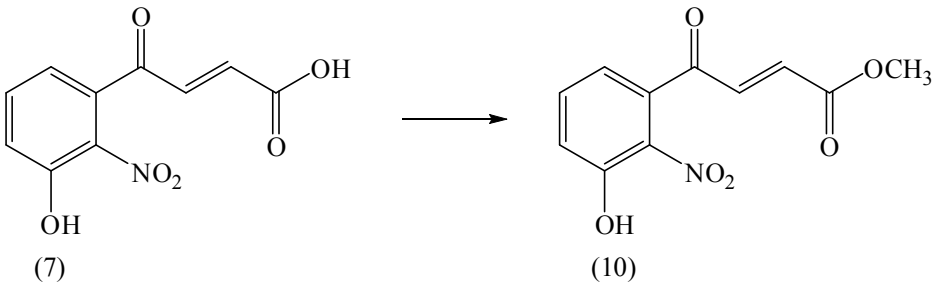

In the method of Manthey *et al.*,[262] the acrylic acid (7) was methylated to protect the carboxylic acid group from glucosylation in the subsequent step. The acrylic acid (7) was

treated with an excess of MeOH in the presence of *N*,*N'*-dicyclohexylcarbodiimide (DCC) to afford the methyl ester (10) in 45% yield after ~16 h. In this study, the methylation of the acrylic acid (7) was conducted in dry MeOH and H_2SO_4 as a catalyst.[282]

2.2.3.1 Method 1 and 2

Initially, different temperature conditions were investigated. The small scale reactions (18-23 mg) were heated to reflux (Method 1, Trial 1) or stirred at RT (Method 1, Trial 2). The progress of the reactions was monitored by TLC. Under both conditions, TLC indicated the formation of two spots, ~10:0.5. After 1.5 h for the reflux conditions and after 8 h for the RT conditions, TLC indicated disappearance of the starting material. The yellow solutions were evaporated under reduced pressure. The yellow solids were redissolved in DCM and dried with $MgSO_4$ to remove the traces of H_2SO_4. The crude products were purified by normal phase column chromatography to yield the methyl ester (10) in similar yields for both conditions (72-78%) along with the methoxy methyl ester (16) in trace quantities. The methoxy methyl ester (16) was formed due to addition of MeOH across the double bond of the acrylic acid (7) (Scheme 2.5). Even though both conditions gave the methyl ester (10) in similar yields, reaction at higher temperature reduced the reaction time by ~5 times compared to the RT conditions.

The bright yellow methyl ester (10) was found to be pure with a melting point of 110-112°C (lit.[262] 111-112°C). The ^{1}H NMR spectrum showed the methyl ester moiety as a single peak at δ 3.8 with an integration of 3H. ES-MS (negative mode) displayed a molecular ion at *m/z* 250 ($M\text{-}H^+$), which is consistent with the expected mass of 251 Da.

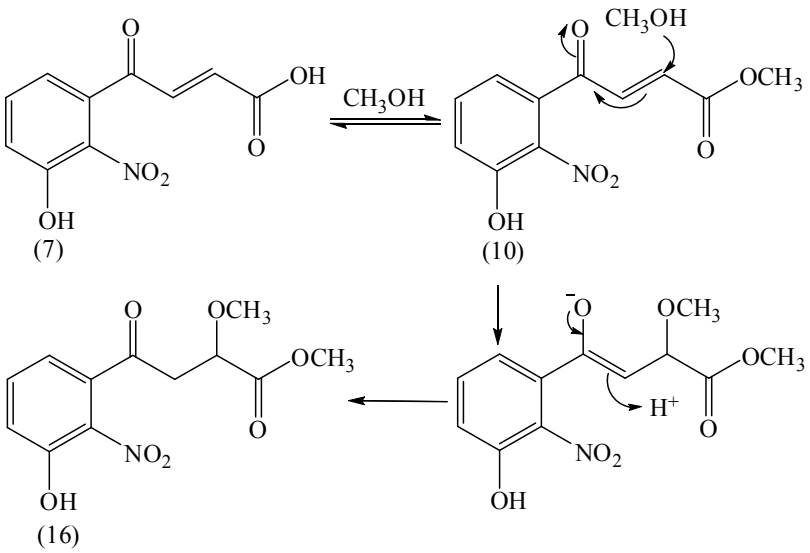

Scheme 2.5: Formation of the methoxy methyl ester (16) *via* Michael addition of MeOH.

Subsequent methylation of the acrylic acid (7) on a larger scale (1.7 g) was carried out under reflux conditions. After 6 h, the reaction mixture was worked up and purified as described above to yield 90% of the methyl ester (10). Upon normal phase column chromatography, the fractions containing a mixture of the methyl ester (10) and methoxy methyl ester (16) were combined (156 mg) and subsequently treated with dry toluene and H_2SO_4 to convert the methoxy methyl ester to the desired methyl ester (Method 2) (Scheme 2.6).[283] This method has been successfully used by Hermanson *et al.*[283] for the demethanolysis of methyl 2-carbomethoxy-3-methoxy-4-oxooctanoate. The reflux conditions, followed by overnight stirring at RT, were the preferred demethylation conditions in the literature.[283] Repetition of the literature procedure resulted in the formation of an additional unknown compound of very similar R_f to the desired material, leading to difficulties in clean up and consequently lower yields of the desired product (Method 2, Trial 1). Therefore, despite taking 4 times longer, overnight demethanolysis (16 h) at RT was the condition of choice, as it gave a cleaner conversion of the methoxy methyl ester (16) to the methyl ester (10) (Method 2, Trial 2). After 16 h, the yellow solution was evaporated and purified as described above for the methyl ester (10) (Method 1). This gave the methyl ester in a combined yield of 94% from the acrylic acid (7). This was a considerable improvement to the 45% yield reported by Manthey *et al.*[262]

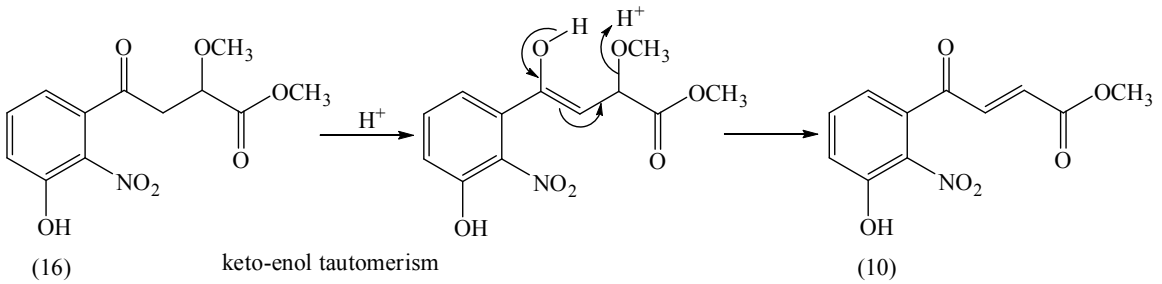

(16) keto-enol tautomerism (10)

Scheme 2.6: Mechanism for acid catalysed demethanolysis of the methoxy methyl ester (16) to the methyl ester (10).

2.2.3.2 Method 3

Due to the presence of the methoxy methyl ester (16) in the above described methylation method (Method 1), the methylation of the acrylic acid (7) was also investigated using diazomethane. Diazomethane methylation is known to be a fast, high yielding reaction with minimal side products. The by-product is nitrogen gas and the reaction conditions are very mild. Diazomethane is known to typically methylate carboxylic acids in a facile manner (Scheme 2.7).[284,285] Methylation using diazomethane of phenols has also been reported, however this occurs typically at a much slower rate than for carboxylic acids.[284,286,287] Therefore, it was believed that methylation of the acrylic acid (7) would be selective for the carboxylic acid moiety.

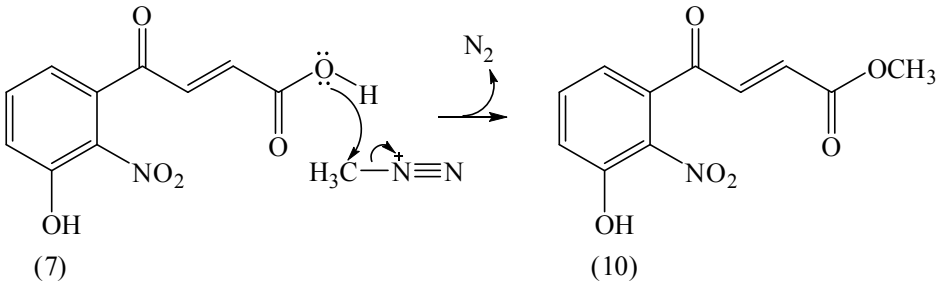

(7) (10)

Scheme 2.7: The mechanism for methylation of the carboxylic acid of the acrylic acid (7) using diazomethane.

Diazomethane was synthesised from *N*-methyl-*N*-nitrosotoluene-*p*-sulphonamine in the presence of KOH, as reported in the literature.[288] Diazomethane was collected as an ethereal solution.

Following the literature methods, the methylation was trialled in diethyl ether at -78 and ~0°C, and in MeOH at ~0°C.[284,288] Diazomethane is a yellow gas, so the completion of the reaction is usually seen once the yellow colour of the solution persists. Under all reaction conditions, TLC showed immediate methylation of the acrylic acid (7) along with generation

of five unknown spots, four of lower and one of higher R_f compared to the desired material. After 1 h, the yellow solutions were evaporated and purified as described above in Method 1. Purification resulted in the recovery of the methyl ester (10) in 41-47% yield, which was substantially lower than that for the methylation in dry MeOH and H_2SO_4 as a catalyst. Furthermore, normal phase column chromatography allowed isolation of 3 crude unknown products. While not formally identified, ^{1}H NMR for each compound showed a singlet at δ ~3.8, consistent with a methoxy group, however, the double bond protons were not detected. This suggests that diazomethane reacted with the double bond. Similar results have been reported for polyunsaturated fatty acids by addition of carbene, formed from diazomethane, to the double bonds.[289,290] Ketones are also known to form undesirable "artifacts" with diazomethane by insertion of methylene to yield epoxides, however this reaction occurs at a much slower rate compared to the conversion of carboxylic acids to methyl esters.[291] Decrease in product yields may also be due to the slow methylation of phenols with diazomethane yielding methyl ethers.[287,292] Careful literature searches suggested that methylation of phenols with diazomethane can be expected in greater quantities if an electron-withdrawing group is present *ortho* to the phenol,[285] such as in the case of the acrylic acid (7).

2.2.3.3 Method 4

In order to simplify the conversion of 3-hydroxy-2-nitroacetophenone (9) to the methyl ester (10), a direct methylation of the acrylic acid (7) obtained from the glyoxylic acid condensation reaction (Section 2.2.2.1), *i.e.* without chromatographic purification, was investigated. Initially, 20 mg of 3-hydroxy-2-nitroacetophenone was condensed with glyoxylic acid monohydrate, as described previously. After 24 h, the brown viscous reaction mixture was cooled to RT and dissolved in dry MeOH and H_2SO_4 as a catalyst. The reaction mixture was fitted with a $CaCl_2$ drying tube and heated to reflux. The progress of the reaction was monitored by normal phase TLC. It revealed formation of the methyl ester (10) as the major product, trace quantities of the methoxy methyl ester (16), a brown baseline spot possibly due to decomposition of glyoxylic acid and at least 2 unknown products. After 3 h, TLC showed the absence of the acrylic acid (7) and the brown solution was evaporated and purified as described above in Method 1. This resulted in 48% yield of the methyl ester (10) from 3-hydroxy-2-nitroacetophenone (9). Scale up to 300 mg of 3-hydroxy-2-nitroacetophenone resulted in 28% yield of the methyl ester from 3-hydroxy-2-nitroacetophenone. The low recovery of the methyl ester (10), compared to the stepwise condensation and methylation reactions (~54%), was partly due to difficulties in handling the very brown and sticky reaction mixture. As a result, two successive normal phase column

chromatography purification steps had to be used, which possibly contributed to a further loss of the desired product.

Thus, the methylation of the purified acrylic acid (7) in refluxing dry MeOH and H_2SO_4 was the preferred method for the synthesis of the methyl ester (10), as it was completed in < 6 h in good yields (~90%). The side product, the methoxy methyl ester (16), was observed in minimal amounts and it was easily demethylated to the desired product. Improvement in the reaction time and product yields was achieved by this study compared to the literature (45% in ~16 h).[262]

2.2.4 Synthesis of ethyl 4-(3-hydroxy-2-nitrophenyl)-4-oxobut-2-enoate (17)

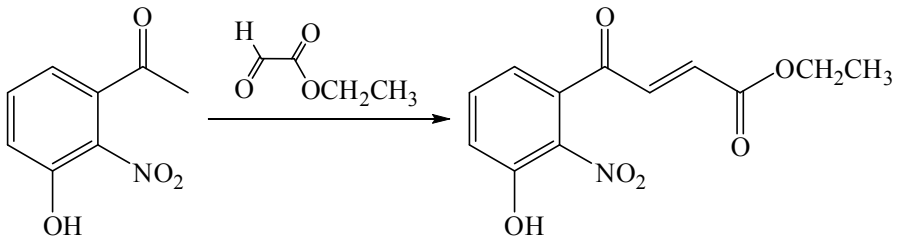

(9) (17)

In order to reduce the number of synthetic steps in the pathway towards 3OHKG, direct condensation of ethyl glyoxylate with 3-hydroxy-2-nitroacetophenone (9) was examined for the synthesis of the ethyl ester (17). The ethyl ester was chosen as the target simply because ethyl glyoxylate was commercially available as a 50% solution in toluene, while methyl glyoxylate was not commercially available.

Sager *et al.*[293] have reported a synthesis of (*E*)-ethyl 4-(naphthalen-2-yl)-4-oxobut-2-enoate from 1-(naphthalen-2-yl)ethanone with ethyl glyoxylate in the presence of polyphosphoric acid (PPA) as a catalyst. PPA has been used as a protic acid catalyst in alkylation, arylation, rearrangement, cyclisation, and other reactions.[294-297] PPA has a phosphorous pentoxide content of about 82-85% and is therefore used as a versatile acid dehydrating agent. Although it was reported that use of PPA, as a catalyst, gave the desired product in > 80% yield, it was impossible to recover PPA from the reaction mixture and reuse it.[294] This becomes important upon the reaction scale up. On the other hand, PPA adsorbed onto normal phase silica (PPA/SiO_2) can be easily recovered from the reaction mixture by simple filtration. PPA/SiO_2 can be readily prepared and handled compared to PPA, which is a viscous liquid at RT. Therefore, PPA/SiO_2 was chosen as a catalyst for this condensation reaction.

PPA/SiO_2 was prepared by dissolving PPA in $CHCl_3$ at 50ºC for 1 h.[294] Normal phase silica (SiO_2) was added and the suspension was stirred for an additional 1 h. The solvent was removed under reduced pressure to obtain PPA/SiO_2 as a white solid.

2.2.4.1 Method 1

3-Hydroxy-2-nitroacetophenone (9) was mixed with 4.5 mol equivalents of ethyl glyoxylate (50% solution in toluene), PPA/SiO_2 and catalytic amounts of PPA at 105°C. An additional 2 Pasteur pipette drops of PPA proved to be necessary for a faster reaction, otherwise it resulted in a significantly longer reaction time (> 18 h). After 4 and 8 h, two separate additions of ethyl glyoxylate (1 mol equivalent) were made, as an obvious brown baseline material increased in intensity on TLC suggesting decomposition of ethyl glyoxylate. A separate incubation of ethyl glyoxylate under the given reaction conditions confirmed that the brown baseline material on TLC was originating from ethyl glyoxylate. After 12 h, the brown reaction mixture was mixed with normal phase silica and cooled to RT. Purification by normal phase column chromatography afforded a bright yellow oily residue of the ethyl ester (17) in 63% yield. The oily residue solidified on standing at RT to bright yellow crystals. The ethyl ester (17) melted at 67-68°C. ^{1}H NMR showed a distinct quartet at δ 4.17 and triplet at δ 1.22 with an integration of 2H and 3H, respectively, representing the ethyl group. Other features in the ^{1}H NMR spectrum were similar to the acrylic acid (7). ES-MS displayed a molecular ion at *m/z* 264 ($M-H^+$), indicating a molecular mass of 265 Da, as expected for the ethyl ester.

2.2.4.2 Method 2

Following the success of the aldol reaction of 3-hydroxy-2-nitroacetophenone (9) and glyoxylic acid monohydrate to give the acrylic acid (7), microwave chemistry was examined for the synthesis of the ethyl ester (17). There is a range of heterogenous acidic/basic catalysts (alumina, silica gels and clays [*e.g.* montmorillonite clay]) that have been successfully used for microwave assisted condensation reactions.[280] In this study, 3-hydroxy-2-nitroacetophenone and ethyl glyoxylate (50% solution in toluene, ~4.5 mol equivalents) were mixed with PPA/SiO_2 and catalytic amounts of PPA, and placed into the cavity of a focused microwave reactor (CEM Discover) at 110°C. A controlled heating system was employed in

conjunction with the rapid cooling system, maintaining the temperature at 110 ± 1°C. A power of ~50 W was applied and the pressure was kept to a minimum (< 5 psi). After 30 and 60 min, two separate additions of ethyl glyoxylate (50% solution in toluene, 1 mol equivalent) were made, as TLC indicated the unreacted starting material, along with an obvious brown baseline spot. A baseline material increased in intensity over time, suggesting decomposition of ethyl glyoxylate. A separate incubation of ethyl glyoxylate under the given reaction conditions confirmed that the brown baseline material was decomposed ethyl glyoxylate. After normal phase column chromatography, the ethyl ester (17) was afforded as a yellow oily residue that solidified by standing at RT. Even though no improvement in the product yield was observed under the microwave conditions (58%) compared to the conventional heating method (Method 1, 63%), there was a significant reduction in the reaction time from 12 h to 130 min.

2.2.4.3 Method 3

All reactions described above were based on use of commercially available ethyl glyoxylate as a 50% solution in toluene. It is known, however, that toluene molecules, due to their low dielectric loss, couple to the applied microwave field very poorly. As a result toluene slowly converts microwave energy into thermal energy, thus the slower the reaction temperature will increase.[278] Toluene is therefore not regarded as a good solvent for use in microwave chemistry. The yields in the microwave reactions may be improved by the addition of a higher microwave absorbing solvent. Formic acid is one of the highest microwave absorbing solvents[278] and in addition can serve as an acid catalyst, obviating the need for PPA/SiO_2. Therefore, 3-hydroxy-2-nitroacetophenone (9) and ethyl glyoxylate in 50% toluene (6 mol equivalents) were treated with formic acid (20 mol equivalents). After 30 and 60 min, two separate additions of ethyl glyoxylate (1 mol equivalent) were made, as the unreacted starting material was still present and no product was seen by TLC. This suggested that formic acid was not providing the acidity necessary for the reaction to occur. Therefore, after 70 and 100 min, two separate additions of formic acid (20 mol equivalents) were made. However, after 130 min, only the starting material and baseline material were observed by TLC. The brown reaction mixture was discarded.

2.2.4.4 Method 4

Montmorillonite clay has been used as a solid support and catalyst for a number of microwave reactions. It is hydrated sodium calcium aluminium magnesium silicate hydroxide $(Na,Ca)_{0.33}(Al,Mg)_2(Si_4O_{10})(OH)_2 \cdot nH_2O$, where n represents the variable amount of water it can contain. Montmorillonite clay is known to provide acidity close to that of H_2SO_4 or HNO_3 and offers several advantages over classical acids, *i.e.* strong acidity, non-corrosive properties, recyclability, cheapness, mild reaction conditions, high yields and ease of set up and work up.[298,299] Furthermore, montmorillonite clay acts as both a Brønsted and Lewis acid in the natural form and ion exchanged form, enabling it to function as an efficient catalyst for various transformations.[299-302]

In this study, montmorillonite clay was added to the reaction mixture of 3-hydroxy-2-nitroacetophenone (9) and ethyl glyoxylate (5 mol equivalents) in toluene. Under microwave conditions at 110 ± 1°C, ~50 W and < 5 psi, the brown reaction mixture was monitored as described above in Method 1. TLC revealed formation of the desired product along with a brown baseline spot. As starting material still appeared on TLC, after 60 and 80 min, 1.5 mol equivalents of 50% ethyl glyoxylate in toluene were added to the brown reaction mixture. After 145 min, TLC showed the absence of the starting material and the reaction mixture was worked up and purified as described above in Method 1. The ethyl ester (17) was recovered in 56% yield. Despite claims that montmorillonite clay can hydrolyse esters,[303] hydrolysis of the ethyl ester (17) was not observed in this study.

Thus, the use of ethyl glyoxylate has made the synthesis of 3OHKG more time efficient by eliminating the stepwise formation of the acrylic acid (7) followed by the synthesis of the methyl ester (10). The yields for formation of the ethyl ester (17) and the methyl ester (10) from 3-hydroxy-2-nitroacetophenone (9) were found to be comparable (~62-63%). In addition, the application of microwave chemistry, lead to a dramatic improvement in reaction time for the condensation of ethyl glyoxylate with 3-hydroxy-2-nitroacetophenone (9) from 12 h to 130-145 min.

2.2.5 Synthesis of methyl (11) and ethyl (18) 4-(2-nitro-3-((2,3,4,5-tetra-*O*-acetyl-β-D-glucopyranosyl)oxyphenyl)-4-oxobut-2-enoate

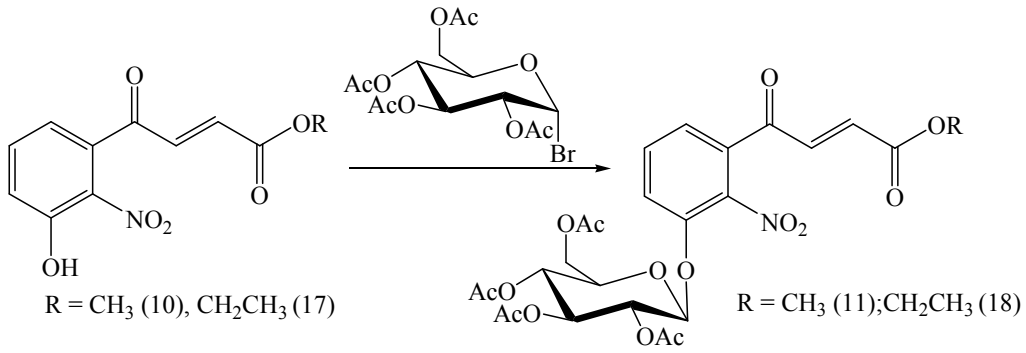

In 1901, Koenigs and Knorr reported the discovery of 2,3,4,6-tetra-*O*-acetyl-α-D-glucopyranosyl bromide (ABG) and more importantly showed that it can be condensed with alcohols and phenols in the presence of silver carbonate to give protected (acetylated) glucosides.[304-306] This was a major breakthrough in the carbohydrate chemistry as the protected carbohydrates were easily deprotected and prevented the unwanted tautomerisation, self condensation and *in situ* anomerisation, seen when using glucose directly in the condensation reactions.[307] Over the years the Koenigs and Knorr reaction has become the most important synthetic pathway for glycosides and oligosaccharides and there has been considerable research conducted to improve the process. Goldschmid and Perlin[308] have shown that acetylated glycosyl halides react with silver carbonate in the absence of a potential aglycone and that this reaction competes with the desired condensation reaction. Helferich and Wedemeyer[309] found that mercury(II) cyanide ($Hg(CN)_2$) could serve as a combined acid acceptor and catalyst in the Koenigs-Knorr reaction between ABG and range of alcohols and phenols in excess MeOH.

The glucosylation mechanism involving soluble catalysts, such as mercury(II) and silver(I) compounds (*e.g.* $Hg(CN)_2$ and silver triflate [AgOTf]), is believed to involve participation of the *trans* 2-*O*-acyl group in the formation of an oxonium ion and displacement at the C-1 position leading to protected glucosides of β-configuration (Scheme 2.8, Path A).[310] The rate determining step is heterolysis of the carbon-halide bond, assisted by the catalysts.[310-313] For the heterogenous process using insoluble mercury(II) and silver(I) salts (*e.g.* Ag_2CO_3), it appears that the reaction occurs by a "bimolecular" mechanism resulting in β-configuration due to the inversion of stereochemistry at the anomeric centre (Scheme 2.8, Path B).[310]

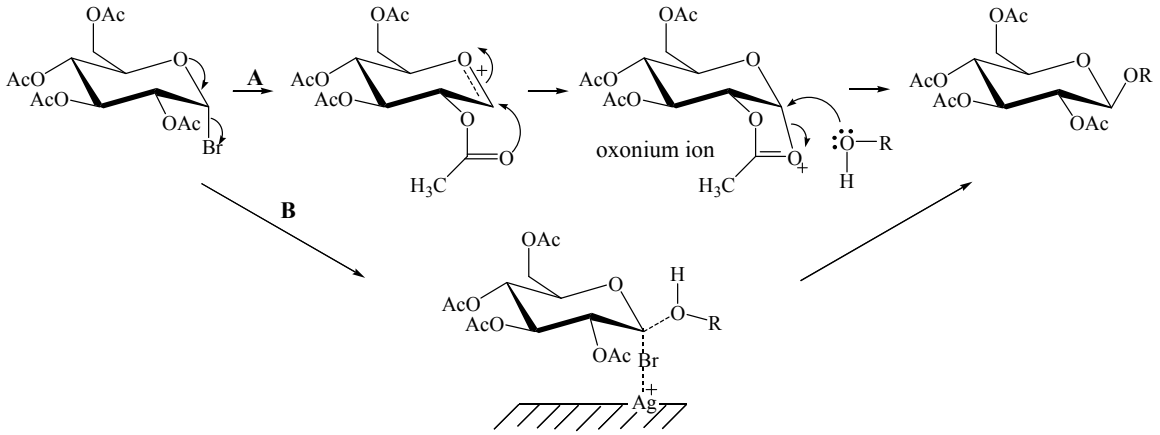

Scheme 2.8: Koenigs-Knorr reaction mechanism. **A**, homogenous process (catalysed by soluble catalysts); **B**, heterogeneous process (catalysed by insoluble catalysts).[310-313]

Manthey *et al.*[262] reported the use of $Hg(CN)_2$ and ABG for the glucosylation of the methyl ester (10), yielding 61% of the desired methyl ester glucoside (11). Despite the good yield, alternative methods were investigated for the synthesis of the methyl ester glucoside (11) as $Hg(CN)_2$ is a highly toxic reagent and it can condense with acetylated glucosyl halides to give acetylated glucosyl cyanides.[304]

2.2.5.1 Reaction trials

In order to find the best glucosylation conditions, a series of small scale reactions was conducted and assessed by TLC without product purification.

2.2.5.1.1 Reactions 1-3

Silver triflate has been reported to be an efficient catalyst for glycosylation of phenols.[314-317] Garegg *et al.*[317] showed that silver triflate, a protected glycosyl bromide and non-polar/non-nucleophilic solvents, such as DCM, are the glycosylation conditions of choice. Use of molecular sieves has also proven to be beneficial to absorb both the liberated hydrogen halide and water present.[314-316] Therefore, the methyl ester (10) was mixed with ABG in the presence of silver triflate and 3 Å molecular sieves at 0°C[315,316] and -10°C[314] in dry DCM (Table 2.1, reactions 1 and 3). The progress of the reactions was monitored by normal phase TLC. After 24 and 36 h, two separate additions of ABG (0.5 mol equivalents) were made, as the unreacted starting material was still present and no product was seen by TLC. After 2.5 days, TLC showed only the unreacted starting material, therefore the reactions were discarded.

Simultaneously, the mixture of the methyl ester (10) and ABG was dissolved in dry $CHCl_3$ in the presence of silver triflate and 3 Å molecular sieves, and reacted at 60°C. A trace amount of the product was seen by TLC, however the reaction did not proceed towards completion even after 2.5 days of heating (Table 2.1, reaction 2). Hence, the reaction was discarded.

2.2.5.1.2 Reactions 4-9

Use of phase-transfer catalysts (*e.g.* quaternary ammonium salts) in glucosylation of phenols with ABG, in the presence of a base (*e.g.* K_2CO_3, KOH), has been reported to give good yields of glucosides.[318-323] Base is used to assist formation of the phenoxide ion. Hongu *et al.*[324] have reported glucosylation of a series of phenols (*e.g.* 2,6-dihydroxyacetophenone, ~0.5 M) with ABG (~2 mol equivalents) in the presence of the phase-transfer catalyst benzyltributyl ammonium chloride (0.2 mol equivalents) and K_2CO_3 (5 mol equivalents) in $CHCl_3$ at RT. This resulted in 46-89% yield of the desired glucosides.

Following the modified literature procedure of Hongu *et al.*,[324] the methyl ester (10) was reacted with ABG, K_2CO_3 and the phase-transfer catalyst tetra-*n*-butyl ammonium bromide in dry DCM or $CHCl_3$ (Table 2.1, reactions 4-5 and 7-9). Tetra-*n*-butyl ammonium bromide was chosen as it was readily available. K_2CO_3 and tetra-*n*-butyl ammonium bromide were dried in an oven at 80°C for 24 h before use. The reactions were carried out under anhydrous conditions (argon) in the dark, due to the moisture sensitivity of ABG. Several initial trials were conducted under different reaction temperatures (Table 2.1); RT (dilute or concentrated conditions), 30°C and reflux in $CHCl_3$. All reactions were carried out for 2.5 days and the progress was monitored by normal phase TLC. During the course of the reactions, additional ABG (0.5 mol equivalents) was added, as TLC indicated the presence of the starting material.

The poorest result was observed for the reactions conducted in $CHCl_3$ either under reflux (reaction 7) or at ~30°C (reaction 5), where only a small amount of product was detected, along with substantial side products. The most promising results seen by TLC were at RT in DCM (reaction 9). Use of greater amounts of ABG, the catalyst and K_2CO_3, addition of the methyl ester (10) in portions (reaction 4) and dilute conditions (reaction 8), seemed not to have an affect.

The methyl ester (10) (mp 110-112°C) was reacted with ABG (mp 89-90°C) in the presence of K_2CO_3 and tetra-*n*-butyl ammonium bromide (mp 102-106°C) under solvent-free conditions at 90°C under vacuum (Table 2.1, reaction 6). The reaction was monitored by TLC, which looked initially promising since the generation of the desired product was seen within 10 min of reaction. During the reaction period of 9 h, approximately 1.5 mol equivalents of ABG were additionally added in portions, as the unreacted starting material was still observed by TLC. However, the reaction did not go to completion and turned dark brown in colour with baseline material observed by TLC.

Table 2.1: Glucosylation of methyl ester (10) with ABG.

#	**Me ester** (mg)	**Solvent** (mL)		**ABG** (mol eq)	**PTC** (mol eq)	**K_2CO_3** (mol eq)	**°C**	**Additional**	**Product**[j]
		DCM	$CHCl_3$						
1[a]	5	0.2	/	1.4[b]	AgOTf (1.4)	/	0	mol. sieves 3 Å	-
2	5	/	0.2	1[b]	AgOTf (1)	/	60	mol. sieves 3 Å	+/-
3[d]	20	0.4	/	1.5[b]	AgOTf (1.5)	/	-10	mol. sieves 3 Å	-
4	20[e]	2	/	4.3[c]	*t*-Butyl-N^+Br^- (1)	9	RT	/	+
5	20	/	2	3[c]	*t*-Butyl-N^+Br^- (1)	9	~30	/	+/-
6[f]	10	/	/	0.5[g]	*t*-Butyl-N^+Br^- (1)	2	90	/	+
7	10	/	1	1[c]	*t*-Butyl-N^+Br^- (1)	1	60	/	+/-
8[h]	5	5	/	1[c]	*t*-Butyl-N^+Br^- (1.5)	10	RT	/	+
9[i]	10	1	/	2[c]	*t*-Butyl-N^+Br^- (0.2)	3.5	RT	/	+

All reactions (except # 6) were stirred in the dark under argon and evaluated by TLC (1:1 EtOAc/pet. spirit (v/v), $R_{f\,(product)}$ 0.40) over a period of 2.5 days.
[a] modified method of Ueda and Takada[315] and Takada *et al.*[316]
[b] ~0.5 mol equivalents ABG added after 24 and 36 h
[c] ~0.5 mol equivalents of ABG added after 9, 24 and 36 h
[d] modified method of Jensen *et al.*[314]
[e] ~4 mg added every 30 min
[f] under vacuum
[g] another 1.5 mol equivalents added over a period of 9 h, reaction time 9 h
[h] dilute conditions
[i] modified method of Hongu *et al.*[324]
[j] +, product observed by TLC; -, product not observed; +/-, product observed in traces

As reactions 6 and 9 looked most promising, these conditions were repeated on higher reaction scales.

2.2.5.2 Method 1 (reaction 6 on a larger scale)

The solvent-free reaction (reaction 6) was repeated on a 100 mg scale of the methyl ester (10). A mixture of the methyl ester, ground anhydrous K_2CO_3 (~2 mol equivalents), ground anhydrous tetra-*n*-butyl ammonium bromide (~1 mol equivalent) and ABG (0.5 mol equivalents) was placed under vacuum (~20 mBar) at 90°C in the dark. Additional ABG (~1.5 mol equivalents) was added in portions over 9 h. In addition to a brown baseline material, TLC showed formation of the desired product. A separate incubation of ABG under the given reaction conditions confirmed that the brown baseline material on TLC was originating from ABG. After 9 h, TLC showed the desired methyl ester glucoside as the major product along with the starting material and a brown baseline spot. As the reaction was quite dark in colour at this point, it was stopped by dissolving it in DCM, filtering through a plug of celite and adsorbing onto normal phase silica (~1 g). The solvent was evaporated under reduced pressure and the remaining solid purified by normal phase column chromatography to yield the methyl ester glucoside (11) in 33% yield. The ^{1}H NMR spectrum of the methyl ester glucoside showed three aromatic resonances at δ 7.58, δ 7.55 and δ 7.47 and a distinct *trans*-configuration of the side chain protons with a coupling constant of 15.7 Hz (2H). This was similar to the methyl ester (10). In addition, resonances were seen at δ 5.30-4.22, δ 2.13-2.05 and δ 3.8, corresponded to the hydrogens from the glucose moiety, the acetyl groups and the methyl ester moiety on the side chain, respectively. These were consistent with the data reported by Manthey *et al.*[262] ES-MS displayed a molecular ion at *m/z* 582 ($M+H^+$), consistent with the expected molecular mass for the methyl ester glucoside (11) of 581 Da.

2.2.5.3 Method 2 (reaction 9 on a larger scale)

The glucosylation reaction that was conducted at RT in DCM also looked promising on a small scale (Table 2.1, reaction 9). Therefore, the reaction was trialled on a 100 mg scale of the methyl ester (10) in dry DCM at a concentration of ~1 mg/mL. Ground anhydrous K_2CO_3 (~3.6 mol equivalents), ground anhydrous tetra-*n*-butyl ammonium bromide (~0.2 mol equivalents) and ABG (~1.5 mol equivalents) were added to the yellow solution. After 9, 24 and 36 h, additional ABG (~0.5 mol equivalents) was added, as the starting material was still observed by TLC. The bright orange suspension gradually faded to a dull red-brown colour after 2.5 days of stirring. The reaction was then filtered, adsorbed onto normal phase silica and purified by normal phase column chromatography to obtain the methyl ester glucoside (11) in 72% yield as a white solid, along with trace amounts of the methyl ester (10). Similar

yields of the desired glucoside (11) were obtained by the use of tetra-*n*-butyl ammonium iodide as a catalyst under similar reaction conditions.[269]

Scaling up to 700 mg of the methyl ester (10) resulted in the recovery of the desired product in 78% yield after 2.5 days of reaction. In contrast, the product was isolated in only 19% yield after 5 days, which was the time needed for total disappearance of the starting material. This was consistent with the TLC monitoring, as it showed time dependent decrease in the intensity of the desired methyl ester glucoside (11) after 2.5 days. This was followed by the formation of two additional spots of very similar R_f to the desired product after 2.5 days. This suggests that even though all starting material may get consumed with prolonged reaction time, simultaneous decomposition of the desired product was occurring. This may be due to side reactions occurring as a result of accumulation of decomposition products of ABG such as the cleavage of the acyl protecting groups of the glycosyl donor. This has been reported for two-phase reaction systems.[321,324] It was therefore concluded that RT conditions in DCM with tetra-*n*-butyl ammonium bromide and K_2CO_3 were the conditions of choice and that subsequent additions of ~1.5-2 mol equivalents of ABG over a period of 2.5 days were optimal for the progress of the reaction.

2.2.5.4 Method 3

Similar reaction conditions to reaction 9 (Table 2.1) were carried out with the ethyl ester (17) on a 250 mg scale. The reaction proved to be of equal success to the glucosylation reaction of the methyl ester (10), as described above, yielding the ethyl ester glucoside (18) in 70% yield as a colourless film after 2 days. Trace amounts of starting material were observed by TLC. ^{1}H NMR was similar to that of the methyl ester glucoside (11), with an ethyl group (δ 4.20 [CH_2] and δ 1.31 [CH_3]) instead of a methyl group. ES-MS displayed a molecular ion at *m/z* 596 ($M+H^+$), a sodium adduct at *m/z* 619 ($M+H^+ + Na$) and an acetylated glucose fragment at *m/z* 331 ($M+H^+$ - $Glu(OAc)_4$). This was in agreement with the expected mass of 595 Da.

As a result of this glucosylation study, an improvement in reaction time of 2 days, compared to the literature procedure of 4 days,[262] and an increase in the product yields to 70-78% from 61%,[262] were achieved. More importantly, toxic $Hg(CN)_2$ was replaced with the more benign phase-transfer catalyst tetra-*n*-butyl ammonium bromide.

2.2.6 Synthesis of 3-hydroxykynurenine-*O*-β-D-glucoside (3OHKG)

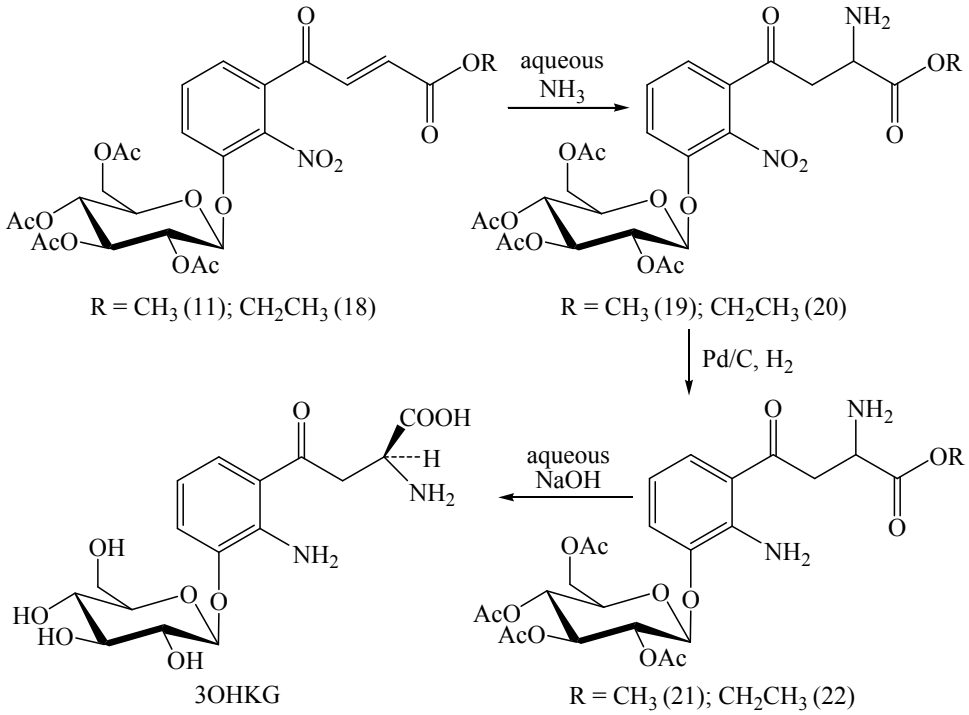

Following the general method of Manthey *et al.*,[262] the last steps to be conducted in the synthesis of 3OHKG were amination of the methyl ester glucoside (11) or the ethyl ester glucoside (18), followed by hydrogenation of the nitro group, and subsequent hydrolysis of the ester and acetyl moieties.

Thus, the methyl ester glucoside (11) was dissolved in aqueous NH_3 (0.03 M) in EtOAc at ~1 mg/mL. EtOAc was employed as the solvent instead of MeOH,[262] due to the ability of MeOH to attack the double bond. A relatively dilute concentration of the methyl ester glucoside (11) were used as concentrated conditions have been previously shown by other members of the research group to give a range of side products, possibly due to the generated amine group attacking the double bond of the starting material to give a dimer.[269] The progress of the reaction was monitored by normal phase TLC, visualising by UV light at 254 and 365 nm, and ninhydrin. A positive reaction with ninhydrin (colour change to purple) indicated the presence of an amine group. No side products were observed. LC-MS analysis confirmed a clean amination (*m/z* 599 ($M+H^+$)). The amination of the methyl ester glucoside (11) was a fast process, typically completed within 3 h. In previous studies by the research group, the amine (19) proved to be unstable, therefore it was not worked up but hydrogenated directly with H_2 (1 atm) and Pd/C as a catalyst. Unsurprisingly, EtOAc proved to be a superior solvent to the water/AcOH (pH 6.0) used by Manthey *et al.*[262] Hydrogenation resulted in a rapid

reduction of the nitro group within 3 h, as observed by normal phase TLC. LC-MS showed the desired product as a major peak (*m/z* 569 ($M+H^+$)). The crude hydrogenation mixture was filtered and evaporated to dryness. The yellow-orange residue was then treated with argon-gassed (~20 min) aqueous NaOH (~0.05 M) and aqueous NH_3 (~8.6 mM) at pH ~12.5 to remove the ester and acetyl moieties. TLC showed formation of two spots with one dominating. LC-MS analysis showed 3OHKG (*m/z* 387 ($M+H^+$)) as the major reaction product in addition to an unknown less polar compound (*m/z* 385 ($M+H^+$)) called U-24. After 8.5 h, the yellow solution was acidified to pH 6 by dropwise addition of 1 M AcOH, lyophilised and purified by RP-HPLC to afford 3OHKG in 27% yield, from the methyl ester glucoside (11), as a pale yellow solid. 3OHKG was seen as a double peak (~1:1). This was due to the formation of two diastereomers of 3OHKG arising from the addition of NH_3 on either side of the double bond. The diastereomers were not resolvable by preparative RP-HPLC, and were therefore collected together.

The identity of 3OHKG was further confirmed by ^1H NMR, which agreed with the literature data.[262] The anomeric carbon appeared at 101.8 ppm and the anomeric proton appeared as a doublet at 4.94 ppm with a coupling constant of 7.3 Hz. This was indicative of a β-configuration of the glucose. ES-MS/MS (positive mode) of 3OHKG showed the molecular ion at *m/z* 387 ($M+H^+$) and fragment ions at *m/z* 370 (loss of NH_3), *m/z* 224 (loss of glucose), *m/z* 208 (3OHKyn yellow), *m/z* 162 (decarboxylated 3OHKyn yellow), *m/z* 152 (2-amino-3-hydroxyacetophenone) and *m/z* 110 (2-aminophenol), consistent with the literature.[262] In phosphate-buffered saline (PBS) at pH 7.0, 3OHKG exhibited absorption maxima at 262 and 365 nm and maximum fluorescence at λ_{ex} 360 and λ_{em} 500 nm. These characteristics are consistent with those reported previously.[86] U-24 was also collected in 20% yield as a white solid. The identity of this compound is discussed in section 2.2.8.

The amination, hydrogenation and hydrolysis reactions were repeated with the ethyl ester glucoside (18). This resulted in 3OHKG and U-24 in 27% and 18% yield, respectively.

2.2.7 Stability of 3OHKG

As relatively low yields of 3OHKG were obtained by the above procedures, despite TLC and LC-MS looking promising during the amination and hydrogenation steps, it was suspected

that U-24 was generated due to decomposition of 3OHKG under the basic hydrolysis conditions.

Previous studies, however, have shown that the model compound 2-amino-4-oxo-4-phenylbutanoic acid deaminates rapidly at pH 9.1 and that the rate of deamination is reduced at higher pH (pH 10.1 examined).[100] Basic conditions (pH ~7-9.5) facilitate the deamination through formation of a carbanion (Scheme 2.9), however the pH values greater than 9.5 lead to substantional deprotonation of the NH_3^+ (pK_a 7.61 ± 0.13) to the uncharged poor leaving group NH_2. Thus, basic hydrolysis at pH ~12.5 was not expected to result in deamination.

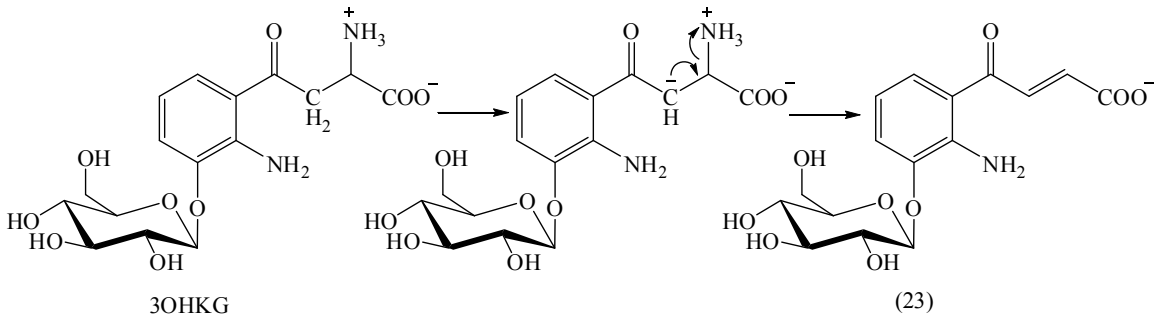

Scheme 2.9: Proposed mechanism for deamination of 3OHKG at pH ~7-9.5.

To investigate this further, the stability of 3OHKG (0.45 mM) was examined in argon-gassed aqueous NaOH (0.05 M) at pH 12.5, mimicking the hydrolysis conditions. Aliquots were taken over a period of 27 h and analysed by RP-HPLC. 3OHKG decomposed 2.2% and 9.0% after 9 and 27 h, respectively (Figure 2.3). LC-MS analysis revealed that the major loss of 3OHKG was due to deamination (*m/z* 370 ($M+H^+$), λ_{max} 283/411 nm). No additional decomposition products were seen. This confirms that U-24 was not formed during the basic hydrolysis. Following the stability conditions for 3OHKG, the stability of Kyn (1.2 mM) was investigated as a positive control. Kyn decomposed 1.5% and 5.7% after 9 and 27 h, respectively. Deamination of Kyn (*m/z* 192 ($M+H^+$), λ_{max} 278/406 nm) was the major cause of decomposition.

As minor deamination of 3OHKG was seen at pH 12.5, the stability of 3OHKG (0.32 mM) was investigated in the presence of aqueous NH_3 (0.04 M). Aqueous NH_3 was added in order to allow amination of the deaminated 3OHKG (23). The loss of 3OHKG was 0% and 5.5% after 9 and 27 h, respectively. Decomposition of 3OHKG was again mainly due to deamination (Figure 2.3). This result suggests that aqueous NH_3 may be beneficial during the first 10 h of basic hydrolysis.

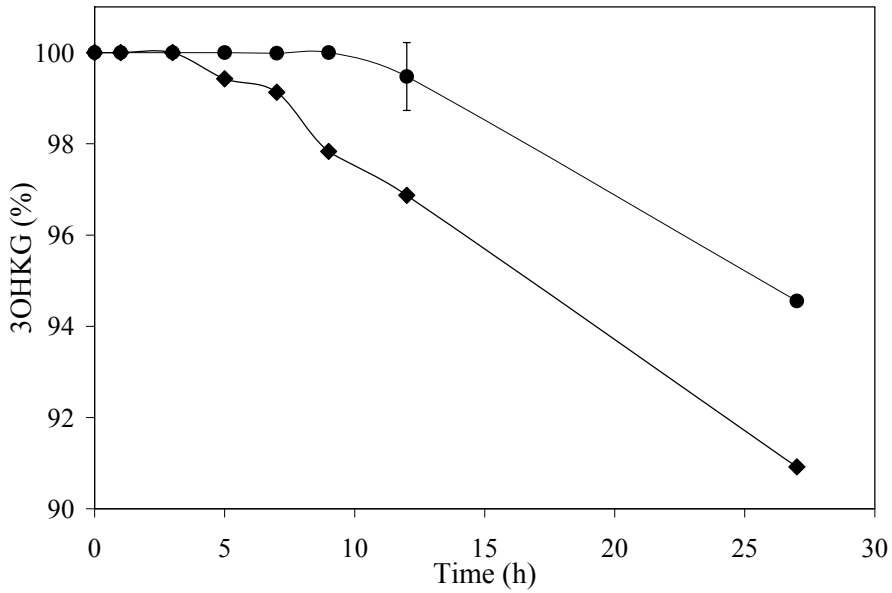

Figure 2.3: Stability of 3OHKG in aqueous NaOH (0.05 M) at pH 12.5 in the absence of NH_3 (◆) and in the presence of NH_3 (0.04 M) (●).

2.2.8 The origin and identity of U-24

In order to determine the origin of U-24, reaction mixtures from the amination, hydrogenation and hydrolysis steps were careful examined by LC-MS in positive mode while monitoring at 254 and 360 nm. Thus, the methyl ester glucoside (11) (~100 mg) was treated with aqueous NH_3 as described above. Approximately 0.2 mL aliquots of the reaction mixture were taken after 1, 2 and 3 h, dried with argon, redissolved in 20% CH_3CN/H_2O (v/v) and analysed by LC-MS. LC-MS showed clean formation of the amine (19) with a molecular ion at *m/z* 599 ($M+H^+$). No side products were detected. After 3 h, the reaction was completed and the pale yellow solution was placed under a H_2 atmosphere (1 atm) in the presence of Pd/C. Approximately 0.2 mL aliquots of the reaction mixture were taken after 1, 2 and 3 h, filtered, dried with argon, redissolved in 20% CH_3CN/H_2O (v/v) and analysed by LC-MS. LC-MS showed the desired reduced amine (21) (*m/z* 569 ($M+H^+$)) as a major product. An additional compound of similar polarity to the reduced amine (21), with a molecular ion at *m/z* 567 ($M+H^+$) and absorption maximum at 324 nm, was observed. This additional compound was most likely the precursor of U-24, as it showed a molecular ion of 2 Da less than the desired product (21) and identical absorbance maxima to U-24. No other major products by LC-MS were observed. After 3 h, the reaction was completed and the reaction mixture was filtered and evaporated under reduced pressure. The crude product was hydrolysed in the presence of aqueous NaOH (~0.05 M) and NH_3 (~8.6 mM) at pH ~12.5. After 2, 4, 6 and 8 h,

approximately 0.2 mL aliquots of the reaction mixture were taken, the pH adjusted to ~6 by 1 M AcOH, and analysed by LC-MS. LC-MS showed formation of 3OHKG (*m/z* 387 ($M+H^+$)) as the major reaction product. In addition, U-24 was observed. It was of lower polarity than 3OHKG and eluted as a double peak (~1:1), suggesting diastereomers, with a molecular ion at *m/z* 385 ($M+H^+$) and an absorption maximum at 324 nm. Upon purification by RP-HPLC, 3OHKG and U-24 were afforded in 25 and 20% yield, respectively, from the methyl ester glucoside (11). These data suggest that the U-24 precursor is probably formed during the hydrogenation step.

HR-MS in the negative mode of U-24 revealed a deprotonated molecular ion at *m/z* 383.107449, which corresponds to the molecular formula of $C_{16}H_{20}N_2O_9$. This is consistent with the structure of 3OHKG with 2 hydrogens less.

The ^{13}C and DEPT NMR spectra of U-24 indicated a total of 16 carbons, with 2 being methylenes (δ 28.8 and 60.9), 9 methines (δ 53.8, 69.7, 73.2, 75.9, 76.7, 100.4, 112.6, 114.3 and 125.5), and 5 quaternary carbons (δ 119.1, 143.9, 152.3, 165.8 and 174.1) (Table 2.2). U-24 had virtually identical ^1H and ^{13}C NMR data in D_2O and DMSO-*d*6 to that for the $CH_2CH(NH_2)COOH$ moiety of 3OHKG, indicating that addition of NH_3 to the double bond had occurred (Table 2.2). Furthermore, an anomeric carbon appeared at δ 100.4 and an anomeric proton appeared as a doublet at δ 5.20 with a coupling constant of 7.5 Hz. This was consistent with the expected β-configuration. Similarly to 3OHKG, other methine and methylene protons from the glucose moiety were seen as overlapping multiplets with coupled resonances at δ 3.82-3.41. The ^1H NMR spectrum clearly showed 3 aromatic resonances at δ 6.88, 6.92 and 7.22, which were coupled to each other (COSY) and arose from the protons at Ar-4, Ar-5 and Ar-6, respectively. Their presence indicated that no addition occurred at the aromatic ring. However, their chemical shifts were quite different to 3OHKG (δ 7.23 [Ar-4], 6.65 [Ar-5] and 7.52 [Ar-6]). No ^{13}C NMR resonance equivalent to the carbonyl at C-4 of 3OHKG (δ 200.0) was observed with U-24 and in contrast to 3OHKG the Ar-6 proton showed no HMBC correlation to C-4. A carbon resonance was observed at δ 165.8, which showed correlation with the protons at C-2 and C-3. This strongly supports a possible structural change at C-4.

Table 2.2: ^{1}H and ^{13}C NMR of 3OHKG and U-24. Spectra were obtained in D_2O.

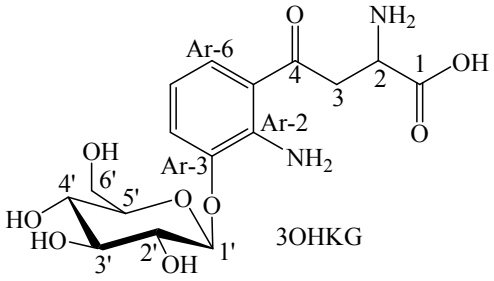

C / H	3OHKG		U-24	
	δ ^{13}C	δ ^{1}H	δ ^{13}C	δ ^{1}H
1	173.8		174.1	
2	50.6	4.05, 1H, m	53.8	4.02, 1H, m
3	39.5	3.65, 2H, m	28.9	3.64, 2H, m
4	200.0		165.8	
Ar-1	118.5		119.1	
Ar-2	141.7		152.3	
Ar-3	145.3		143.9	
Ar-4	121.3	7.23, 1H, d, *J* 8.1	112.7	6.88, 1H, m
Ar-5	116.5	6.65, 1H, dd, *J* 8.1, 8.1	125.5	6.92, 1H, m
Ar-6	126.1	7.52, 1H, d, *J* 8.1	114.3	7.22, 1H, d, *J* 8.2
1’	101.8	4.94, 1H, d, *J* 7.3	100.4	5.20, 1H, d, *J* 7.5
2’	75.9	3.48-3.53, 2 x 1H, m	75.8	3.55-3.60, 2 x 1H, m
3’	73.2		73.2	
4’	69.7	3.47, 1H, m	69.8	3.41, 1H, m
		3.38, 1H, m		
5’	76.6	3.44, 1H, m	76.7	3.52, 1H, m
		3.42, 1H, m		
6’	60.8	3.82, 1H, dd, *J* 1.6, 12.5	60.9	3.82, 1H, m
		3.68, 1H dd, *J* 5.5, 12.5		3.65, 1H, m

Given the above data, the benzisoxazole structure shown in Figure 2.4 was proposed for U-24. The isoxazole ring carbon corresponding to C-4 in the proposed structure of U-24 has been reported to be at δ ~169.[325] This structure is also consistent with the aromatic resonances and the molecular formula confirmed for U-24.

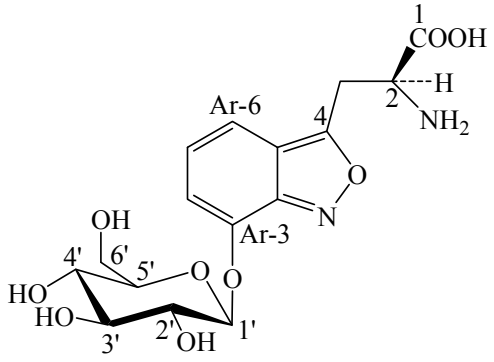

Figure 2.4: Proposed structure of U-24.

ES-MS/MS in the positive mode of U-24 revealed a molecular ion at *m/z* 385 ($M+H^+$), with accompanying fragment ions at *m/z* 368 and *m/z* 223 due to loss of NH_3 and loss of glucose. ES-MS/MS of a protonated ion at *m/z* 223 resulted in fragment ions at *m/z* 206, *m/z* 150 and *m/z* 135 due to loss of NH_3, loss of $HC(NH_2)COOH$ on the side chain and further loss of CH_2 on the side chain (Figures 2.5 (B) and 2.6 (B)). ES-MS/MS of U-24 performed in the negative mode revealed a corresponding molecular ion at *m/z* 383 ($M+H^+$) and accompanying fragment ions at *m/z* 366, *m/z* 221, *m/z* 204, *m/z* 148 and *m/z* 133. This fragmentation pattern is consistent with ES-MS/MS of 3OHKG in the positive mode displaying a molecular ion at *m/z* 387 ($M+H^+$) and accompanying fragment ions at *m/z* 370, *m/z* 225, m/z 208 and *m/z* 152, although with 2 additional hydrogens compared to U-24 (Figures 2.5 (A) and 2.6 (A)). A fragment ion at *m/z* 110 due to loss of the side chain of 3OHKG was not observed in the U-24 spectrum indicating a structural change at C-4 (Figures 2.5 and 2.6). These MS data provided further evidence for the proposed structure of U-24 having an isoxazole ring (Figure 2.4).

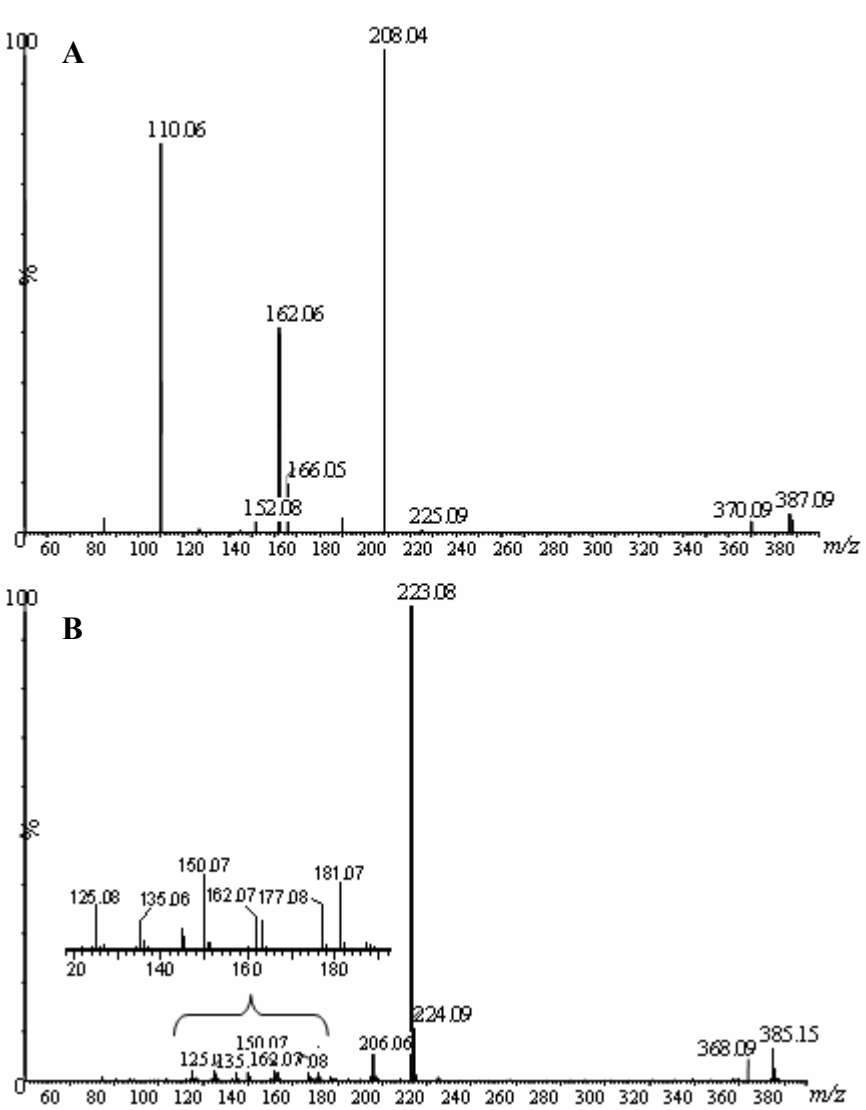

Figure 2.5: ES-MS/MS of authentic 3OHKG (**A**) and U-24 (**B**) in positive mode.

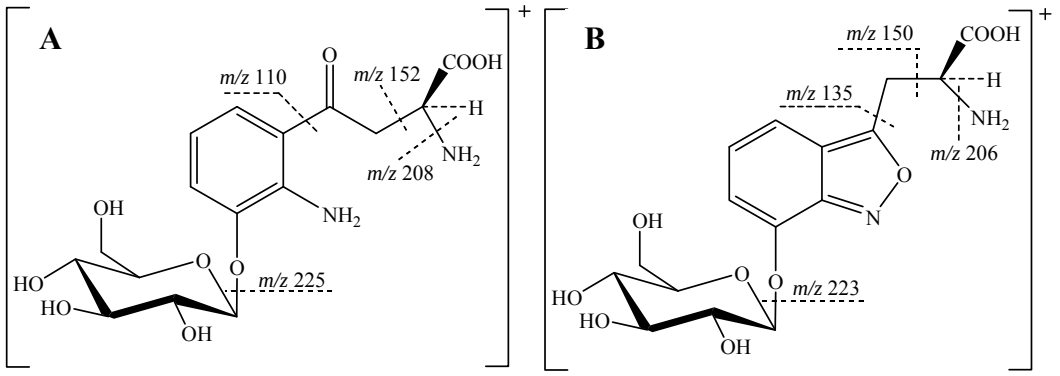

Figure 2.6: 3OHKG (A) and the proposed structure of U-24 (B) with the assigned major protonated fragments by ES-MS/MS (positive mode).

In PBS at pH 7.0, U-24 showed an absorption maximum at 323 nm and no fluorescence. These characteristics do not resemble those of 3OHKG (λ_{max} 262 and 365 nm, λ_{ex} 360 and λ_{em} 500 nm) under similar conditions. This indicates that U-24 has a different chromophoric structure to 3OHKG and is consistent with the suggested isoxazole structure.

From the LC-MS data, it was evident that U-24 was formed during the hydrogenation step or the reaction work up. Isoxazoles are known to readily reduce under the experimental conditions used in this study, resulting in the formation of the corresponding primary amine and ketone (Figure 2.10, an example given for the proposed structure of U-24).[325-330] The facile reductive cleavage of the N-O bond has been attributed to the greater electronegativity of the oxygen atom adjacent to the nitrogen in an isoxazole ring.[331] To further investigate this, U-24 was dissolved in water and ~0.01% TFA (v/v) and reduced under a H_2 atmosphere (1 atm) in the presence of Pd/C in the dark at RT. TFA was added to the reaction mixture to keep the amine group in the protonated state and to prevent possible deamination of the side chain. After 10 min, TLC clearly indicated disappearance of U-24 and formation of 3OHKG. The reaction mixture was filtered and the yellow solution was lyophilised. RP-HPLC showed a peak consistent with 3OHKG along with at least 3 unknown products of higher polarity. Their identity was not investigated further. 3OHKG was obtained in 65% yield.

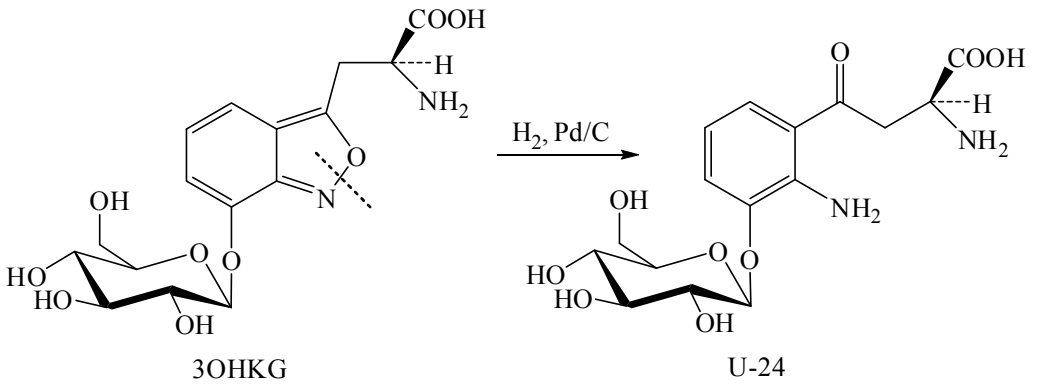

3OHKG U-24

Scheme 2.10: Reduction of U-24 to 3OHKG.

Due to the formation of the side products under the conditions described above, the U-24 reduction was repeated under similar conditions in the absence of TFA. After 10 min, TLC indicated complete conversion of U-24 to 3OHKG. The crude product was worked up and purified as described above to obtain nearly quantitative (92%) yield of 3OHKG. This suggests that U-24 may be unstable under the hydrogenation conditions in the presence of 0.01% TFA (v/v). The isolated 3OHKG coeluted with authentic 3OHKG and showed identical ES-MS/MS and ^{1}H NMR. These data strongly support the proposed structure of U-24 (Figure 2.4).

Overall, the formation of the isoxazole ring was surprising. It was suggested that U-24 occurs due to incomplete reduction of the nitro group to hydroxylamine. This has been observed by Carrion *et al.*[325] They reported the reduction of pyrazoline derivatives with $SnCl_2$ in EtOH resulting in the formation of the isoxazole derivatives (Scheme 2.11). It was suggested that the formation of an isoxazole ring occurs *via* an attack of the hydroxyl group of the hydroxylamine intermediate to the carbonyl group followed by loss of water and rearrangement of the conjugated system (Scheme 2.11).[325]

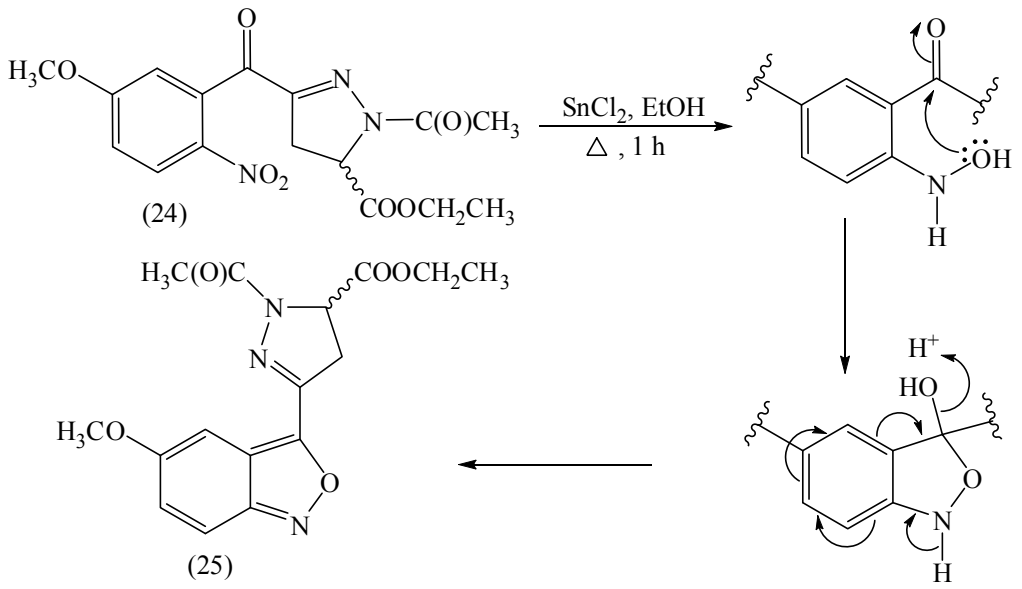

Scheme 2.11: The reduction of ethyl 1-acetyl-3-(5-methoxy-2-nitrobenzoyl)-Δ^2-pyrazoline-5-carboxylate (24) to ethyl 1-acetyl-3-(5-methoxybenzo[c]isoxazol-3-yl)-Δ^2-pyrazoline-5-carboxylate (25).[325]

Isoxazole derivatives are important structural units of many molecules of biological interest, for example, antiinflammatory agents (4-(5-methyl-3-phenylisoxazol-4-yl)benzenesulfonamide [Bextra®] and 5-methyl-*N*-(4-(trifluoromethyl)phenyl)-isoxazole-4-carboxamide [Arava®]), herbicidal agents (isoxazole-4-carboxylate) and antibacterial agents (4-amino-*N*-(3,4-dimethyloxazol-5-yl)-benzenesulfonamide [Sulfisoxazole]).[331] Thus, it would be of interest to find out if U-24 has any biological function.

In this study 3OHKG was synthesised in 25-27% overall yield from the methyl (11) and ethyl (18) ester glucoside *via* successive amination, reduction and hydrolysis reactions. A reduction in the product yield was observed compared to the literature (48%), which may be due to the formation of U-24 in 18-20% yield. Subsequent hydrogenation of U-24 resulted in nearly quantitative recovery of 3OHKG. This gave 3OHKG in ~46% yield from either the methyl (11) or ethyl (18) ester glucoside. This was comparable to the literature.[262] It was therefore postulated that hydrogenation of the crude reaction mixture after hydrolysis may result in greater recovery of 3OHKG. This remains to be investigated.

2.3 Conclusions

Several procedures have been reported for the synthesis of the major UV filter, 3OHKG,[260-262] however some of these methods involve the use of expensive and/or toxic reagents. Apart from the method of Manthey *et al.*,[262] these procedures are generally inflexible and can not be

applied to the synthesis of a range of UV filter compounds. Through the expansion and optimisation of the procedure reported by Manthey *et al.*,[262] a new strategy has been developed to allow for the synthesis of a range of known UV filter compounds and their derivatives using commercially available and inexpensive reagents. Green chemistry principles have been applied in the synthesis of the acrylic acid (7) and the ethyl ester (17), with toxic and corrosive reagents being replaced with benign reagents and use of solvent-free and microwave chemistry. A detailed investigation of different reaction conditions was conducted for most reaction steps, resulting in either the improvement of reaction yields or reaction time. The versatility of this modified method was shown by the synthesis of other UV filter compounds. This will be discussed in Chapters 3 and 4. As a result of this study ready access to 3OHKG was obtained for protein binding and UV illumination studies. These are described in Chapters 5 and 6, respectively.

2.4 Experimental

2.4.1 General experimental

Organic solvents, ammonia (NH_3, 28%) and formic acid (99%) were from Ajax Chemicals (NSW, Australia). Acetonitrile (CH_3CN) was of HPLC grade. All other organic solvents were AR grade and distilled prior to use. Petroleum spirit (pet. spirit) was of bp 40-60 ºC. Glyoxylic acid monohydrate (98%), 2,3,4,6-tetra-*O*-acetyl-α-D-glucopyranosyl bromide (ABG, > 95%), copper nitrate hemi(pentahydrate) ($Cu(NO_3)_2 \cdot 2.5H_2O$, 99%), tetra-*n*-butyl ammonium bromide (≥ 99%), trifluoroacetic acid (TFA, > 99%), polyphosphoric acid (PPA, equivalent to 112-116% H_3PO_4), silver triflate (AgOTf, + 99%), montmorillonite KSF clay, decolourising carbon and Pd/C (10 wt % on activated carbon) were from Sigma-Aldrich. Ethyl glyoxylate (50% solution in toluene) was from Lancaster Synthesis (England). Glacial acetic acid (AcOH) (> 99.9%) and acetic anhydride (99.0%) were purchased from BDH. CD_3OD (99.8%), $CDCl_3$ (99.8%) and D_2O (99.9%) were from Cambridge Isotope Laboratories. Dulbelcco's phosphate-buffered saline (PBS), without calcium and magnesium, consisted of KCl (2.7 mM), KH_2PO_4 (1.4 mM), NaCl (137 mM) and Na_2HPO_4 (7.68 mM).[257] Pre-washed chelex resin was added to the PBS buffer (~2 g/L) and left for 24 h prior to use. The pH was adjusted to 7.0 with 1 M NaOH. Milli-Q® H_2O (purified to 18.2 MΩ cm^{-2}) was used in preparation of RP-HPLC aqueous solutions and PBS. Thin-layer chromatography (TLC) plates of normal phase 60 F_{254} and reversed phase 18 F_{254}, and normal phase silica gel

(SiO_2, 230-400 mesh) were from Merck (Germany). Normal phase TLC plates were developed using the mobile phase *n*-butanol/AcOH/H_2O (12:3:5 BAW, v/v), where indicated. TLC plates were visualised under UV light (254 and 365 nm) and sprayed with ninhydrin (ninhydrin [0.2%, w/v] in *n*-butanol [94.8%, v/v] and AcOH [5%, v/v]),[288] where indicated. Melting points were determined on a SMP 10 Stuart scientific (UK) apparatus and are uncorrected. Infrared spectra were recorded on a PerkinElmer Paragon 1000 PC FT-IR spectrometer. A labconco FreeZone 12 plus freeze drier (0.04 mBa, -80°C) from Crown Scientific was used for aqueous lyophilisation. Microwave assisted aldol condensation reactions were conducted in a focused microwave reactor (CEM Discover) at ~50 W and < 5 psi. Other aldol condensation reactions were conducted in a 12 place head carousel reactor station from Radley Discovery Technologies. A vacuum pump used for reactions under vacuum and evaporation of organic solvents was of ~20 mBar.

2.4.2 UV-visible (UV-vis) absorbance and fluorescence spectrometric measurements

UV-vis absorbance spectra were obtained using a Varian DMS 90 UV-vis spectrometer and UV cuvettes of 0.75 mL. Fluorescence spectra were recorded on a PerkinElmer LS55 Luminescence spectrometer using SUPRASIL® PerkinElmer fluorescence cells (0.3 or 3mL). Slit widths were 10 nm for excitation and emission. PBS (pH 7.0) was used as solvent for all measurements at ~0.5 mg/mL of organic compounds.

2.4.3 Reversed phase-high performance liquid chromatography (RP-HPLC)

RP-HPLC was performed on a Shimadzu HPLC equipped with LC-10ADvp pumps, a SIL-10Avp autoinjector and SPD-M10Avp diode array detector. The analytical analyses were performed on a Phenomenex (Luna, 100 Å, 5 μm, 4.6 x 250 mm, C18) column fitted with a Phenomenex (Synergy Fusion, 100 Å, 4 μm, 2 x 4 mm, C18) guard column, while preparative purifications were performed on a Phenomenex (Luna, 100 Å, 10 μm, 15 x 250 mm, C18) column fitted with a Phenomenex (Synergy Fusion, 100 Å, 4 μm, 10 x 10 mm, C18) guard column. The following mobile phase system; buffer A (H_2O/0.05% TFA, v/v) and buffer B (80% CH_3CN/0.05% TFA, v/v) and the flow rate 1 mL/min for analytical and 5 mL/min for preparative separations were kept constant. Preparative purification of 3OHKG was performed using the following mobile phase gradient: 0-15 min (5% buffer B), 15-35 min (5-40% buffer B), 35-40 min (40% buffer B), 40-45 min (40-5% buffer B) and 45-55 min (5% buffer B). The stability experiments of 3OHKG and Kyn under basic conditions were

analysed using the following mobile phase gradient: 0-5 min (5% buffer B), 5-18 min (5-70% buffer B), 18-23 min (70% buffer B), 23-28 min (70-5% buffer B) and 28-38 min (5% buffer B). The spiking experiments of 3OHKG and U-24 were analysed using an Alltech (Prevail, 100 Å, 5 μm, 4.6 x 250 mm, C18) column fitted with a Phenomenex (Synergy Fusion, 100 Å, 4 μm, 2 x 4 mm, C18) guard column and the following mobile phase gradient: 0-10 min (0% buffer B), 10-20 min (0-50% buffer B), 20-23 min (50% buffer B), 23-26 min (50-0% buffer B) and 26-32 min (0% buffer B).

2.4.4 Liquid chromatography-mass spectrometry (LC-MS)

LC-MS was run on a Shimadzu LC-MS-2010EV unit attached to an electrospray ionisation mass spectrometer (ES-MS). A Phenomenex (Synergi, 100 Å, 4 μm, 2 x 150 mm, C18) column fitted with a Phenomenex (Synergy Fusion, 100 Å, 4 μm, 2 x 4 mm, C18) guard column was used at 30°C. The mobile phase system consisted of buffer A (H_2O/0.1% formic acid, v/v) and buffer B (CH_3CN/0.1% formic acid, v/v). The mobile phase gradient was as follows: 0-10 min (0% buffer B), 10-25 min (0-80% buffer B), 25-30 min (80% buffer B), 30-35 min (80-0% buffer B) and 35-40 min (0% buffer B). The flow rate was 0.2 mL/min and the source temperature was maintained at 200°C. All spectra were acquired in positive continuum mode and monitored at 254 and 360 nm.

2.4.5 Nuclear magnetic resonance (NMR) spectroscopy

^{1}H, ^{13}C, COSY (^{1}H-^{1}H correlation spectroscopy), HSQC (^{1}H-^{13}C heteronuclear single quantum correlation) and HMBC (^{1}H-^{13}C heteronuclear multiple bond correlation) NMR experiments were acquired on a Bruker Avance 400 spectrometer (^{1}H, 400 MHz; ^{13}C, 100 MHz) at 25°C. NMR spectra were run in deuterated solvent as specified. The solvent signal was used as the internal reference. Resonances are quoted in ppm and coupling constants (*J*) are given in Hz.

2.4.6 Mass spectrometry (MS)

Synthetic compounds were resuspended in aqueous 50% CH_3CN/0.5% formic acid (v/v) and analysed by electrospray ionisation MS (ES-MS) in positive ion mode using a Micromass Q-

TOF2 equipped with a nanospray source. MS settings were as follows: cone voltage 25 V, LM/HM 12/12, MCP 2300 V, mass range 50-800 *m/z*.

For tandem MS (ES-MS/MS) analyses, ions were subjected to a range of collision energy settings (typically between 10-25 eV). All measurements were done in positive mode, unless stated otherwise.

High resolution mass spectrometry (HR-MS) was run on a Bruker Apex 3 4.7 T Bruker Daltonics (Billerrica, MA, USA). Samples were scanned with PEG 200 internal calibrant and accurate mass data was formulated on a VG Opus 3.6 Data station using Elemental Analysis software. Samples were flow injected by a Syringe pump into the Bruker electrospray source. The capillary exit voltage was 50 V.

2.4.7 Synthesis of 3-hydroxy-2-nitroacetophenone (9) (modified method of Butenandt *et al.*[263])

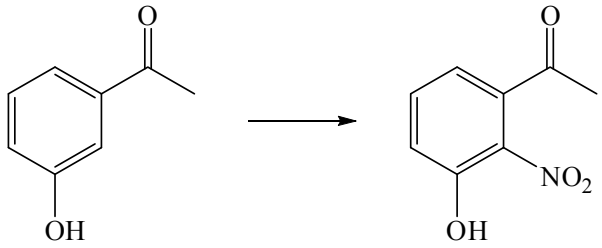

(8) (9)

3-Hydroxyacetophenone (8) (20.0 g, 0.15 mol) was dissolved in a mixture of glacial AcOH (110 mL, 1.92 mol) and acetic anhydride (12.0 mL, 0.13 mol). The colourless solution was stirred at 10-15°C in a water/ice bath. Ground $Cu(NO_3)_2 \cdot 2.5H_2O$ (40.0 g, 0.17 mol) was added over 3 h and the reaction mixture changed in colour to green. The reaction was monitored by TLC (DCM). This revealed formation of three spots, including the desired product. After 8 h, the green solution was stored in the fridge overnight. The next day the reaction was continued at 10-15°C for 8 h, with initial addition of ground $Cu(NO_3)_2 \cdot 2.5H_2O$ (20.0 g, 0.08 mol) over a period of 1 h. Upon completion, water (~200 mL) was added to the green solution and the reaction mixture was stirred at 10-15°C for ~1 h. The yellow precipitate was collected by vacuum filtration, rinsed with cold water and air dried. The filtrate was extracted with DCM (5 x ~200 mL), washed with saturated brine (3 x ~200 mL), dried with $MgSO_4$ and decolourised with activated carbon. The dried yellow solid was purified by two sequential

normal phase chromatography steps (DCM, followed by 5:1 toluene/EtOAc, v/v) to afford 3-hydroxy-2-nitroacetophenone (6.65 g, 25%, R_f 0.60 (DCM), R_f 0.35 (5:1 toluene/EtOAc, v/v), mp 138°C (lit. 134-6°C[268] and 138°C[263]) as a yellow solid. 3-Hydroxy-4-nitroacetophenone (12) and 3-hydroxy-6-nitroacetophenone (13) were collected as yellow solids, however, not being the desired products, accurate yields were not determined due to allowed losses during purification.

3-Hydroxy-2-nitroacetophenone (9): ν_{max}(KBr disc) 3144 (br, OH), 1668 (C=O), 1531 (NO_2), 1376 (NO_2), 1291 (C-O), 798 (out-of-plane aromatic C-H bend) cm^{-1}; ^{1}H NMR δ ($CDCl_3$) 10.50 (1H, s, OH), 7.59 (1H, dd, *J* 7.3, 8.5, ArH-5), 7.23 (1H, dd, *J* 1.2, 8.5, ArH-6), 6.85 (1H, dd, *J* 1.2, 7.3, ArH-4), 2.50 (3H, s, CH_3); ^{13}C NMR δ ($CDCl_3$) 199.4 (CO-2), 155.0 (ArC-3), 140.6 (ArC-2, ArC-1), 136.9 (ArC-5), 121.0 (ArC-6), 118.1 (ArC-4), 30.3 (C-1).

3-Hydroxy-4-nitroacetophenone (12) (R_f 0.09 (DCM), R_f 0.15 (5:1 toluene/EtOAc, v/v)): ^{1}H NMR δ ($CDCl_3$) 8.10 (1H, d, *J* 9.0, ArH-5), 6.94 (1H, dd, *J* 2.7, 9.0, ArH-6), 6.72 (1H, d, *J* 2.7, ArH-2), 6.58 (1H, s, OH), 2.50 (3H, s, CH_3).

3-Hydroxy-6-nitroacetophenone (13) (R_f 0.79 (DCM), R_f 0.57 (5:1 toluene/EtOAc, v/v)): ^{1}H NMR δ ($CDCl_3$) 10.25 (1H, s, OH), 8.17 (1H, dd, *J* 0.3, 9.0, ArH-5), 7.68 (1H, dd, *J* 0.3, 1.8, ArH-2), 7.50 (1H, dd, *J* 1.8, 9.0, ArH-4), 2.60 (3H, s, CH_3).

2.4.8 Synthesis of 4-(3-hydroxy-2-nitrophenyl)-4-oxobut-2-enoic acid (7)

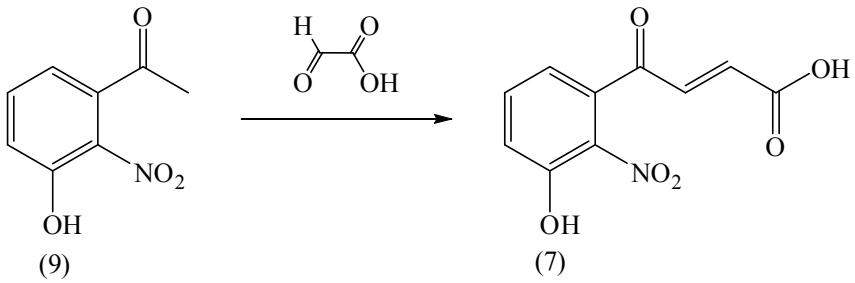

(9) (7)

2.4.8.1 Method 1 (modified method of Bianchi *et al.*[276])

3-Hydroxy-2-nitroacetophenone (9) (0.40 g, 2.2 mmol) was combined with melted glyoxylic acid monohydrate (2.0 g, 22 mmol) at 60°C. The yellow reaction mixture was further heated

to 120°C under vacuum. The reaction progress was monitored by normal phase TLC (EtOAc/1% AcOH, v/v). After 7 and 14 h, glyoxylic acid monohydrate (0.20 g, 2.17 mmol) was added. After 24 h, the brown viscous reaction mixture was set aside to cool to RT, dissolved in brine, extracted with DCM (5-6 x ~100 mL) and evaporated to ~50 mL. The crude reaction mixture was mixed with normal phase silica (~2 g) and the solvent evaporated. The crude product was purified by normal phase column chromatography (DCM/1% AcOH, v/v) to yield 4-(3-hydroxy-2-nitrophenyl)-4-oxobut-2-enoic acid (0.22 g, 42%, R_f 0.48 (EtOAc/1% AcOH, v/v), mp 157-159°C (lit.[263] 158°C)) as a yellow solid.

4-(3-Hydroxy-2-nitrophenyl)-4-oxobut-2-enoic acid (7): ν_{max}(KBr disc) 3500-2300 (br, OH, with C-H superimposed), 1704 (C=O), 1676 (C=O), 1601 (NO_2), 1518, 1431, 1348 (NO_2), 1273 (C-O), 1168 cm^{-1}; ^{1}H NMR δ ($CDCl_3$) 10.51 (1H, s, OH), 7.66 (1H, dd, *J* 7.3, 8.5, ArH-5), 7.31 (1H, dd, *J* 1.2, 8.5, ArH-6), 7.31 (1H, d, *J* 16.2, H-3), 6.90 (1H, dd, *J* 1.2, 7.3, ArH-4), 6.40 (1H, d, *J* 16.2, H-2); ^{13}C NMR δ ($CDCl_3$) 190.8 (CO-4), 166.3 (CO-1), 152.9 (ArC-3), 138.9 (C-3), 136.6 (ArC-2), 134.9 (ArC-1), 134.8 (ArC-5), 134.5 (C-2), 123.0 (ArC-6), 121.1 (ArC-4); ES-MS *m/z* 238.0 ($M+H^+$, 67%).

2.4.8.2 Method 2 (modified method of Bianchi *et al.*[276])

The reaction was repeated on the same scale as described above. After 24 h, the brown viscous reaction mixture was mixed with normal phase silica (~2 g) and set aside to cool to RT. The mixture was purified by normal phase column chromatography (DCM/1% AcOH, v/v) to yield 4-(3-hydroxy-2-nitrophenyl)-4-oxobut-2-enoic acid (0.28 g, 55%, R_f 0.48 (EtOAc/1% AcOH, v/v), mp 157-159°C (lit.[263] 158°C)) as a yellow solid. ^{1}H NMR, ^{13}C NMR and ES-MS were consistent with above.

2.4.8.3 Method 3

3-Hydroxy-2-nitroacetophenone (9) (88 mg, 0.46 mmol) was combined with glyoxylic acid monohydrate (0.5 g, 5.4 mmol) and placed into the cavity of a focused microwave reactor (CEM Discover) at 110°C. The reaction progress was monitored by normal phase TLC (EtOAc/1% AcOH, v/v). After 6 and 12 min, glyoxylic acid monohydrate (50 mg, 0.54 mmol) was added. After 17 min, the brown viscous reaction mixture was mixed with normal phase silica (~0.5 g) and set aside to cool to RT. The mixture was purified by normal phase

chromatography (DCM/1% AcOH, v/v) to yield 4-(3-hydroxy-2-nitrophenyl)-4-oxobut-2-enoic acid (69 mg, 60%, R_f 0.48 (EtOAc/1% AcOH, v/v), mp 157-159°C (lit.[263] 158°C)) as a yellow solid. ^{1}H NMR, ^{13}C NMR and ES-MS were consistent with above.

2.4.9 Synthesis of methyl 4-(3-hydroxy-2-nitrophenyl)-4-oxobut-2-enoate (10)

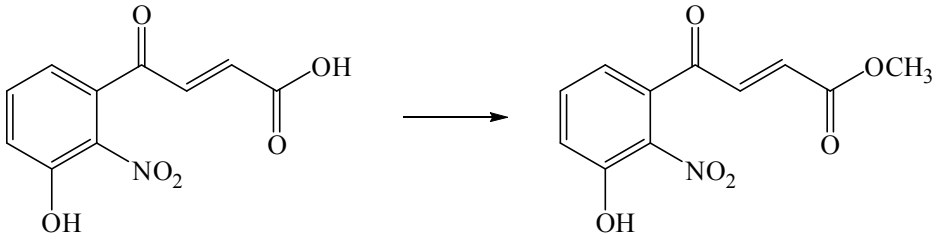

(7) (10)

2.4.9.1 Method 1

2.4.9.1.1 Preparation of dry MeOH[332]

A solution containing dry magnesium turnings (5 g), iodine (0.5 g) and distilled MeOH (50 mL) was heated to reflux until the iodine disappeared and all the magnesium had converted to magnesium methoxide (white). During distillation the condenser was fitted with a $CaCl_2$ drying tube to exclude moisture from the system. After 1 h, ~400 mL of distilled MeOH was added and the solution was refluxed for an additional 2 h. The MeOH was distilled into a brown bottle and stored under argon. The residue was cooled to RT, treated with 1 M HCl and discarded into organic waste.

2.4.9.1.2 Trial 1

4-(3-Hydroxy-2-nitrophenyl)-4-oxobut-2-enoic acid (7) (23 mg, 0.09 mmol) was dissolved in dry MeOH (2 mL) and concentrated H_2SO_4 (25 μL, 0.47 mmol) was added. The condenser was fitted with a $CaCl_2$ drying tube and the yellow reaction mixture was heated to reflux. The progress of the reaction was monitored by normal phase TLC (1:1 EtOAc/pet. spirit, v/v). After 1.5 h, the yellow solution was evaporated, redissolved in DCM, dried with $MgSO_4$ and concentrated to ~50 mL. The crude product was mixed with normal phase silica (~0.3 g) and purified by normal phase column chromatography (1:5 EtOAc/pet. spirit, v/v) to afford

methyl 4-(3-hydroxy-2-nitrophenyl)-4-oxobut-2-enoate (19 mg, 79%, R_f 0.65 (1:1 EtOAc/pet. spirit, v/v), 110-112°C (lit.[262] 111-112°C)) as a yellow solid. ^{1}H NMR was in agreement with the literature.[262]

Methyl 4-(3-hydroxy-2-nitrophenyl)-4-oxobut-2-enoate (10): ^{1}H NMR δ ($CDCl_3$) 10.50 (1H, OH, s), 7.65 (1H, dd, *J* 7.3, 8.6, ArH-5), 7.30 (1H, dd, *J* 1.3, 8.6, ArH-6), 7.25 (1H, d, *J* 16.1, H-3), 6.88 (1H, dd, *J* 1.3, 7.3, ArH-4), 6.40 (1H, d, *J* 16.1, H-2), 3.80 (3H, s, C$\underline{H_3}$); ES-MS *m/z* 250 ($M\text{-}H^+$, 100%).

2.4.9.1.3 Trial 2

4-(3-Hydroxy-2-nitrophenyl)-4-oxobut-2-enoic acid (7) (18 mg, 0.07 mmol) was dissolved in dry MeOH (2 mL) and concentrated H_2SO_4 (25 μL, 0.47 mmol). The condenser was fitted with a $CaCl_2$ drying tube and the yellow solution was stirred at RT. After 8 h, the yellow solution was evaporated and purified as described above to afford methyl 4-(3-hydroxy-2-nitrophenyl)-4-oxobut-2-enoate (14 mg, 72%, R_f 0.65 (1:1 EtOAc/pet. spirit, v/v)) as a yellow solid. ^{1}H NMR, ES-MS and mp were consistent with above and the literature.[262]

2.4.9.1.4 Trial 3

The reaction conditions described in Trial 1 were repeated with 4-(3-hydroxy-2-nitrophenyl)-4-oxobut-2-enoic acid (7) (1.7 g, 6.9 mmol), dry MeOH (170 mL) and concentrated H_2SO_4 (65 μL, 1.2 mmol). The condenser was fitted with a $CaCl_2$ drying tube and the yellow solution was heated to reflux. The progress of the reaction was monitored by normal phase TLC (1:1 EtOAc/pet. spirit (v/v) and EtOAc/1%AcOH (v/v)). After 6 h, the yellow solution was evaporated, redissolved in DCM, dried with $MgSO_4$ and concentrated to ~50 mL. The crude product was mixed with normal phase silica (~4 g) and evaporated. The dried mixture was purified by normal phase column chromatography (1:5 EtOAc/pet. spirit, v/v) to afford methyl 4-(3-hydroxy-2-nitrophenyl)-4-oxobut-2-enoate (1.6 g, 90%, R_f 0.65 (1:1 EtOAc/pet. spirit, v/v), R_f 0.84 (EtOAc/1%AcOH, v/v)) and a mixture of methyl 4-(3-hydroxy-2-nitrophenyl)-4-oxobut-2-enoate (10) and methyl 4-(3-hydroxy-2-nitrophenyl)-2-methoxy-4-oxo-butanoate (16) (156 mg, ~2:1) as yellow solids. ^{1}H NMR, ES-MS and mp of methyl 4-(3-hydroxy-2-nitrophenyl)-4-oxobut-2-enoate were consistent with above and the literature.[262]

2.4.9.2 Method 2

2.4.9.2.1 Preparation of dry toluene[332]

Distilled toluene was pre-dried overnight with anhydrous $CaCl_2$ and distilled into a brown bottle containing 4 Å molecular sieves over an atmosphere of argon. The toluene was stored in the dark under argon. The residue was cooled to RT, treated with isopropanol and subsequently with EtOH, and discarded into organic waste.

2.4.9.2.2 Trial 1 (modified method of Hermanson *et al.*[283])

The mixture of methyl 4-(3-hydroxy-2-nitrophenyl)-4-oxobut-2-enoate (10) and methyl 4-(3-hydroxy-2-nitrophenyl)-2-methoxy-4-oxobutanoate (16) (34 mg, ~2:1) was dissolved in a minimum amount of dry toluene (3 mL), concentrated H_2SO_4 (15 μL, 0.28 mmol) was added and the mixture was heated to reflux. The reaction progress was monitored by normal phase TLC (1:1 EtOAc/pet. spirit, v/v). After 4 h, the reaction mixture was evaporated and purified as described in Method 1 to afford methyl 4-(3-hydroxy-2-nitrophenyl)-4-oxobut-2-enoate (21 mg, R_f 0.65 (EtOAc/pet. spirit, v/v)) as a yellow solid. ^{1}H NMR, ES-MS and mp were consistent with above and the literature.[262]

2.4.9.2.3 Trial 2

The mixture of methyl 4-(3-hydroxy-2-nitrophenyl)-4-oxobut-2-enoate (10) and methyl 4-(3-hydroxy-2-nitrophenyl)-2-methoxy-4-oxobutanoate (16) (122 mg, ~2:1) were dissolved in a minimum amount of dry toluene (5 mL), concentrated H_2SO_4 (25 μL, 0.47 mmol) was added and the mixture was stirred at RT. The reaction progress was monitored by normal phase TLC (1:1 EtOAc/pet. spirit, v/v). After 16 h, the reaction mixture was evaporated and purified as described above to afford methyl 4-(3-hydroxy-2-nitrophenyl)-4-oxobut-2-enoate (105 mg, R_f 0.65 (1:1 EtOAc/pet. spirit, v/v)) as a yellow solid. ^{1}H NMR, ES-MS and mp were consistent with above and the literature.[262]

2.4.9.3 Method 3

2.4.9.3.1 Preparation of diazomethane[288]

WORK IN FUMEHOOD! EXPLOSIVE! Avoid rough or sharp glass surfaces and exposure to strong direct light.

Solution A, consisting of KOH (3 M, 2 mL) and EtOH (5 mL), was placed in a round bottom flask equipped with a dropping funnel and condenser. Solution B**,** consisting of *N*-methyl-*N*-nitrosotoluene-*p*-sulfonamide (1.0 g, 4.6 mmol) and diethyl ether (10 mL), was placed in the dropping funnel. Solution A was heated to 40°C and solution B was introduced into the flask over a period of ~30 min. The distilled ethereal diazomethane was collected in a round bottom flask while being cooled to -78°C (dry ice/acetone). The ethereal solution of diazomethane was stored at -80°C until used. The final concentration of diazomethane was not determined. It has been reported that the ethereal solution of diazomethane, prepared by the above procedure, contains ~70% of diazomethane.[288] The residual mixture of solutions A and B was neutralised by dropwise addition of AcOH (1 M) until no bubbling was observed and discarded into organic waste.

2.4.9.3.2 Trial 1

4-(3-Hydroxy-2-nitrophenyl)-4-oxobut-2-enoic acid (7) (190 mg, 0.80 mmol) was dissolved in diethyl ether (4 mL) and stirred at -78°C. The ethereal solution of diazomethane was added dropwise to the pale yellow solution over a period of 30-45 min until the reaction mixture changed in colour to a darker yellow. The progress of the reaction was monitored by normal phase TLC (1:1 EtOAc/pet. spirit, v/v). After 1 h, the yellow solution was evaporated and purified as described in Method 1. Methyl 4-(3-hydroxy-2-nitrophenyl)-4-oxobut-2-enoate (85 mg, 43%, R_f 0.65 (1:1 EtOAc/pet. spirit, v/v)) was afforded as a yellow solid. ^{1}H NMR, ES-MS and mp were consistent with above and the literature.[262]

2.4.9.3.3 Trial 2

The above reaction was repeated with 4-(3-hydroxy-2-nitrophenyl)-4-oxobut-2-enoic acid (7) (160 mg, 0.67 mmol) in diethyl ether (4 mL) at ~0°C. The ethereal solution of diazomethane

was added to the pale yellow solution, as described above. After 1 h of stirring, the yellow solution was worked up and purified, as described above, to afford methyl 4-(3-hydroxy-2-nitrophenyl)-4-oxobut-2-enoate (69 mg, 41%, R_f 0.65 (1:1 EtOAc/pet. spirit, v/v)) as a yellow solid. ^{1}H NMR, ES-MS and mp were consistent with above and the literature.[262]

2.4.9.3.4 Trial 3

The above reaction was repeated with 4-(3-hydroxy-2-nitrophenyl)-4-oxobut-2-enoic acid (7) (30 mg, 0.13 mmol) in MeOH (2 mL) at ~0°C. The ethereal solution of diazomethane was added to the pale yellow solution, as stated above. After 1 h, the yellow solution was worked up and purified, as described above, to afford methyl 4-(3-hydroxy-2-nitrophenyl)-4-oxobut-2-enoate (12 mg, 37%, R_f 0.65 (1:1 EtOAc/pet. spirit, v/v)) as a yellow solid. ^{1}H NMR, ES-MS and mp were consistent with above and the literature.[262]

2.4.9.4 Method 4

2.4.9.4.1 Trial 1

3-Hydroxy-2-nitroacetophenone (9) (20 mg, 0.11 mmol) was combined with melted glyoxylic acid monohydrate (100 mg, 1.09 mmol) at 60°C. The yellow reaction mixture was further heated to 120°C under vacuum. The formation of 4-(3-hydroxy-2-nitrophenyl)-4-oxobut-2-enoic acid was monitored by normal phase TLC (EtOAc/1% AcOH (v/v), R_f 0.48). After 7 h, a further portion of glyoxylic acid monohydrate (100 mg, 1.09 mmol) was added. After 24 h, the brown viscous reaction mixture was cooled to RT and dissolved in a mixture of dry MeOH (3 mL) and concentrated H_2SO_4 (25 μL, 0.47 mmol). The condenser was fitted with a $CaCl_2$ drying tube and the brown solution was stirred and heated to reflux. The progress of the reaction was monitored by normal phase TLC (1:1 EtOAc/pet. spirit, v/v). After 3 h, the brown solution was evaporated and purified 2 times as described in Method 1. Methyl 4-(3-hydroxy-2-nitrophenyl)-4-oxobut-2-enoate (13 mg, 48%, R_f 0.65 (1:1 EtOAc/pet. spirit, v/v)) was afforded as a yellow solid. ^{1}H NMR and ES-MS were consistent with above and the literature.[262]

2.4.9.4.2 Trial 2

The above procedure was repeated on a 300 mg (1.65 mmol) scale of 3-hydroxy-2-nitroacetophenone (9) and glyoxylic acid monohydrate (1.50 g, 16.3 mmol). After 4 and 8 h, a further portion of glyoxylic acid monohydrate (0.15 g, 1.63 mmol) was added. After 24 h, the brown viscous reaction mixture was cooled to RT and dissolved in a mixture of dry MeOH (25 mL) and concentrated H_2SO_4 (40 μL, 0.75 mmol). The condenser was fitted with a $CaCl_2$ drying tube and the brown reaction mixture was heated to reflux. The progress of the reaction was monitored as described above. After 8 h, the brown solution was evaporated and purified, as described in Method 1. Methyl 4-(3-hydroxy-2-nitrophenyl)-4-oxobut-2-enoate (117 mg, 28.0%, R_f 0.65 (1:1 EtOAc/pet. spirit, v/v)) was afforded as a yellow solid. ^{1}H NMR and ES-MS were consistent with above and the literature.[262]

2.4.10 Synthesis of ethyl 4-(3-hydroxy-2-nitrophenyl)-4-oxobut-2-enoate (17)

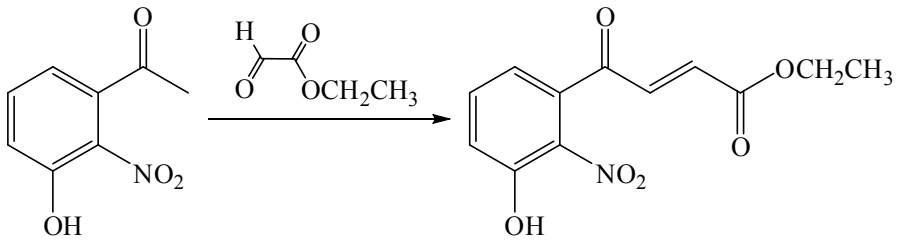

(9) (17)

2.4.10.1 Preparation of PPA/SiO_2 catalyst[294]

PPA (2.1 g) was added to $CHCl_3$ (100 mL) and stirred at 50°C for 1 h. Normal phase silica (5 g, 230-400 mesh size SiO_2) was added to the solution and the suspension was stirred for a further 1 h. The solvent was removed by rotary evaporation and the resulting solid was dried under vacuum (~20 mm Hg) at RT for ~4 h.

2.4.10.2 Method 1 (modified method of Sager *et al.*[293])

3-Hydroxy-2-nitroacetophenone (9) (100 mg, 0.55 mmol) was mixed with ethyl glyoxylate solution in toluene (0.5 mL (50%), 2.4 mmol), PPA/SiO_2 (~40 mg) and 2 Pasteur pipette drops of PPA (~30 μL). The reaction was left at 105°C and monitored by normal phase TLC

(5:1 toluene/EtOAc, v/v). After 4 and 8 h, a further portion of ethyl glyoxylate solution in toluene (0.1 mL (50%), 0.5 mmol) was added. After 12 h, the brown viscous reaction mixture was mixed with normal phase silica (~0.5 g) and set aside to cool to RT. The mixture was purified by normal phase column chromatography (1:5 EtOAc/pet. spirit, v/v) to afford ethyl 4-(3-hydroxy-2-nitrophenyl)-4-oxobut-2-enoate (92 mg, 63%, R_f 0.35 (5:1 toluene/EtOAc, v/v), mp 67-68°C) as a yellow solid.

Ethyl 4-(3-hydroxy-2-nitrophenyl)-4-oxobut-2-enoate (17): M-H^+, 264.049934 Da. Calculated for $C_{12}H_{10}NO_6$: M-H^+, 264.050812 Da; M+H^+ + Na, 288.049567 Da. Calculated for $C_{12}H_{11}NO_6Na$: M+H^+ + Na, 288.048407 Da; ν_{max}(KBr disc) 3303 (br, OH), 2993 (br, aromatic and aliphatic C-H), 1722 (C=O), 1677 (C=O), 1604 (NO_2), 1528, 1461, 1440, 1349 (NO_2), 1303, 1270, 1187 (C-O), 818 (out-of-plane aromatic C-H bend), 698 (out-of-plane aromatic C-H bend) cm^{-1}; ^{1}H NMR δ ($CDCl_3$) 10.60 (1H, s, OH), 7.60 (1H, dd, *J* 7.6, 8.0, ArH-5), 7.26 (1H, dd, *J* 1.2, 8.0, ArH-6), 7.23 (1H, d, *J* 16.1, H-3), 6.85 (1H, dd, *J* 1.2, 7.6, ArH-4), 6.34 (1H, d, *J* 16.1, H-2), 4.17 (2H, q, *J* 7.1, $C\underline{H_2}CH_3$), 1.22 (3H, t, *J* 7.1, $CH_2C\underline{H_3}$); ^{13}C NMR δ ($CDCl_3$) 191.3 (CO-4), 164.8 (CO-1), 155.4 (ArC-3), 139.4 (C-3), 137.1 (ArC-1), 136.9 (ArC-5), 132.7 (C-2), 131.4 (ArC-2), 122.1 (ArC-6), 119.9 (ArC-4), 61.6 ($\underline{C}H_2CH_3$), 14.0 ($CH_2\underline{C}H_3$); ES-MS *m/z* 264.0 (M-H^+, 100%).

2.4.10.3 Method 2

3-Hydroxy-2-nitroacetophenone (9) (100 mg, 0.55 mmol) was mixed with ethyl glyoxylate solution in toluene (0.5 ml (50%), 2.4 mmol), PPA/SiO_2 (~100 mg) and 2 drops of PPA. The reaction mixture was placed into the cavity of a focused microwave reactor (CEM Discover) at 110°C and monitored by TLC (5:1 toluene/EtOAc, v/v). After 30 and 60 min, a further portion of ethyl glyoxylate solution in toluene (0.1 mL (50%), 0.5 mmol) was added. After 130 min, the brown reaction mixture was mixed with normal phase silica (0.5 g) and set aside to cool to RT. The mixture was purified, as described in Method 1, to afford ethyl 4-(3-hydroxy-2-nitrophenyl)-4-oxobut-2-enoate (85 mg, 58%, R_f 0.35 (5:1 toluene/EtOAc, v/v)) as a yellow solid. ^{1}H NMR, ^{13}C NMR, ES-MS and mp were consistent with above.

2.4.10.4 Method 3

3-Hydroxy-2-nitroacetophenone (9) (24 mg, 0.13 mmol) was mixed with ethyl glyoxylate solution in toluene (0.17 mL (50%), 0.83 mmol) and formic acid (0.10 mL, 2.7 mmol). The reaction mixture was placed into a microwave reactor at 110°C and monitored by TLC (5:1 toluene/EtOAc, v/v). After 30 and 60 min, a further portion of ethyl glyoxylate solution in toluene (0.10 mL (50%), 0.5 mmol) was added. After 70 and 100 min, formic acid (0.10 mL, 2.7 mmol) was added to the brown reaction mixture. After 130 min, the brown reaction mixture showed only starting material by TLC and was therefore discarded.

2.4.10.5 Method 4

3-Hydroxy-2-nitroacetophenone (9) (53 mg, 0.29 mmol) was mixed with ethyl glyoxylate solution in toluene (0.3 ml (50%), 1.5 mmol) and montmorillonite KSF clay (0.5 g). The reaction mixture was placed into a microwave reactor at 110°C and monitored by TLC (5:1 toluene/EtOAc, v/v). After 40 and 80 min, a further portion of ethyl glyoxylate solution in toluene (0.1 mL (50%), 0.5 mmol) was added and after 145 min the brown reaction mixture was mixed with normal phase silica (0.1 g) and set aside to cool to RT. The mixture was purified, as described in Method 1, to afford ethyl 4-(3-hydroxy-2-nitrophenyl)-4-oxobut-2-enoate (44 mg, 57%, R_f 0.35 (5:1 toluene/EtOAc, v/v)) as a yellow solid. ^{1}H NMR, ^{13}C NMR, ES-MS and mp were consistent with above.

2.4.11 Synthesis of methyl (11) and ethyl (18) 4-(2-nitro-3-((2,3,4,5-tetra-*O*-acetyl-β-D-glucopyranosyl)oxyphenyl)-4-oxobut-2-enoate

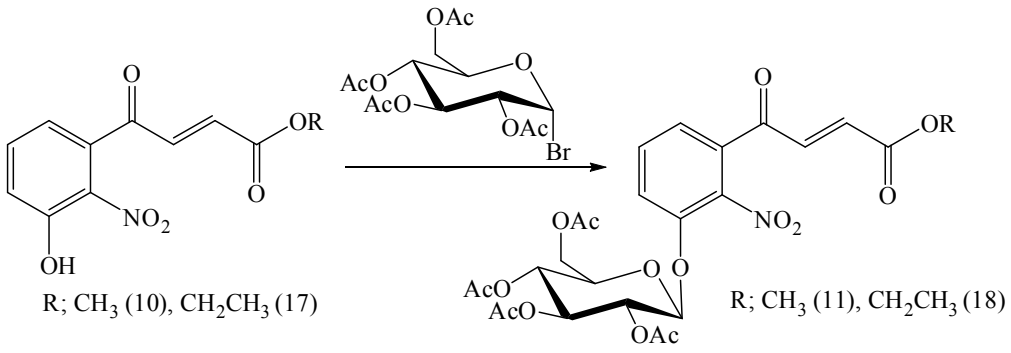

2.4.11.1 Preparation of dry DCM[332]

DCM was dried as described for toluene in Section 2.4.9.2.1.

2.4.11.2 Method 1

Methyl 4-(3-hydroxy-2-nitrophenyl)-4-oxobut-2-enoate (10) (100 mg, 0.40 mmol), ground anhydrous K_2CO_3 (108 mg, 0.78 mmol), ground anhydrous tetra-*n*-butyl ammonium bromide (0.10 g, 0.37 mmol) and ABG (82 mg, 0.20 mmol) were mixed and placed under vacuum at 90°C in the dark. K_2CO_3 and tetra-*n*-butyl ammonium bromide were kept in an oven at 80°C for 24 h before use. The progress of the reaction was monitored by TLC (1:1 EtOAc/pet. spirit, v/v). Additional ABG (246 mg, 0.60 mmol) was added in portions over 9 h. After 9 h, the dark brown reaction mixture was dissolved in DCM, filtered through a plug of celite and mixed with normal phase silica (~1 g). The crude mixture was chromatographed (1:2 EtOAc/pet. spirit, v/v) to yield ethyl 4-(2-nitro-3-((2,3,4,5-tetra-*O*-acetyl-β-D-glucopyranosyl)oxyphenyl)-4-oxobut-2-enoate (75 mg, 33%, R_f 0.40 (1:1 EtOAc/pet. spirit, v/v)) as a white solid.

Methyl 4-(2-nitro-3-((2,3,4,5-tetra-*O*-acetyl-β-D-glucopyranosyl)oxyphenyl)-4-oxobut-2-enoate (11): ^{1}H NMR δ ($CDCl_3$) 7.58 (1H, m, ArH-5), 7.55 (1H, m, ArH-6), 7.54 (1H, d, *J* 15.7, H-3), 7.47 (1H, m, ArH-4), 6.72 (1H, d, *J* 15.7, H-2), 5.20-5.30 (2H, m, H-2' and H-3'), 5.14 (1H, m, H-4'), 5.06 (1H, m, H-1'), 4.22 (2H, d, *J* 3.9, H-6'), 3.86 (1H, m, H-5'), 3.80 (3H, s, C$\underline{H_3}$), 2.13 (3H, s, COC$\underline{H_3}$), 2.10 (3H, s, COC$\underline{H_3}$), 2.05 (3H, s, COC$\underline{H_3}$), 2.03 (3H, s, COC$\underline{H_3}$); ^{13}C NMR δ ($CDCl_3$) 187.5 (CO-4), 170.4 ($\underline{C}OCH_3$), 170.1 ($\underline{C}OCH_3$), 169.3 ($\underline{C}OCH_3$), 169.3 ($\underline{C}OCH_3$), 165.2 (CO-1), 148.5 (ArC-3), 141.2 (ArC-2), 136.4 (C-3), 134.2 (C-2), 131.5 (ArC-5), 131.5 (ArC-1), 124.1 (ArC-4), 123.7 (ArC-6), 100.4 (C-1'), 72.4, 70.3, 67.9 (C-3', C-2', C-4'), 72.1 (C-5'), 61.6 (C-6'), 52.5 ($\underline{C}H_3$), 21.0, 20.6, 20.5, 20.4 (4 x CO$\underline{C}H_3$); ES-MS *m/z* 582.0 ($M+H^+$, 100%).

2.4.11.3 Method 2

Methyl 4-(3-hydroxy-2-nitrophenyl)-4-oxobut-2-enoate (10) (0.70 g, 2.8 mmol) was dissolved in dry DCM (70 mL). Ground anhydrous K_2CO_3 (1.4 g, 0.01 mol), ABG (1.8 g, 4.4 mmol) and ground anhydrous tetra-*n*-butyl ammonium bromide (0.17 g, 0.53 mmol) were

added and the bright orange suspension was allowed to stir at RT in the dark under argon. The reaction was monitored by TLC (1:1 EtOAc/pet. spirit, v/v). Additional ABG (500 mg, 1.2 mmol) was added after 9, 24 and 36 h. After 2.5 days, the red-brown reaction mixture was filtered through a plug of celite, mixed with normal phase silica (~4 g) and evaporated to dryness. The crude mixture was chromatographed, as described in Method 1, to yield methyl 4-(2-nitro-3-((2,3,4,5-tetra-*O*-acetyl-β-D-glucopyranosyl)oxyphenyl)-4-oxobut-2-enoate (1.3 g, 78%, R_f 0.40 (1:1 EtOAc/pet. spirit, v/v)) as a white solid. ^{1}H NMR, ^{13}C NMR and ES-MS were in agreement with above and the literature.[262]

2.4.11.4 Method 3

Ethyl 4-(3-hydroxy-2-nitrophenyl)-4-oxobut-2-enoate (17) (252 mg, 0.95 mmol) was dissolved in dry DCM (30 mL). Ground anhydrous K_2CO_3 (660 mg, 4.78 mmol), ground anhydrous tetra-*n*-butyl ammonium bromide (70 mg, 0.21 mmol) and ABG (810 mg, 2.0 mmol) were added and the bright orange suspension was allowed to stir at RT in the dark under argon. The reaction was monitored by TLC (1:1 EtOAc/pet. spirit, v/v). Additional ABG (200 mg, 0.49 mmol) was added after 9, 24 and 36 h. After 2 days, the red-brown reaction mixture was filtered through a plug of celite, mixed with normal phase silica (~1.5 g) and evaporated to dryness. The crude mixture was chromatographed, as described above (Method 1), to yield ethyl 4-(2-nitro-3-((2,3,4,5-tetra-*O*-acetyl-β-D-glucopyranosyl)oxyphenyl)-4-oxobut-2-enoate (395 mg, 70%, R_f 0.20 (1:1 EtOAc/pet. spirit, v/v)) as a colourless film.

Ethyl 4-(2-nitro-3-((2,3,4,5-tetra-*O*-acetyl-β-D-glucopyranosyl)oxyphenyl)-4-oxobut-2-enoate (18): M+H$^+$, 596.160931 Da. Calculated for $C_{26}H_{30}N_1O_{15}$: M+H$^+$, 596.161545 Da; M+H$^+$ + Na, 618.143494 Da. Calculated for $C_{26}H_{29}N_1O_{15}Na$: M+H$^+$ + Na, 618.143489 Da; ν_{max}(KBr disc) 3473 (br, OH), 2974 (br, aromatic and aliphatic C-H), 1752 (br, C=O), 1679 (C=O), 1543 (NO_2), 1455, 1369 (NO_2), 1304, 1227 (br, C-O), 1075 (C-O-C), 1037 cm^{-1}; ^{1}H NMR δ ($CDCl_3$) 7.58-7.45 (3H, m, ArH-4, ArH-5, ArH-6), 7.48 (1H, d, *J* 15.8, H-3), 6.72 (1H, d, *J* 15.8, H-2), 5.20-5.28 (2H, m, H-2' and H-3'), 5.14 (1H, m, H-4'), 5.06 (1H, m, H-1'), 4.25 (2H, m, H-6'), 4.20 (2H, m, C$\underline{H_2}$-CH_3) 3.85 (1H, m, H-5'), 2.11 (3H, s, COC$\underline{H_3}$), 2.07 (3H, s, COC$\underline{H_3}$), 2.03 (3H, s, COC$\underline{H_3}$), 2.01 (3H, s, COC$\underline{H_3}$), 1.31 (3H, t, *J* 7.1, CH_2C$\underline{H_3}$); ^{13}C NMR δ ($CDCl_3$) 187.7 (CO-4), 170.4 (C$\underline{O}$$CH_3$), 170.1 (C$\underline{O}$$CH_3$), 169.6 (C$\underline{O}$$CH_3$), 169.3 (C$\underline{O}$$CH_3$), 164.8 (CO-1), 148.5 (ArC-3), 141.2 (ArC-2), 136.3 (C-3), 134.8 (C-2), 131.6 (ArC-5), 131.0

(ArC-1), 124.1 (ArC-4), 123.6 (ArC-6), 100.7 (C-1'), 72.4, 70.3, 67.9 (C-2', C-3', C-4'), 72.1 (C-5'), 67.9 ($\underline{C}H_2CH_3$) 61.6 (C-6'), 20.6, 20.6, 20.5, 20.4 (4 x CO$\underline{C}H_3$), 14.1 ($CH_2\underline{C}H_3$); ES-MS *m/z* 596.0 ($M+H^+$, 100%), 618.0 ($M+H^+$ + Na, 70%), 331.0 (56%).

2.4.12 **Synthesis of 3-hydroxykynurenine-*O*-β-D-glucoside (3OHKG)** (modified method of Manthey *et al.*[262])

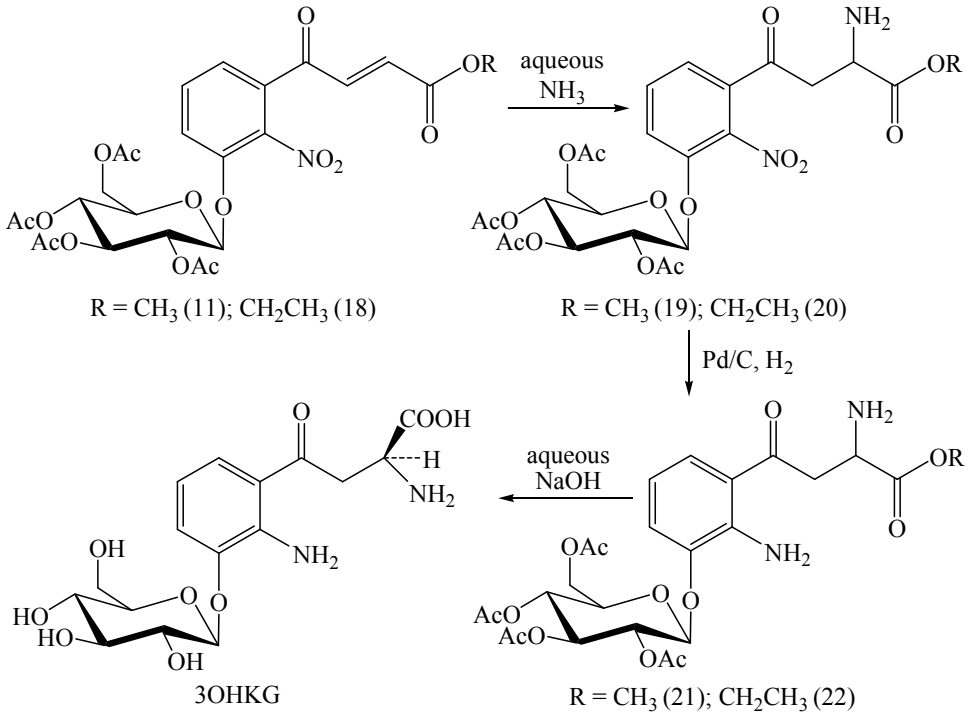

2.4.12.1 Method 1

A colourless solution of methyl 4-(2-nitro-3-((2,3,4,5-tetra-*O*-acetyl-β-D-glucopyranosyl)oxyphenyl)-4-oxobut-2-enoate (11) (0.27 g, 0.46 mmol), EtOAc (250 mL) and aqueous NH_3 (0.50 mL (28%), 8.2 mmol) was stirred at RT under argon in the dark. The formation of methyl 2-amino-4-(2-nitro-3-((2,3,4,5-tetra-*O*-acetyl-β-D-glucopyranosyl)oxyphenyl)-4-oxobutanoate (19) was monitored by normal phase TLC (EtOAc, R_f 0.03), visualising by UV (254 nm) and ninhydrin, and by LC-MS (*m/z* 599 ($M+H^+$, 100%), λ_{max} 245/301 nm). After 3 h, Pd/C (20 mg) was added and the reaction mixture was placed under an atmosphere of H_2 (1 atm). The formation of methyl 2-amino-4-(2-amino-3-((2,3,4,5-tetra-*O*-acetyl-β-D-glucopyranosyl)oxyphenyl)-4-oxobutanoate (21) was monitored by normal phase TLC (BAW, R_f 0.37), visualising by UV (365 nm) and ninhydrin, and by LC-MS (*m/z* 569 ($M+H^+$, 100%), λ_{max} 231/371 nm). After 3 h, the reaction mixture

was filtered through a plug of celite and the yellow solution was evaporated under reduced pressure. The yellow-orange residue was mixed with argon-gassed (~20 min) aqueous NaOH (190 mL, 0.05 mM) and aqueous NH_3 (0.10 mL (28%), 1.6 mmol) and left to stir at RT under argon in the dark. The formation of 3OHKG was monitored by TLC of normal phase (BAW) and reversed phase (water/0.05% TFA, v/v), visualising by UV (254 and 365 nm) and ninhydrin, and by LC-MS (*m/z* 387 ($M+H^+$, 100%), λ_{max} 263/365 nm). An additional compound (U-24) was observed by normal phase (BAW, R_f 0.25) and reversed phase (H_2O, R_f 0.52) TLC, and by LC-MS (*m/z* 385 ($M+H^+$, 100%), 407 ($M+H^+$ + Na), λ_{max} 324 nm). After 8.5 h, the yellow solution was acidified by AcOH (1 M) to pH 6 and purified by preparative RP-HPLC to afford 3OHKG (51 mg, 27%, R_f 0.12 (BAW), R_f 0.66 (water/0.05% TFA, v/v), Rt 10.2 min) as a pale yellow solid and U-24 (35 mg, 20%, R_f 0.25 (BAW), R_f 0.52 (water), Rt 20.5 min) as a white solid. ^{1}H NMR, absorbance and fluorescence of 3OHKG were consistent with the literature.[260,262]

3-Hydroxykynurenine-*O*-β-D-glucoside (3OHKG): $M-H^+$, 385.123035. Calculated for $C_{16}H_{21}N_2O_9$: $M-H^+$, 385.124706; ν_{max}(KBr disc) 3600-2300 (br, zwitterionic NH_3^+, COO^-, NH_2, OH, with C-H superimposed), 1642 (br, C=O), 1618, 1219 (C-O), 1075 (C-O-C) cm^{-1}; ^{1}H NMR δ (D_2O) 7.52 (1H, d, *J* 8.1, ArH-6), 7.23 (1H, d, *J* 8.1, ArH-4), 6.65 (1H, dd, *J* 8.1, 8.1, ArH-5), 4.94 (1H, d, *J* 7.3, H-1'), 4.05 (1H, m, H-2), 3.82 (1H, dd, *J* 1.6, 12.5, H-6'), 3.68 (1H, dd, *J* 5.3, 12.5, H-6'), 3.65 (2H, m, H-3), 3.53-3.48 (2 x 1H, m, H-2' and H-3'), 3.47 (0.5H, m, H-4'), 3.44 (0.5H, m, H-5'), 3.42 (0.5H, m, H-5'), 3.38 (0.5H, m, H-4'); ^{13}C NMR δ (D_2O) 200.0 (CO-4), 173.8 (CO-1), 145.3 (ArC-3), 141.7 (ArC-2), 126.1 (ArC-6), 121.3 (ArC-4), 118.5 (ArC-1), 116.5 (ArC-5), 101.8 (C-1'), 76.6 (C-5'), 75.9 (C-2'), 73.2 (C-3'), 69.7 (C-4'), 60.8 (C-6'), 50.6 (C-2), 39.5 (C-3); ES-MS/MS *m/z* 387.0 ($M+H^+$, 5%), 370.0 ($M+H^+$ - NH_2, 3%), 225.1 ($M+H^+$ - Glu, 2%), 208.1 ($M+H^+$ - NH_2 - Glu, 100%), 162.0 (40%), 152.0 ($M+H^+$ - Glu - $HC(NH_2)COOH$, 5%), 127.0 (1%), 110.0 ($M+H^+$ - Glu - $C(O)CH_2CH(NH_2)COOH$, 78%), 84.9 (3%). λ_{max} 262 and 365 nm and maximum fluorescence at λ_{ex} 360 / λ_{em} 500 nm.

U-24: $M+H^+$, 385.123035. Calculated for $C_{16}H_{21}N_2O_9$: $M+H^+$, 385.124706; $M-H^+$, 383.1027. Calculated for $C_{16}H_{19}N_2O_9$: $M-H^+$, 383.1091; ν_{max}(KBr disc) 3600-2300 (br, zwitterionic NH_3^+, COO^-, OH, with C-H superimposed), 1649 (br, C=O), 1202 (C-O), 1076 (C-O-C) cm^{-1}; ^{1}H NMR δ (D_2O) 7.22 (1H, d, *J* 8.2, ArH-6), 6.92 (1H, m, ArH-5), 6.88 (1H, m, ArH-4), 5.20 (1H, d, *J* 7.5, H-1'), 4.02 (1H, m, H-2), 3.82 (1H, m, H-6'), 3.65 (1H, m, H-6'), 3.64 (2H, m,

H-3), 3.60-3.55 (2 x 1H, m, H-2'and H-3'), 3.52 (1H, m, H-5'), 3.41 (1H, m, H-4'); ^{13}C NMR δ (D_2O) 174.1 (CO-1), 165.8 (CO-4), 152.3 (ArC-2), 143.9 (ArC-3), 125.5 (ArC-5), 119.1 (ArC-1), 114.3 (ArC-6), 112.7 (ArC-4), 100.4 (C-1'), 76.7 (C-5'), 75.8 (C-2'), 73.2 (C-3'), 69.8 (C-4'), 60.9 (C-6'), 53.8 (C-2), 28.9 (C-3); ES-MS/MS *m/z* 385.2 ($M+H^+$, 8%), 368.1 ($M+H^+$ - NH_2, 6%), 224.1 (14%), 223.1 ($M+H^+$ - Glu, 100%), 206.1 ($M+H^+$ - NH_2 - Glu, 8%), 181.1 (2%), 177.1 (1%), 162.1 (1%), 150.1 ($M+H^+$ - Glu - $HC(NH_2)COOH$, 8%), 135.1 ($M+H^+$ - Glu - $CH_2CH(NH_2)COOH$, 1%), 125.1 (2%); ES-MS/MS *m/z* 383.5 ($M-H^+$, 18%), 366.4 ($M-H^+$ - NH_2, 100%), 310.4 (4%), 249.2 (3%), 221.2 ($M-H^+$ - Glu, 5%), 204.2 ($M-H^+$ - NH_2 - Glu, 3%), 181.1 (10%), 160.2 (69%), 145.0 ($M-H^+$ - Glu - $HC(NH_2)COOH$, 2%), 133.1 ($M-H^+$ - Glu - $CH_2CH(NH_2)COOH$, 5%), 113.1 (25%). λ_{max} 323 nm.

2.4.12.2 Method 2

A colourless solution of ethyl 4-(2-nitro-3-((2,3,4,5-tetra-*O*-acetyl-β-D-glucopyranosyl)oxyphenyl)-4-oxobut-2-enoate (18) (0.384 g, 0.65 mmol), EtOAc (250 mL) and aqueous NH_3 (0.50 mL (28%), 8.2 mmol) was stirred in the dark under argon. The formation of ethyl 2-amino-4-(2-nitro-3-((2,3,4,5-tetra-*O*-acetyl-β-D-glucopyranosyl)oxyphenyl)-4-oxobutanoate (20) was monitored by normal phase TLC (EtOAc, R_f 0.05), as described in Method 1, and by LC-MS (*m/z* 613 ($M+H^+$, 100%), 635 ($M+H^+$ + Na), λ_{max} 246/300 nm). After 3 h, Pd/C (20 mg) was added and the reaction mixture was placed under an atmosphere of H_2 (1 atm). The formation of ethyl 2-amino-4-(2-amino-3-((2,3,4,5-tetra-*O*-acetyl-β-D-glucopyranosyl)oxyphenyl)-4-oxobutanoate (22) was monitored by TLC (BAW, R_f 0.37) as described in Method 1, and by LC-MS (*m/z* 583 ($M+H^+$, 100%), λ_{max} 230/265/372 nm). After 3 h, the reaction mixture was filtered through a plug of celite and the yellow solution was evaporated under reduced pressure. The yellow-orange residue was mixed with argon-gassed (~20 min) aqueous NaOH (200 mL, 3.5 mM) and aqueous NH_3 (0.10 mL (28%), 1.6 mmol) and left to stir at RT under argon in the dark. The formation of 3OHKG and U-24 was monitored by TLC and LC-MS, as described above. After 8.5 h, the yellow solution was worked up and purified, as described above, to afford 3OHKG (66 mg, 27%, R_f 0.12 (BAW), R_f 0.66 (water/0.05% TFA, v/v), Rt 10.3 min) as a pale yellow solid and U-24 (45 mg, 18%, R_f 0.25 (BAW), R_f 0.53 (water), Rt 20.6 min) as a white solid. ^{1}H NMR, ^{13}C NMR, ES-MS/MS, IR, absorbance and fluorescence of 3OHKG and U-24 were consistent with above. ^{1}H NMR, absorbance and fluorescence of 3OHKG were consistent with the literature.[260,262]

2.4.13 Stability of 3OHKG and Kyn under basic conditions

3OHKG was dissolved in argon-gassed (~20 min) aqueous NaOH (0.05 M, 4 mL, pH ~12.5) to give a final concentration of 0.45 mM. The colourless solutions (3 × 4 mL) were sealed and incubated in the dark at 37°C with gentle shaking. Single aliquots were taken from each solution over 24 h, acidified with AcOH (1 M) to pH ~5-6 and analysed by RP-HPLC. Separate stability studies were repeated with Kyn (1.2 mM) under similar conditions.

2.4.14 Stability of 3OHKG under basic conditions in the presence of NH_3

3OHKG was dissolved in argon-gassed (~20 min) NaOH (0.05 M, 4 mL, pH ~12.5) to give a final concentration of 0.32 mM. Aqueous NH_3 (10 µL (28%), 0.04 M) was added and the colourless solutions (3 × 4 mL) were sealed and incubated in the dark at 37°C with gentle shaking. Single aliquots were taken from each solution over 24 h, acidified with AcOH (1 M) to pH ~5-6 and analysed by RP-HPLC.

2.4.15 Hydrogenation of U-24

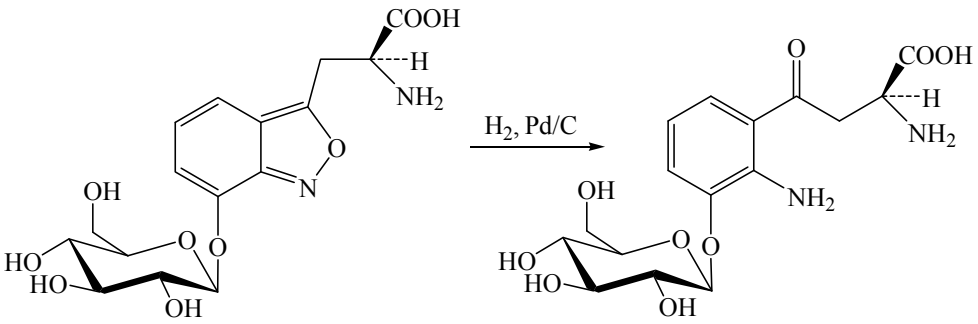

3OHKG U-24

2.4.15.1 Method 1

A colourless solution of U-24 (16 mg, 0.04 mmol) and aqueous TFA (3 mL, 0.05%, v/v) at pH ~4 was placed under an atmosphere of H_2 (1 atm) in the presence of Pd/C (10 mg) at RT in the dark. The progress of the reaction was monitored by TLC of reversed phase (5% CH_3CN/0.05% TFA, v/v), visualising by UV and ninhydrin. After 10 min, the reaction mixture was filtered through a plug of celite and the pale yellow solution was lyophilised. The crude product was dissolved in 5% CH_3CN/0.05% TFA (v/v) and purified by preparative RP-

HPLC, as described above for 3OHKG. The fractions containing the product (Rt 10.3 min) were collected and lyophilised to yield 3OHKG (11 mg, 65%, R_f 0.65, (5% CH_3CN/0.05% TFA, v/v)) as a light yellow solid. ^1H NMR, ES-MS/MS, absorbance and fluorescence were consistent with above and the literature.[260,262]

2.4.15.2 Method 2

A colourless solution of U-24 (13 mg, 0.03 mmol) and water (2 mL) was placed under an atmosphere of H_2 (1 atm) in the presence of Pd/C (10 mg) at RT in the dark. The progress of the reaction was monitored, as described above in Method 1. After 10 min, the reaction mixture was worked up and purified, as described above in Method 1, to yield 3OHKG (12 mg, 92%, R_f 0.65, (5% CH_3CN/0.05% TFA, v/v)) as a light yellow solid. ^1H NMR, ES-MS/MS, absorbance and fluorescence were consistent with above and the literature.[260,262]

CHAPTER 3

FACILE SYNTHESIS OF THE UV FILTER COMPOUNDS 3OHKyn AND AHBG

The overall aim of this chapter was to use precursors in the synthesis of 3OHKG for the facile synthesis of 3-hydroxykynurenine (3OHKyn) and 4-(2-amino-3-hydroxyphenyl)-4-oxobutanoic acid-*O*-β-D-glucoside (AHBG).

3.1 Introduction

With the success of the 3OHKG synthesis (described in Chapter 2), an additional study was undertaken to expand the synthetic strategy to the synthesis of other UV filter compounds. Of particular interest was the synthesis of 3OHKyn and AHBG. 3OHKyn is commercially available, but very expensive (AU$103/25 mg), while AHBG is not commercially available and must be synthesised. Therefore, the specific aims of this chapter were to allow cost effective synthesis of 3OHKyn and AHBG using a common pathway to that introduced for 3OHKG in Chapter 2 and to provide AHBG in sufficient quantities for subsequent identification and quantification studies in Chapter 4. 3OHKyn[263,333,334] and AHBG[262,335] have been previously synthesised by different groups. An overview of their synthetic procedures is given below.

3.1.1 Previous synthesis of 3OHKyn

In 1951, Kotake *et al.*[333] reported the syntheses of 3OHKyn from 2-nitro-3-methoxytoluene (26) in 10 steps and 9.6% overall yield (Scheme 3.1). The acid chloride (28) of 2-nitro-3-methoxybenzoic acid (27), prepared by oxidation of (26), was condensed with ethyl acetoacetate and subsequently converted to the benzoylacetate (30). This was then alkylated and acid cleaved to yield the butanoic acid (32). The butanoic acid was brominated to the bromoketonic acid (33), which was then hydrolysed to the acrylic acid (34). Addition of NH_3 to the unsaturated intermediate and reduction of the aromatic nitro group yielded the amino acid (36). Subsequent demethylation and neutralisation gave 3OHKyn.

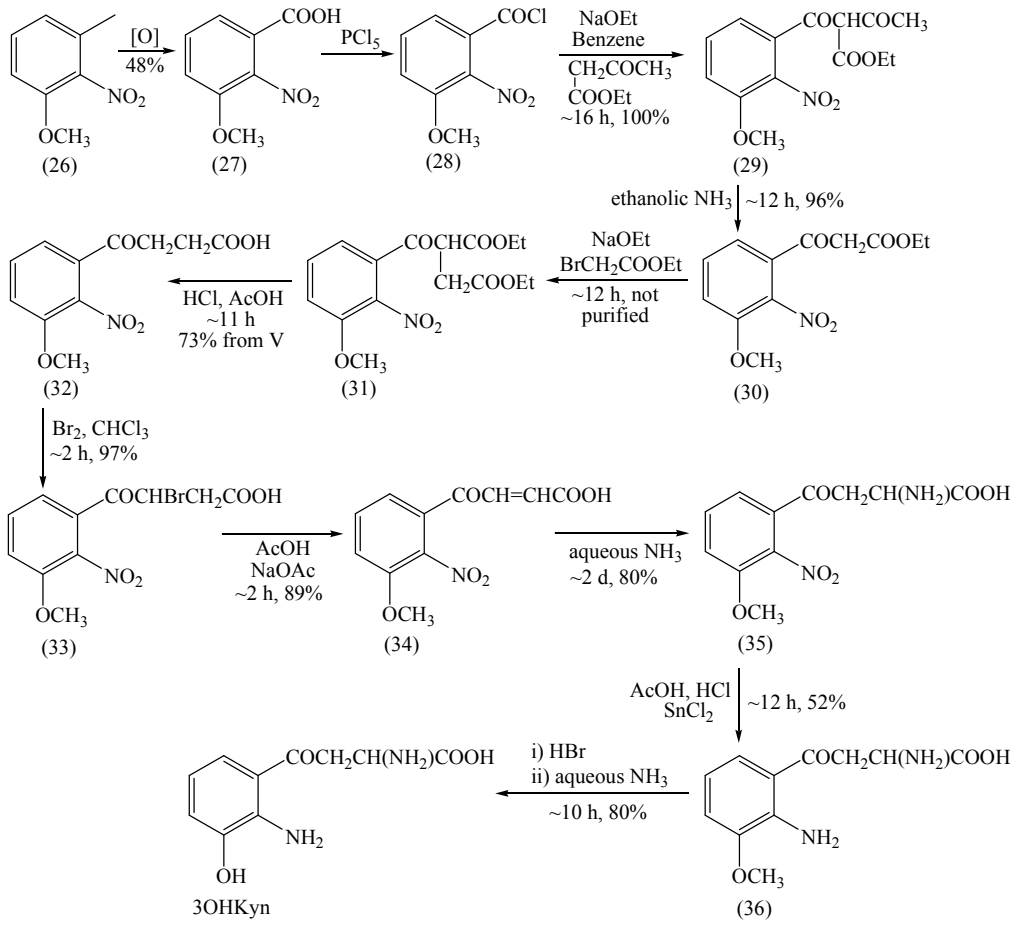

Scheme 3.1: Synthesis of 3OHKyn by Kotake *et al.*[333]

In 1957, Butenandt *et al.*[263] reported two alternative synthetic pathways towards 3OHKyn, starting with nitration of 3-hydroxyacetophenone (8) to 3-hydroxy-2-nitroacetophenone (9), as described in Chapter 2 (Scheme 3.2). In pathway A, the acetophenone (9) was protected as the benzyl ether (37) and then condensed with diethyl oxalate to give (38). Treatment with NH_4OH gave the hydroxylimine (39), which was reduced with Raney Ni and Pd/C to 3OHKyn in 6.4% yield from (8) (5 steps). In pathway B, regarded as the simpler pathway by the authors, the acetophenone (9) was condensed with Ba glyoxylate to give the acrylic acid (7). While this condensation gave the authors the acrylic acid in 64% yield, it proved to be a difficult reaction in our laboratory (Chapter 2). The acrylic acid was subsequently aminated with aqueous NH_3 and the nitro group reduced to yield 3OHKyn in 6.6% yield from (8) (4 steps).

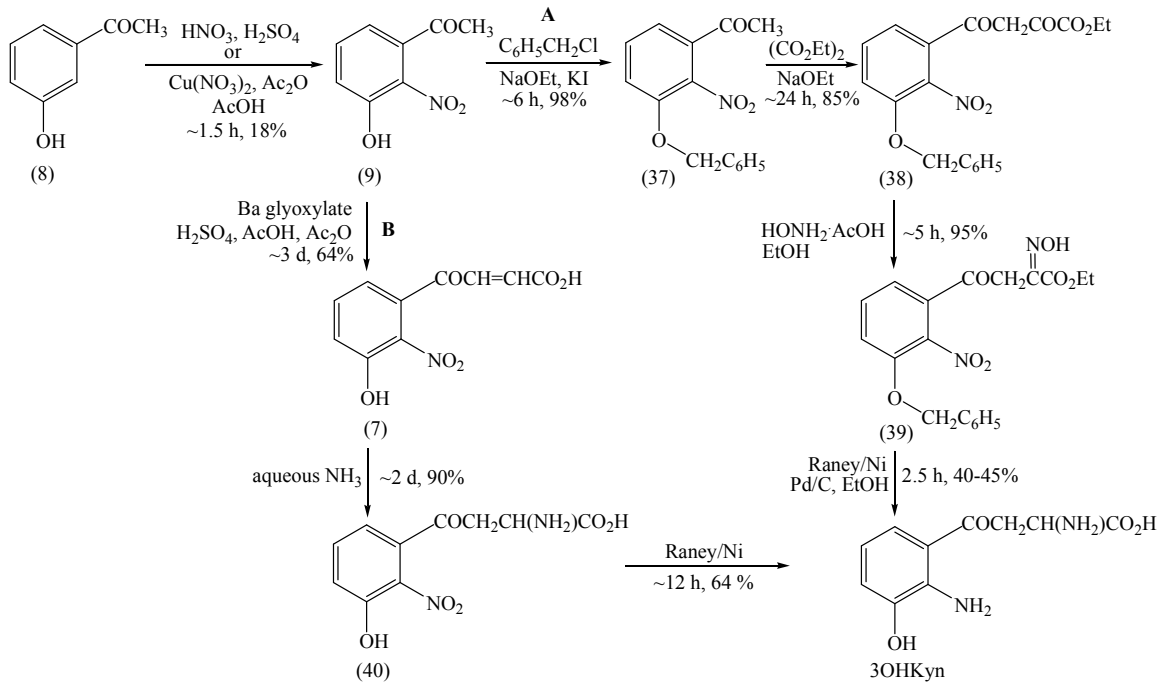

Scheme 3.2: Synthesis of 3OHKyn by Butenandt *et al.*[263]

In 1962, the procedure for the synthesis of the carbonyl-C^{14}-labelled 3OHKyn was reported by Brown *et al.*[334] This method employed 2-nitro-3-methoxybenzoic acid (27), which was converted to the acid chloride (28) (Scheme 3.3). Upon treatment with diazomethane, the resulting diazoketone (41) was brominated and condensed with diethyl acetamidomalonate to give (43). Deprotection and reduction with HI and red phosphorous gave 3OHKyn in an overall yield of 35% based on the radiocarbon.

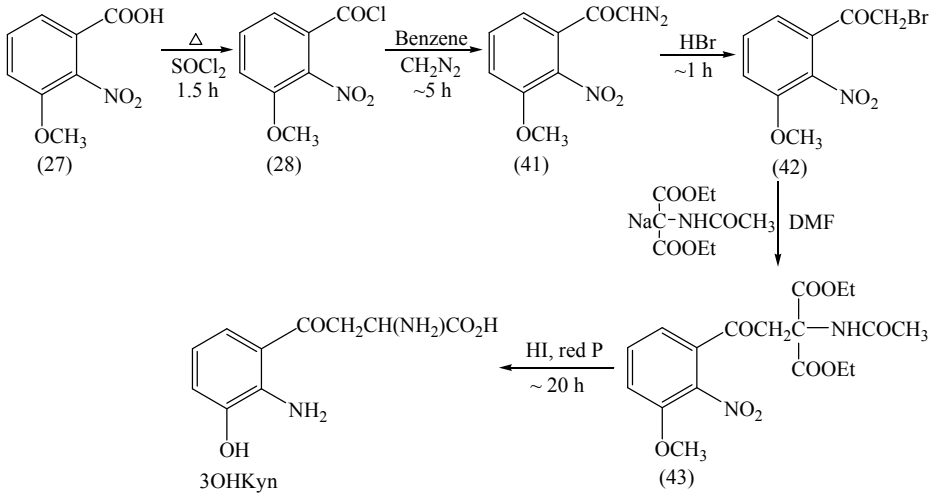

Scheme 3.3: Synthesis of 3OHKyn by Brown *et al.*[334]

3.1.2 Previous synthesis of AHBG

Two syntheses have been reported for AHBG, the first by Manthey *et al.*[262] in 1999 and the second by Chenault *et al.*[335] in 2000. Chenault *et al.*[335] employed 3-methoxy-2-nitrobenzaldehyde (44) as the starting material (Scheme 3.4). This was allylated to the corresponding alcohol (45), which was subsequently hydrated *via* hydroboration-oxidation to yield the diol (46). The diol was oxidised with Jones reagent to give the butanoic acid (47), which was then demethylated and esterified to yield the ester (48). The ester was coupled with ABG in the presence of a silver catalyst to produce the protected glucoside (49), which upon hydrogenation and deprotection yielded AHBG in 9.5% overall yield (7 steps).

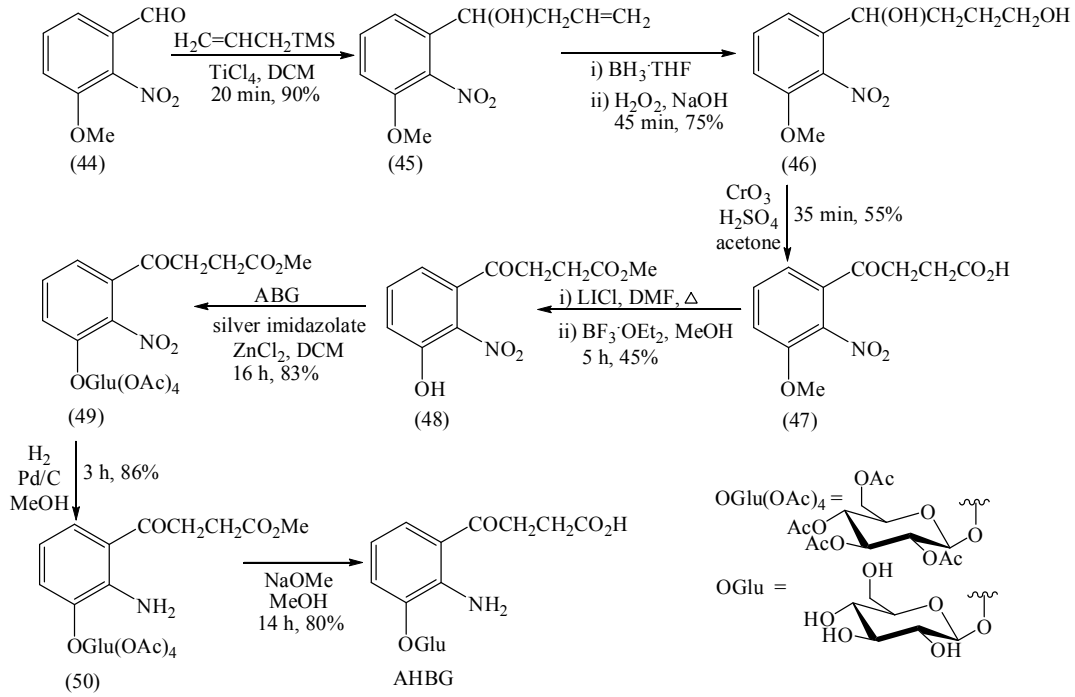

Scheme 3.4: Synthesis of AHBG by Chenault *et al.*[335]

In a similar manner to Butenandt *et al.'s* method,[263] Manthey *et al*.[262] obtained the acrylic acid (7) from 3-hydroxyacetophenone (8) (Scheme 3.5). This was then esterified to the methyl ester (10) and coupled with ABG in the presence of $Hg(CN)_2$ to form the methyl ester glucoside (11). Hydrogenation to reduce the nitro group and double bond, followed by hydrolysis of the ester and acetyl moieties by NaOEt in EtOH and then aqueous base, gave AHBG in 10.4% yield from the methyl ester (10).

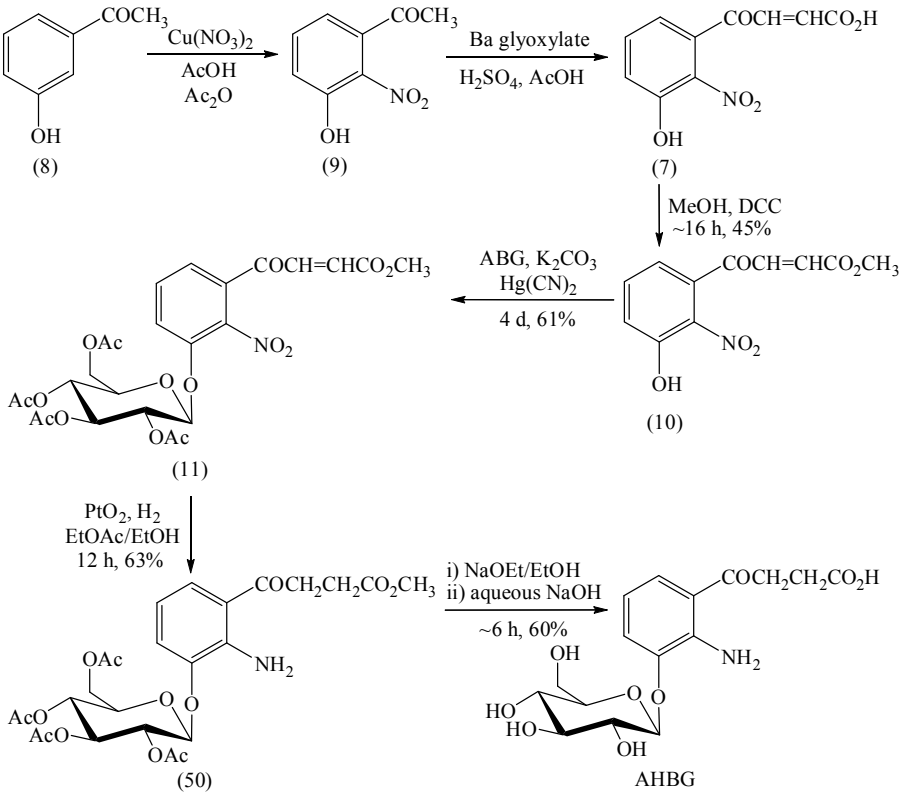

Scheme 3.5: Synthesis of AHBG by Manthey *et al.*[262]

In this study, the aim was to synthesise 3OHKyn and AHBG by expanding the optimised synthetic strategy of Butenandt *et al.*[263] and Manthey *et al.*[262] used for the synthesis of 3OHKG, as described in Chapter 2. The proposed synthetic pathway for the synthesis of 3OHKyn and AHBG is given in Scheme 3.6. The key precursor for the synthesis of 3OHKyn was the acrylic acid (7), which was synthesised from 3-hydroxy-2-nitroacetophenone (9) by an aldol condensation with glyoxylic acid monohydrate under microwave conditions (see Chapter 2). The AHBG precursor, the methyl ester glucoside (11), was obtained by glucosylation of the methyl ester (10) with ABG in the presence of a phase transfer catalyst and base (Chapter 2). The synthesis of 3OHKyn and AHBG were conducted only on a small (mg) scale to explore their feasibility and to obtain sufficient AHBG for use as a standard in Chapter 4.

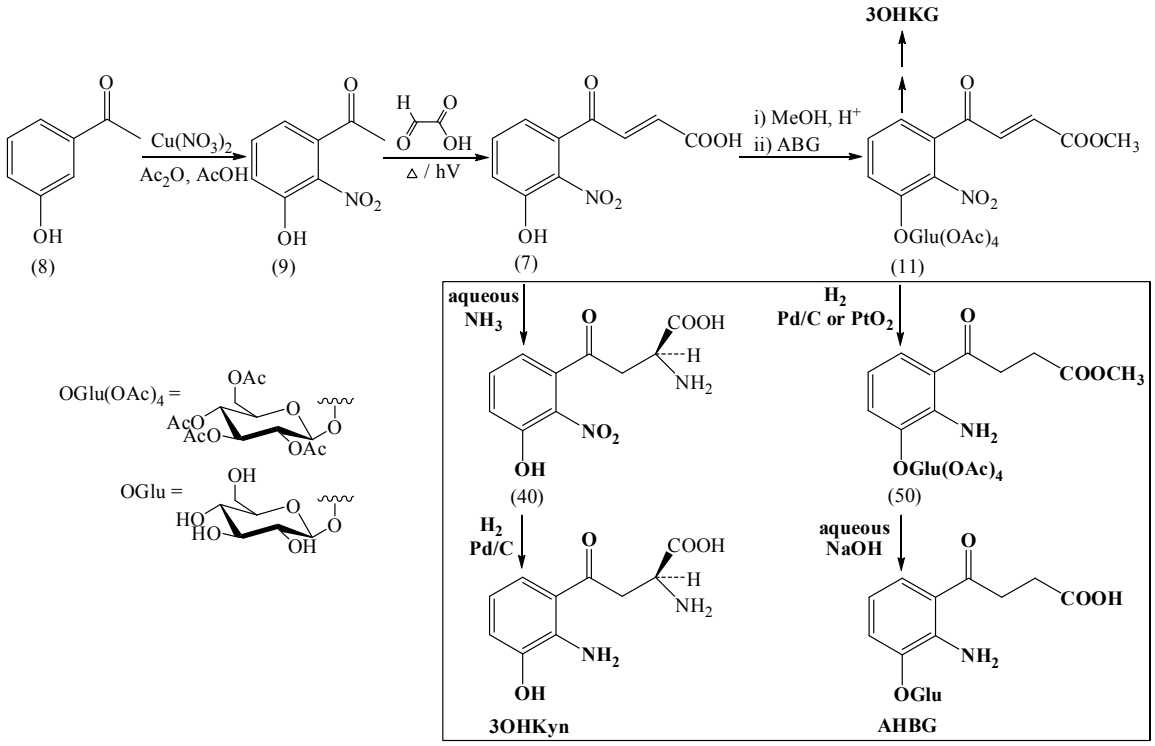

Scheme 3.6: Proposed synthetic pathway for 3OHKyn and AHBG from the acrylic acid (7) and the methyl ester glucoside (11), respectively.

3.2 Results and Discussion

3.2.1 Synthesis of 3-hydroxykynurenine (3OHKyn)

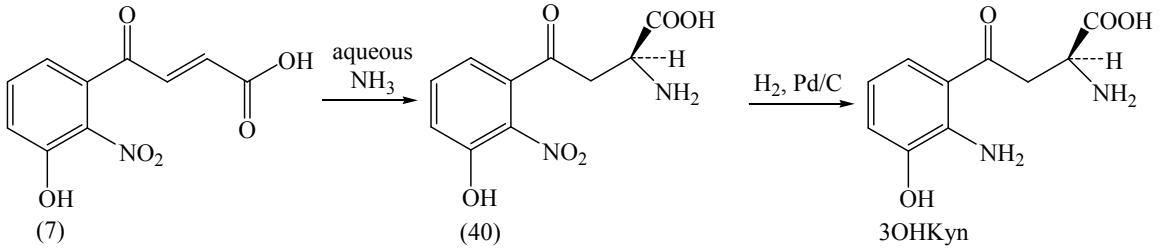

(7) (40) 3OHKyn

3.2.1.1 Synthesis of 2-amino-4-(3-hydroxy-2-nitrophenyl)-4-oxobutanoic acid (40) - Amination

In a similar manner to Butenandt *et al.'s* method[263] for the amination of the acrylic acid (7), the acrylic acid (7) was treated with aqueous NH_3 (28%) under argon in the dark at RT. The progress of the reaction was monitored by TLC, which almost immediately revealed formation of the desired product. The product was found to produce a purple spot on TLC when sprayed with ninhydrin, indicating the formation of an amine group. LC-MS analysis showed clean amination of the acrylic acid (7) to form the amine (40) (*m/z* 255 ($M+H^+$). The reaction was found to be complete within 1 h. The white suspension was acidified with 1 M AcOH and purified by RP-HPLC to obtain the amine (40) in 73% yield as a white solid. This was lower than the reported 90% yield by Butenandt *et al*.,[263] which could be due to the higher reaction scale (~700 mg) used by Butenandt *et al*.[263] compared to the 20 mg scale used in this study. Nevertheless, the reaction was complete within 1 h compared to two days, as reported by Butenandt *et al*.[263] The aromatic region of the ^1H NMR spectrum revealed three adjacent aromatic resonances with chemical shifts and coupling patterns similar to the aromatic ring of the acrylic acid (7). The aliphatic side chain contained characteristic signals for a CH_2-CH moiety (δ 3.68 and 3.52 [2H] and δ 4.10 [1H]), similar to the 3OHKyn amino acid side chain.[202] ES-MS/MS displayed a molecular ion at *m/z* 255 ($M+H^+$) and fragment ions at *m/z* 238 (loss of NH_3), *m/z* 237 (loss of H_2O), *m/z* 182 (loss of $CH(NH_2)COOH$) and *m/z* 166 (loss of $CH(NH_2)COOH$ and OH). The melting point of 170-172°C indicated that the product was obtained in high purity as it was consistent with the literature value of 171-173°C.[263]

3.2.1.2 Synthesis of 3OHKyn - Hydrogenation

Butenandt *et al*.[263] reduced the nitro group of the amine (40) with Raney Ni and Pd/C in EtOH to afford 3OHKyn. In this study, the nitro group of the amine (40) (52 mg) was reduced under an atmosphere of H_2 (1 atm) in aqueous NH_3 (28%) in the presence of Pd/C. This method was chosen since the relatively non-hazardous Pd/C was preferred over Raney Ni, which is a pyrophoric (can ignite spontaneously) and carcinogenic catalyst. In addition, aqueous NH_3 (28%) was chosen as a solvent as it was expected to prevent deamination of the side chain. The reaction was monitored by TLC (UV and ninhydrin) and LC-MS. These indicated clean formation of 3OHKyn (*m/z* 225 ($M+H^+$). After 2 h, TLC showed complete disappearance of the starting material. The yellow solution was filtered to remove the catalyst and acidified to pH ~6 by 1 M AcOH. 3OHKyn was isolated from this small scale reaction by filtration in 67% yield. The yield was comparable to the 64% reported by Butenandt *et al*.[263] on a ~200 mg scale after 12 h of reaction time. The synthetic sample coeluted with a commercial 3OHKyn standard and showed identical ^1H NMR and ES-MS/MS.[202] The aliphatic side chain contained characteristic signals for the methylene protons at δ 3.48 and 3.73 and a methine proton at δ 3.89. ES-MS/MS (positive mode) revealed a molecular ion at *m/z* 225 ($M+H^+$), which fragmented to ions at *m/z* 208 (loss of NH_3), *m/z* 162 (loss of NH_3 and HCOOH), *m/z* 152 (2-amino-3-hydroxyacetophenone) and *m/z* 110 (2-aminophenol). Absorbance (λ_{max} 269 and 371 nm) and fluorescence (λ_{ex} 370 and λ_{em} 460 nm) profiles in PBS at pH 7.0 were identical to an authentic sample of 3OHKyn and the literature.[202,336]

3.2.1.3 Synthesis of 3OHKyn - The "One pot" reaction

The above amination reaction was repeated on a 51 mg scale of the acrylic acid (7) and the reaction mixture was subsequently hydrogenated without intermediate (amine (40)) purification. The amination progress was monitored by TLC (UV and ninhydrin) and LC-MS, which indicated a clean amination over 1.5 h. Hydrogenation was then commenced as described above. After 30 min, TLC and LC-MS indicated clean formation of 3OHKyn. After 2 h, TLC indicated complete disappearance of the amine (40), and the yellow solution was worked up and purified as described above to yield 3OHKyn in 72% yield from the acrylic acid (7).

As a result of this study, 3OHKyn was synthesised from the acrylic acid (7) using modified conditions from Butenandt *et al.'s* method.[263] The amination of the acrylic acid (7) was

conducted in aqueous NH_3 (28%) in 1 h and 73% yield, compared to 2 days and 90% yield as reported by Butenandt *et al.*[263] The catalytic hydrogenation was conducted by Pd/C in preference to Raney Ni due to its non-hazardous properties. The amine (40) was hydrogenated in 2 h and 67% yield, compared to 12 h and 64% yield for Butenandt *et al.'s* method.[263] The synthesis was also conducted as a "one pot" reaction to obtain 3OHKyn in 72% yield, resulting in an improvement in the overall reaction yield, cost, reaction time and benignness of the reaction conditions compared to the literature.

3.2.2 Synthesis of 4-(2-amino-3-hydroxyphenyl)-4-oxobutanoic acid-*O*-β-D-glucoside (AHBG)

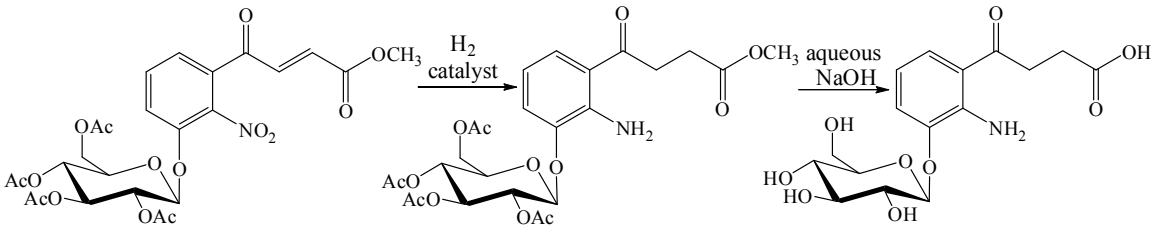

(11) (50) AHBG

3.2.2.1 Synthesis of 4-(2-amino-3-((2,3,4,5-tetra-*O*-acetyl-β-D-glucopyranosyl)oxyphenyl)-4-oxobut-2-anoate (50) - Hydrogenation

In order to obtain AHBG in sufficient quantities for studies conducted in Chapter 4, both hydrogenation conditions of Chenault *et al.*[335] and Manthey *et al.*[262] were investigated. The methyl ester glucoside (11), the precursor in the synthesis of 3OHKG (Chapter 2), was separately hydrogenated under an atmosphere of H_2 (1 atm) in the presence of PtO_2 in EtOAc/EtOH (4:1, v/v)[262] and Pd/C in MeOH.[335] Both reactions were monitored by TLC (UV and ninhydrin) and LC-MS. TLC was consistent with the formation of an amine, producing a ninhydrin positive spot, and LC-MS indicated clean reduction of the methyl ester glucoside (*m/z* 582 ($M+H^+$) to the amine (50) (*m/z* 554 ($M+H^+$)). After 2 h, TLC showed no starting material. The pale yellow solutions were separately filtered through a plug of celite, evaporated and purified by RP-HPLC to afford the amine (50) as a white solid in similar yields (62-67%) for both conditions. These yields were comparable to the 63% yield reported by Manthey *et al.*[262] and slightly lower then the 86% reported by Chenault *et al.*[335]

In the ^1H NMR spectrum, the aliphatic side chain showed clear resonances for a CH_2-CH_2 moiety, with signals at δ 3.27 and 2.68, each with an integration of 2H. These chemical shifts

were consistent with that reported by Manthey *et al*.[262] and Chenault *et al*.[335] The signal at δ 3.27 was a triplet (*J* 6.7 Hz), as seen by both Manthey *et al*.[262] and Chenault *et al*.[335] However, the signal at δ 2.68 showed a triplet, with a further splitting of 2.2 Hz. Manthey *et al*.[262] only noted a triplet for the signal (at 300 MHz) and Chenault *et al*.[335] noted a multiplet (at 400 MHz). This splitting was not seen for the related compounds, AHA and AHB, suggesting that it was possibly due to the effect of the chiral glucose moiety making the methylene protons diasterotopic. The aromatic region revealed three adjacent protons with chemical shifts and coupling patterns consistent with the literature.[262,335] ES-MS/MS displayed a molecular ion at *m/z* 554 ($M+H^+$) and fragment ions at *m/z* 482 (loss of CH_2COOCH_3) and *m/z* 331 ($Glu(OAc)_4$).

3.2.2.2 Synthesis of AHBG - Deprotection

To remove the ester and acetyl moieties, the amine (50) was hydrolysed by the modified method of Manthey *et al*.[262] under the basic conditions (aqueous NaOH) used in Chapter 2 for the synthesis of 3OHKG. TLC (UV and ninhydrin) indicated almost immediate formation of two additional products of higher polarity than the starting material. LC-MS analysis showed AHBG (*m/z* 372 ($M+H^+$) and three unknown small peaks (~19% peak area at 254 nm). After 5 h, TLC indicated no starting material, and the pale yellow solution was acidified to pH ~6 by 1 M AcOH and purified by RP-HPLC to yield AHBG in 48% yield as a pale yellow solid. The yield was lower than that reported in the literature (60%), possibly due to the small scale of the reaction (20 mg) conducted in this study.[262] ^1H NMR and ES-MS/MS were identical to the literature.[262,335] The aromatic region of the ^1H NMR spectrum revealed three adjacent aromatic resonances with chemical shifts and coupling patterns consistent with the literature.[262,335] The aliphatic side chain contained characteristic signals for a CH_2-CH_2 moiety seen as isolated triplets at δ 2.47 (2H) and 3.22 (2H), consistent with the literature.[262,335] The anomeric proton appeared as a broad doublet centered at δ 4.94 with coupling of ~7.5 Hz and integration of 1H. This was indicative of a β-configuration. ES-MS/MS displayed a molecular ion at *m/z* 372 ($M+H^+$) and fragment ions at *m/z* 210 (loss of glucose), *m/z* 192 (loss of glucose and water) and *m/z* 164 (loss of glucose and COOH). Absorbance (λ_{max} 260 and 358 nm) and fluorescence (λ_{ex} 357 and λ_{em} 495 nm) profiles in PBS at pH 7.0 were identical to the literature.[86]

3.2.2.3 Synthesis of AHBG – Without intermediate purification

The above hydrogenation reaction was repeated on a 10 mg scale of the methyl ester glucoside (11), following Manthey *et al.'s* conditions.[262] The progress of the reaction was monitored by TLC and LC-MS, as described above. After 2 h, the pale yellow solution was filtered through a plug of celite and evaporated to yield the crude amine (50). The crude product was hydrolysed under basic conditions (aqueous NaOH), as described above. The progress of the reaction was monitored by TLC and LC-MS and after 5 h the pale yellow solution was worked up and purified as above to yield AHBG in 41% overall yield, as a pale yellow solid.

As a result of this study, AHBG was synthesised *via* the methyl ester glucoside (11) following the literature hydrogenation procedures of Manthey *et al.*[262] and Chenault *et al.*[335] and optimised deprotection conditions of Manthey *et al.*[262] (Chapter 2). This gave AHBG in ~31% overall yield (2 steps). Under an atmosphere of H_2, Pd/C and PtO_2 proved to be equally effective catalysts in hydrogenation of the methyl ester glucoside (11) in EtOAc/EtOH (4:1, v/v) and MeOH, respectively. The synthesis was also conducted without intermediate purification, to obtain AHBG in 41% overall yield.

These reactions were conducted on relatively small scales (≤ 22 mg). While this gave sufficient material for this study, further investigation on larger scale is required. It is proposed that in future studies similar amination and deprotection reactions could be performed with the ethyl ester glucoside (18) (see Chapter 2) for the synthesis of AHBG, given that this would eliminate one step in the synthesis of the ethyl ester glucoside (18).

3.3 Conclusions

Using intermediates from the synthesis of 3OHKG, the UV filters, 3OHKyn and AHBG, were successfully synthesised. 3OHKyn was synthesised in good yield *via* step-wise amination of the acrylic acid (7) by aqueous NH_3 and subsequent hydrogenation with H_2 in the presence of Pd/C as a catalyst. The synthesis was also conducted without intermediate purification, resulting in improvement in the reaction yields and reaction time. AHBG was synthesised from the methyl ester glucoside (11) *via* catalytic hydrogenation under an atmosphere of H_2, following the methods of Manthey *et al.*[262] and Chenault *et al.*,[335] and subsequent deprotection under basic conditions using modified conditions of Manthey *et al.*[262] (Chapter

2). AHBG was also synthesised without intermediate purification. This made the reaction more time efficient and it resulted in an improvement in the reaction yield.

In general, these reactions were relatively low scale reactions, therefore further investigation on a larger scale would be valuable. Nevertheless, the synthetic pathway optimised in Chapter 2 for the synthesis of 3OHKG has been proven to be a versatile method that allows entry into a range of UV filter compounds, including 3OHKyn and AHBG, and as discussed later in Chapter 4, 4-(2-aminophenyl)-4-oxobutanoic acid (AHA), 4-(2-amino-3-hydroxyphenyl)-4-oxobutanoic acid (AHB) and cysteinyl-3-hydroxykynurenine-*O*-β-D-glucoside (Cys-3OHKG). The ready access of these compounds has allowed further work to be conducted, as presented in Chapters 4, 5 and 6.

3.4 Experimental

3.4.1 General experimental

Organic solvents, aqueous ammonia (NH_3, 28%), acetonitrile (CH_3CN, HPLC grade) and formic acid (99%) were from Ajax Chemicals (NSW, Australia). All other organic solvents were AR grade and distilled prior to use. Trifluoroacetic acid (TFA, > 99%), PtO_2 (Pt 81-83%), deactivated carbon and Pd/C (10 wt % on activated carbon) were from Sigma-Aldrich. Glacial acetic acid (AcOH) (> 99.9%) was purchased from BDH. CD_3OD (99.8%), $CDCl_3$ (99.8%) and D_2O (99.9%) were from Cambridge Isotope Laboratories. Filter paper (AA grade, 20-25 μm) was from Whatman. Dulbelcco's phosphate-buffered saline (PBS), without calcium and magnesium, consisted of KCl (2.7 mM), KH_2PO_4 (1.4 mM), NaCl (137 mM) and Na_2HPO_4 (7.68 mM).[257] Pre-washed chelex resin was added to the PBS buffer (~2 g/L) and left for 24 h prior to use. The pH was adjusted to 7.0 with 1 M NaOH. Milli-Q® H_2O (purified to 18.2 MΩ cm^{-2}) was used in preparation of RP-HPLC aqueous solutions and PBS. Thin-layer chromatography (TLC) plates of normal phase 60 F_{254} and reversed phase 18 F_{254} were from Merck (Germany). TLC plates were visualised under UV light (254 and 365 nm) and sprayed with ninhydrin (ninhydrin [0.2%, w/v] in *n*-butanol [94.8%, v/v] and AcOH [5%, v/v]),[288] where indicated. Normal phase TLC plates were developed using *n*-butanol/AcOH/H_2O (12:3:5 BAW, v/v), where indicated. Normal phase silica gel (SiO_2, 230-400 mesh) was from Merck (Germany). Melting points were determined on an SMP 10 Stuart scientific (UK) apparatus and are uncorrected. Infrared spectra were recorded on a

PerkinElmer Paragon 1000 PC FT-IR spectrometer. A Labconco FreeZone 12 plus freeze drier (0.04 mBa, -80°C) from Crown Scientific was used for lyophilisation of aqueous solutions. Organic solvents were removed by rotary evaporation without application of heat.

3.4.2 UV-visible (UV-vis) absorbance and fluorescence spectrometric measurements

See Section 2.4.2 for details.

3.4.3 Reversed phase-high performance liquid chromatography (RP-HPLC)

RP-HPLC was performed on a Shimadzu HPLC equipped with LC-10ADvp pumps, a SIL-10Avp autoinjector and SPD-M10Avp diode array detector. The preparative purifications were performed on a Phenomenex (Luna, 100 Å, 10 μm, 15 x 250 mm, C18) column fitted with a Phenomenex (Fusion, 100 Å, 4 μm, 10 x 10 mm, C18) guard column. The following mobile phase system; buffer A (H_2O/0.05% TFA, v/v) and buffer B (80% CH_3CN/0.05% TFA, v/v) and the flow rate of 5 mL/min were kept constant. Preparative purifications of 2-amino-4-(3-hydroxy-2-nitrophenyl)-4-oxobutanoic acid (40) and AHBG were performed using the following mobile phase gradient: 0-10 min (5% buffer B), 10-35min (0-50% buffer B), 35-40 min (50% buffer B), 40-45 min (50-5% buffer B) and 45-55 min (5% buffer B). Preparative purification of methyl 4-(2-amino-3-((2,3,4,5-tetra-*O*-acetyl-β-D-glucopyranosyl)oxyphenyl)-4-oxobutanoate (50) was performed using the following mobile phase gradient: 0-5 min (55% buffer B), 5-25 min (55-90% buffer B), 25-30 min (90% buffer B), 30-35 min (90-55% buffer B) and 35-45 min (55% buffer B).

3.4.4 Liquid chromatography-mass spectrometry (LC-MS)

See Section 2.4.4 for details.

3.4.5 Nuclear magnetic resonance (NMR) spectroscopy

See Section 2.4.5 for details.

3.4.6 Mass spectrometry (MS)

See Section 2.4.6 for details.

3.4.7 Synthesis of 3-hydroxykynurenine (3OHKyn)

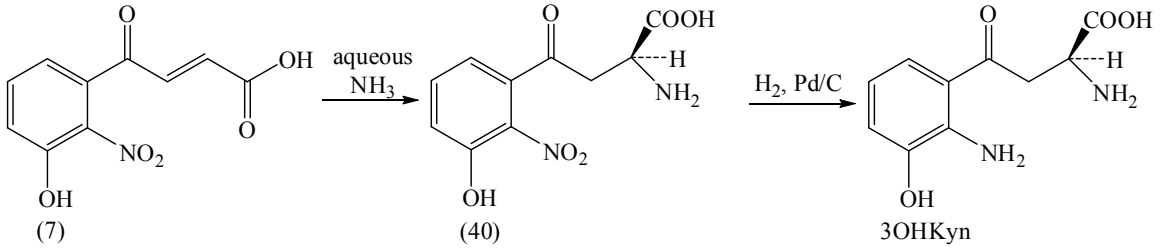

3.4.7.1 Synthesis of 2-amino-4-(3-hydroxy-2-nitrophenyl)-4-oxobutanoic acid (40) – Amination (modified method of Butenandt *et al*.[263])

4-(3-Hydroxy-2-nitrophenyl)-4-oxobut-2-enoic acid (7) (20 mg, 0.08 mmol) was dissolved in aqueous NH_3 (1.0 mL (28%), 16 mmol) and stirred under argon in the dark at RT. The progress of the reaction was monitored by normal phase TLC (BAW, UV and ninhydrin) and LC-MS (*m/z* 255 ($M+H^+$), λ_{max} 245 and 312 nm). After 1 h, the white suspension was acidified to pH 6 by AcOH (1 M) and lyophilised. The white solid was purified by RP-HPLC to obtain 2-amino-4-(3-hydroxy-2-nitrophenyl)-4-oxobutanoic acid (16 mg, 73%, R_f 0.38 (BAW), mp 170-172°C (lit.[263] 171-173°C)) as a white solid.

2-Amino-4-(3-hydroxy-2-nitrophenyl)-4-oxobutanoic acid (40): ^{1}H NMR δ (MeOD) 7.52 (1H, dd, *J* 8.0, 8.0, ArH-5), 7.42 (1H, br d, *J* ~8.0, ArH-6), 7.27 (1H, br d, *J* ~8.0, ArH-4), 4.10 (1H, m, H-2), 3.68 (1H, dd, *J* 1.6, 19.3, H-3), 3.52 (1H, dd, *J* 8.5, 19.3, H-3); ES-MS/MS *m/z* 255.0 ($M+H^+$, 100%), 245.7 (10%), 238.4 ($M+H^+$ - NH_3, 10%), 236.7 ($M+H^+$ - H_2O, 12%), 209.1 (72%), 182.0 ($M+H^+$ - $CH(NH_2)COOH$, 27%), 166.0 ($M+H^+$ - $CH(NH_2)COOH$ - OH, 10%), 92.0 (8%).

3.4.7.2 Synthesis of 3-hydroxykynurenine (3OHKyn) - Hydrogenation

A mixture of 2-amino-4-(3-hydroxy-2-nitrophenyl)-4-oxobutanoic acid (40) (52 mg, 0.22 mmol), aqueous NH_3 (1.0 mL (28%), 16 mmol) and Pd/C (~4 mg) was treated with H_2 gas (1 atm) at RT in the dark for 2 h. The reaction was monitored by TLC of normal phase (BAW)

and reversed phase (5% CH_3CN/0.05% TFA, v/v), and LC-MS. The yellow solution was filtered through a plug of celite and acidified to pH ~6 by AcOH (1 M), decolourised with deactivated carbon, refiltered through filter paper and lyophilised. The yellow solid was washed with cold water (~5 mL) and dried under vacuum to obtain 3OHKyn (31 mg, 67%, R_f 0.42 (BAW), R_f 0.54 (5% CH_3CN/0.05% TFA, v/v)) as a bright yellow solid.

3-Hydroxykynurenine (3OHKyn): ν_{max}(KBr disc) 3492 (NH_2), 3370 (NH_2), 3250-2500 (br, zwitterionic NH_3^+, COO^-, NH_2, OH, with C-H superimposed), 1642 (C=O), 1548, 1504, 1236, 752 (out-of-plane aromatic C-H bend) cm^{-1}; ^{1}H NMR δ (MeOD) 7.27 (1H, d, *J* 8.1, ArH-6), 6.82 (1H, d, *J* 7.9, ArH-4), 6.48 (1H, dd, *J* 7.9, 8.1, ArH-5), 3.89 (1H, dd, *J* 2.6, 9.3, H-2), 3.73 (1H, dd, *J* 2.6, 18.6, H-3), 3.48 (1H, dd, *J* 9.3, 18.6, H-3); ES-MS *m/z* 225.0 ($M+H^+$, 8%), 208.0 ($M+H^+$ - NH_3, 100%), 190.0 ($M+H^+$ - NH_3 - H_2O, 38%), 180.0 (12%), 171.0 (12%), 166.0 (52%), 162.0 ($M+H^+$ - NH_3 - HCOOH, 83%), 152.0 ($M+H^+$ - $CH(NH_2)COOH$, 40%), 136.0 (18%), 110.0 ($M+H^+$ - $C(O)CH_2CH(NH_2)COOH$, 82%). λ_{max} at 269 and 371 nm and maximum fluorescence at λ_{ex} 370 / λ_{em} 460 nm.

3.4.7.3 Synthesis of 3-hydroxykynurenine (3OHKyn) - The “One pot” reaction

4-(3-Hydroxy-2-nitrophenyl)-4-oxobut-2-enoic acid (7) (51 mg, 0.22 mmol) was dissolved in aqueous NH_3 (1.5 mL (28%), 25 mmol). The white solution was stirred in the dark at RT under argon and monitored by TLC and LC-MS, as described above. After 1.5 h, Pd/C (~4 mg) was added and the white suspension was placed under an atmosphere of H_2 (1 atm). The progress of the reaction was monitored by TLC and LC-MS, as described above. After 2 h, the yellow solution was worked up and purified, as described above, to obtained 3OHKyn (44 mg, 73%) as a bright yellow solid. ^{1}H NMR, ES-MS, absorbance and fluorescence were consistent with above.

3.4.8 Synthesis of 4-(2-amino-3-hydroxyphenyl)-4-oxobutanoic acid-*O*-β-D-glucoside (AHBG)

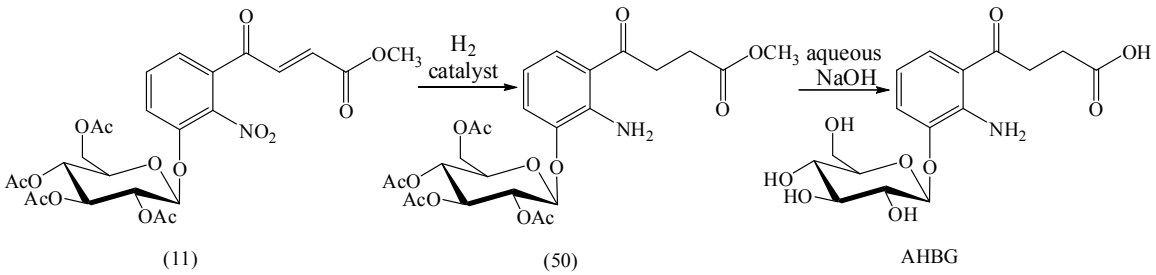

3.4.8.1 Synthesis of 4-(2-amino-3-((2,3,4,5-tetra-*O*-acetyl-β-D-glucopyranosyl)oxyphenyl)-4-oxobutanoate (50) - Hydrogenation

3.4.8.1.1 Method 1 (modified method of Manthey *et al*.[262])

A solution of methyl 4-(2-nitro-3-((2,3,4,5-tetra-*O*-acetyl-β-D-glucopyranosyl)oxyphenyl)-4-oxobut-2-enoate (11) (22 mg, 0.04 mmol) and EtOAc/EtOH (2 mL, 4:1, v/v) was placed under an atmosphere of H_2 (1 atm) in the presence of PtO_2 (3 mg, 0.01 mmol) in the dark at RT. The reaction was monitored by normal phase TLC (BAW, 1:1 EtOAc/hexane, v/v, and 5:95 DCM/EtOAc, v/v) and LC-MS (*m/z* 554 ($M+H^+$, 100%), 576 ($M+H^+$ + Na, 30%); λ_{max} 258 and 361 nm). After 2 h, the pale yellow solution was filtered through a plug of celite, evaporated and purified by preparative RP-HPLC to afford methyl 4-(2-amino-3-((2,3,4,5-tetra-*O*-acetyl-β-D-glucopyranosyl)oxyphenyl)-4-oxobutanoate (14 mg, 67%, R_f 0.86 (BAW), R_f 0.50 (1:1 EtOAc/hexane, v/v), R_f 0.60 (5:95 DCM/EtOAc, v/v)) as a white solid. ^{1}H NMR and ES-MS/MS were in agreement with the literature.[262,335]

Methyl 4-(2-amino-3-((2,3,4,5-tetra-*O*-acetyl-β-D-glucopyranosyl)oxyphenyl)-4-oxobutanoate (50): ^{1}H NMR δ ($CDCl_3$) 7.52 (1H, dd, *J* 1.2, 8.1, ArH-6), 7.02 (1H, dd, *J* 1.2, 7.9, ArH-4), 6.53 (1H, dd, *J* 7.9, 8.1, ArH-5), 5.31-5.25 (2H, m, H-2', H-3'), 5.13 (1H, m, H-4'), 4.95 (1H, m, H-1'), 4.28 (1H, m, H-6'), 4.16 (1H, m, H-6'), 3.83 (1H, m, H-5'), 3.67 (3H, s, C$\underline{H_3}$), 3.27 (2H, t, *J* 6.7, H-2), 2.68 (2H, t, *J* 6.7, further fine splitting ~2.2, H-3), 2.07 (3H, s, COC$\underline{H_3}$), 2.05 (3H, s, COC$\underline{H_3}$), 2.03 (3H, s, COC$\underline{H_3}$), 2.02 (3H, s, COC$\underline{H_3}$); ES-MS/MS *m/z* 554.0 ($M+H^+$, 100%), 539.0 (8%), 482.5 ($M+H^+$ - CH_2COOCH_3, 6%), 331.0 ($Glu(OAc)_4$, 81%), 270.9 (14%).

3.4.8.1.2 Method 2 (modified method of Chenault *et al*.[335])

The above procedure was repeated with methyl 4-(2-nitro-3-((2,3,4,5-tetra-*O*-acetyl-β-D-glucopyranosyl)oxyphenyl)-4-oxobut-2-enoate (11) (22 mg, 0.04 mmol) in MeOH (3 mL) and Pd/C (~3 mg) as a catalyst. After 2 h, the pale yellow solution was worked up and purified, as described above, to yield methyl 4-(2-amino-3-((2,3,4,5-tetra-*O*-acetyl-β-D-glucopyranosyl)oxyphenyl)-4-oxobutanoate (13 mg, 62%, R_f 0.86 (BAW), R_f 0.50 (1:1 EtOAc/hexane, v/v), R_f 0.60 (5:95 DCM/EtOAc, v/v)) as a white solid. ^{1}H NMR and ES-MS/MS were consistent with above and the literature.[262,335]

3.4.8.2 Synthesis of 4-(2-amino-3-hydroxyphenyl)-4-oxobutanoic acid-*O*-β-D-glucoside (AHBG) - Deprotection (modified method of Manthey *et al*.[262])

Methyl 4-(2-amino-3-((2,3,4,5-tetra-*O*-acetyl-β-D-glucopyranosyl)oxyphenyl)-4-oxobutanoate (50) (20 mg, 0.04 mmol) was dissolved in argon-gassed (~20 min) aqueous NaOH (5 mL, 0.08 mM). The reaction was stirred under argon and monitored by normal phase TLC (BAW) and LC-MS (*m/z* 372 ($M+H^+$, 100%), 394 ($M+H^+$ + Na, 25%); λ_{max} 261 and 362 nm). After 5 h, the pale yellow solution was acidified to pH 6 using AcOH (1 M) and lyophilised. The light yellow solid was purified by preparative RP-HPLC to afford AHBG (6.4 mg, 48%, R_f 0.57 (BAW)) as a pale yellow solid. ^{1}H NMR, ES-MS/MS, absorbance and fluorescence were in agreement with the literature.[85,86,262,335]

4-(2-Amino-3-hydroxyphenyl)-4-oxobutanoic acid-*O*-β-D-glucoside (AHBG): ^{1}H NMR δ (D_2O) 7.64 (1H, dd, *J* 1.1, 8.1, ArH-6), 7.22 (1H, dd, *J* 1.1, 8.1, ArH-4), 6.88 (1H, dd, *J* 8.1, 8.1, ArH-5), 4.94 (1H, br d, *J* ~7.5, H-1'), 3.83 (1H, dd, *J* 2.1, 12.5, H-6'), 3.67 (1H, dd, *J* 5.5, 12.5, H-6'), 3.58-3.48 (3H, m, H-2', H-3', H-5'), 3.43 (1H, m, H-4'), 3.22 (2H, t, *J* 6.8, H-2), 2.47 (2H, t, *J* 6.8, H-3); ES-MS/MS *m/z* 372.1 ($M+H^+$, 32%), 210.1 ($M+H^+$ - Glu, 100%), 192.1 ($M+H^+$ - Glu - H_2O, 43%), 164.1 ($M+H^+$ - Glu - COOH, 12%), 145.0 (11%), 127.0 (5%), 110.1 ($M+H^+$ - Glu - $C(O)CH_2CH_2COOH$, 51%), 97.0 (3%), 85.0 (10%). λ_{max} at 260 and 358 nm and maximum fluorescence at λ_{ex} 357 / λ_{em} 495 nm.

3.4.8.3 Synthesis of 4-(2-amino-3-hydroxyphenyl)-4-oxobutanoic acid-*O*-β-D-glucoside (AHBG) - Without intermediate purification (modified method of Manthey *et al*.[262])

A mixture of methyl 4-(2-nitro-3-((2,3,4,5-tetra-*O*-acetyl-β-D-glucopyranosyl)oxyphenyl)-4-oxobut-2-enoate (11) (10 mg, 0.02 mmol), EtOAc/EtOH (2 mL, 4:1, v/v) and PtO_2 (3 mg, 0.01 mmol) was treated with H_2 gas (1 atm) at RT in the dark. The reaction was monitored by normal phase TLC and LC-MS, as described above. After 2 h, the pale yellow reaction mixture was filtered through a plug of celite, evaporated and mixed with argon-gassed (~20 min) aqueous NaOH (5 mL, 0.08 mM). After 5 h, the reaction mixture was acidified to pH 6 using AcOH (1 M) and worked up and purified, as described above, to afford AHBG (2.6 mg, 41%) as a pale yellow solid. ^{1}H NMR, ES-MS, absorbance and fluorescence were consistent with the literature and above.[85,86,262,335]